NPS ARCHIVE
1968
LENZINI, M.

# CALIBRATION OF TURBINE TEST RIG WITH IMPULSE TURBINE AT HIGH PRESSURE RATIOS

by

Martin Joseph Lenzini

DUDLEY KNOX LIBRARY
NAVAL POSTGRADUATE SCHOOL
MONTEREY, CA 93943-5101

Gaylord
SHELF BINDER
Syracuse, N. Y.
Stockton, Calif.

# UNITED STATES
# NAVAL POSTGRADUATE SCHOOL

# THESIS

CALIBRATION OF TURBINE TEST RIG WITH
IMPULSE TURBINE AT HIGH PRESSURE RATIOS

by

Martin Joseph Lenzini

June 1968

This document is subject to special export controls and each transmittal to foreign government or foreign nationals may be made only with prior approval of the U. S. Naval Postgraduate School.

# CALIBRATION OF TURBINE TEST RIG WITH IMPULSE TURBINE AT HIGH PRESSURE RATIOS

by

Martin Joseph Lenzini
Captain, United States Marine Corps
B.S., University of New Mexico, 1961

Submitted in partial fulfillment of the

requirements for the degree of

AERONAUTICAL ENGINEER

from the

NAVAL POSTGRADUATE SCHOOL
June 1968

NPS ARCHIVE
1968
LENZINI, M
~~Thesis L527 c.1~~

ABSTRACT

The Transonic Turbine Test Rig of the Turbo-Propulsion Laboratory, Department of Aeronautics, of the Naval Post-graduate School was designed to investigate the performance of turbines with transonic or supersonic rotor inlet velocities. The test rig has provisions for testing single stage axial turbines at high pressure ratios and at variable axial and radial clearances. The present study describes the calibration of the turbine test rig with an impulse turbine at high pressure ratios. The turbine stage consists of a double circular-arc rotor with sharp leading edges and a stator with converging nozzle type blading. The results of the flow rate calibration and labyrinth seal leakage tests are described. The instrumentation necessary to separate rotor and stator losses is also discussed.

DUDLEY KNOX LIBRARY
NAVAL POSTGRADUATE SCHOOL
MONTEREY, CA 93943-5101

TABLE OF CONTENTS


| SECTION | | PAGE |
|---|---|---|
| 1. | INTRODUCTION | 13 |
| 2. | TURBINE DESCRIPTION | 15 |
| 3. | TEST INSTALLATION | 17 |
| 4. | FLOW NOZZLE CALIBRATION | 22 |
| 5. | PLENUM LABYRINTH SEAL LEAK RATE | 25 |
| 6. | ANALYSIS AND DATA REDUCTION | 29 |
| | 6.1 General | 29 |
| | 6.2 Flow Rate Determination | 29 |
| | 6.3 Stator Entrance Properties | 31 |
| | 6.4 Stator Discharge Properties | 31 |
| | 6.5 Rotor Discharge Properties | 37 |
| | 6.6 Performance Parameters | 41 |
| 7. | DESCRIPTION OF TURBINE TESTS | 44 |
| 8. | RESULTS AND DISCUSSION OF TURBINE TESTS | 47 |
| 9. | RECOMMENDATIONS | 55 |
| REFERENCES | | 88 |
| APPENDIX I: | COMPUTER PROGRAMS FOR FLOW RATE DETERMINATION AND TURBINE TEST DATA REDUCTION | 89 |
| APPENDIX II: | EVALUATION OF THE FORCE ACTING ON THE STATOR ASSEMBLY BY THE STATOR DISCHARGE PRESSURE. | 140 |

DUDLEY KNOX LIBRARY
NAVAL POSTGRADUATE SCHOOL
MONTEREY, CA 93943-5101

LIST OF ILLUSTRATIONS


| FIGURE | | PAGE |
|---|---|---|
| 1. | Blade Profiles Circular-Arc Rotor Converging Stator | 57 |
| 2. | Converging Stator (View showing stator entrance) | 58 |
| 3. | Circular-Arc Rotor (View showing rotor entrance) | 59 |
| 4. | Mean Radius Blade Profile Converging Stator | 60 |
| 5. | Mean Radius Blade Profile Circular-Arc Rotor with Sharp Leading Edges | 61 |
| 6. | Blade Profile Circular-Arc Rotor with Blunt Leading Edges | 62 |
| 7. | Blade Profile Contoured Rotor | 63 |
| 8. | Blade Profile Converging-Diverging Stator. | 64 |
| 9. | Piping Installation, Transonic Turbine Test Rig | 65 |
| 10. | Transonic Turbine Test Rig. | 66 |
| 11. | Turbine Blading Arrangement | 67 |
| 12. | Closure Plate Assembly Transonic Turbine Test Rig. | 68 |
| 13. | Closure Plate Calibration Rig (View showing closure plate assembly setup for calibration run) | 69 |

14. Closure Plate Assembly Installation
Transonic Turbine Test Rig . . . . . 70
15. Turbine and Shroud Details . . . . . 71
16. Circular-Arc Rotor and Bearing Assembly
Mounted in Rotor Bearing Stand . . . . . 72
17. Floating Stator Assembly . . . . . 73
18. Flow Nozzle Discharge Coefficient
Transonic Turbine Test Rig . . . . . 74
19. Referred Labyrinth Seal Leak Rate
Transonic Turbine Test Rig . . . . . 75
20. Referred Labyrinth Seal Leak Rate
Transonic Turbine Test Rig . . . . . 76
21. Modified Referred Labyrinth Seal Leak
Rate Transonic Turbine Test Rig . . . . . 77
22. Pressure Survey at Stator Entrance
Pressure Ratio = 2.0 . . . . . 78
23. Velocity Diagram of Turbine Stage . . . . . 79
24. Thermodynamic Process of Fluid
in an Axial Turbine Stage . . . . . 80
25. Total-Static Efficiency at Various
Axial Clearances . . . . . 81
26. Referred Moment versus Referred RPM
Pressure Ratio = 2.0 . . . . . 82
27. Efficiency Total-Static Initial
Turbine Tests . . . . . 83
28. Referred Moment versus Referred RPM
Initial Turbine Tests . . . . . 84

29. Stator Torque Capsule Variation with RPM Transonic Turbine Test Rig . . . . . 85
30. Stator Torque Capsule Variation with Temperature Transonic Turbine Test Rig . . . . . 86
31. Stator and Rotor Loss Coefficient versus Hood Temperature at 13080 RPM and Pressure Ratio of 2.5 . . . . . 87

## TABLE OF SYMBOLS

Latin

| | |
|---|---|
| A | Cross-sectional area ($in^2$) |
| a | Flow channel throat diameter (in) |
| a | Speed of sound (ft/sec) |
| b | Blade width (in) |
| C | Conversion factor, $2gJc_p$ ($ft^2/sec^2 - {}^oR$) |
| $c_p$ | Specific heat at constant pressure ($BTU/lb_m - {}^oR$) |
| D | Diameter (in) |
| F | Force ($lb_f$) |
| g | Gravitational constant ($32.174\ lb_m - ft/lb_f - sec^2$) |
| h | Blade height (in) |
| HP | Horsepower |
| $h_w$ | Differential pressure across turbine flow nozzle ($in\ H_2O$) |
| J | Conversion factor ($778.16\ ft - lb_f/BTU$) |
| K | Work coefficient (dimensionless) |
| $K_{is}$ | Head coefficient (dimensionless) |
| $K_n$ | Flow nozzle discharge coefficient (dimensionless) |
| M | Moment ($ft - lb_f$) |
| M | Absolute Mach number (dimensionless) |
| $M_R$ | Relative Mach number (dimensionless) |
| N | Rotational speed (rpm) |
| $P_t$ | Total pressure (psia) |
| P | Static pressure (psia) |
| R | Gas constant ($ft - lb_f/lb_m - {}^oR$) |
| $R_e$ | Reynolds number (dimensionless) |

| | |
|---|---|
| $R_m$ | Mean radius (in) |
| r | Radius (in) |
| r | Labyrinth pressure ratio (dimensionless) |
| r* | Theoretical degree of reaction (dimensionless) |
| s | Distance between blades (in) |
| s | Entropy ($BTU/lb_m - {}^\circ R$) |
| T | Static temperature ($^\circ R$) |
| $T_t$ | Total temperature ($^\circ R$) |
| t | Blade thickness at trailing edge (in) |
| t | Static temperature ($^\circ F$) |
| $t_t$ | Total temperature ($^\circ F$) |
| U | Peripheral velocity (ft/sec) |
| V | Absolute velocity (ft/sec) |
| W | Relative velocity (ft/sec) |
| $\dot{W}$ | Flow rate ($lb_m$/sec) |
| $Y_1$ | Expansion factor (dimensionless) |
| Z | Number of blades in a row |

Greek

| | |
|---|---|
| $\alpha$ | Absolute flow discharge angle (degrees) |
| $\alpha_n$ | Coefficient of thermal expansion of flow nozzle (dimensionless) |
| $\beta$ | Relative flow discharge angle (degree) |
| $\gamma$ | Ratio of specific heats (dimensionless) |
| $\delta$ | Referred pressure (dimensionless) |
| $\zeta$ | Loss coefficient (dimensionless) |
| $\eta$ | Efficiency (dimensionless) |
| $\theta$ | Referred temperature (dimensionless) |
| $\xi$ | Area restriction factor (dimensionless) |

$\Phi$ Flow function (dimensionless)

$\Phi_L$ Referred labyrinth seal leak rate ($in^2$)

$\Phi_{LM}$ Modified referred labyrinth seal leak rate ($in^2$)

Angular velocity (radians/sec)

Subscripts

a Axial direction

ax Area normal to the axial direction

Cl Closure plate

D Dynamometer

E Equivalent thermodynamic property

h Blade hub

h Hood

is Isentropic

L Labyrinth seals

m Mean streamline

n Flow nozzle properties

o Stator entrance properties

P Labyrinth plenum properties

R Rotor

REF Referred value

S Stator

t Blade tip

th Theoretical value

u Peripheral direction

1 Stator discharge properties

2 Rotor discharge properties

# SECTION 1

# INTRODUCTION

Turbines for modern gas turbine plants and jet propulsion units must operate at high pressure ratios. It is advantageous to use stages with supersonic or transonic flows in the rotating rows thereby limiting the number of stages and increasing the specific work output. Although the efficiency of such stages may prove to be somewhat lower than that of rotating rows with subsonic flows, they are desirable for use in low-weight power plants. An application presently under consideration by NASA is the use of a single-stage supersonic turbine in a hydrogen-fueled open-cycle auxiliary space power plant [1].

Very little quantitative information on supersonic and transonic turbine performance is available in the literature. Therefore, a Transonic Turbine Test Rig was built at the Naval Postgraduate School, Monterey, California. The test rig was designed by Dr. M. H. Vavra of the Department of Aeronautics to determine the effect of different blading arrangements on turbine efficiency and to separate the total losses of the turbine into those of the rotating and the stationary rows of blades. With the Transonic Turbine Test Rig, investigation of turbine performance for transonic and supersonic rotor inlet velocities is possible.

The present study is concerned with the installation modifications and calibration tests necessary to obtain meaningful data for transonic or supersonic turbine performance analysis at high pressure ratios. Initial calibration

tests using an impulse turbine with a stator, consisting of converging nozzle type blading, and a rotor with circular-arc profiles with sharp leading edges are described. Several instrumentation difficulties were experienced during the initial tests which required a number of modifications to the test installation. Tests are described which were carried out with the turbine after the different modifications of the Turbine Test Rig.

The author wishes to express his deep appreciation to Dr. M. H. Vavra for his guidance during the experimental work and for his help in the reporting of the study. Thanks are also given to Mr. J. E. Hammer for his generous assistance during the project.

## SECTION 2

## TURBINE DESCRIPTION

The turbine investigated is a single stage axial flow turbine of the impulse type which was designed for transonic rotor inlet velocities. The rotor has double circular-arc blade profiles with sharp leading edges and is one of three rotors presently available for the Transonic Turbine Test Rig, which hereafter is referred to as the TTR. The stator used during the present turbine tests has converging type nozzles. Also available is a stator with converging-diverging type nozzles for supersonic stator discharge velocities. The three rotors and the two stators are interchangable, and any stator-rotor combination can be tested with the TTR. Of the six available combinations only one was tested because of time considerations and the delays because of the TTR modifications. Figures 1, 2, and 3 are photographs of the stator and rotor of the turbine stage tested. Scale drawings of the mean radius blade profiles of this stator and rotor are shown in Figs. 4 and 5, respectively. Pertinent turbine dimensions are listed in Table I. The blading parameters indicated in Table I are at the mean radius of the stage.

Another rotor which can be run in the TTR has double circular-arc blade profiles with blunt leading edges. This type of rotor, which is shown in Fig. 6, could be used in high temperature applications where blade cooling is necessary. A third rotor, whose blade profiles are shown in Fig.

7, has blade profiles with gradually changing curvature. Figure 8 is a photograph of the blade profiles of the converging-diverging stator.

TABLE I

IMPULSE TURBINE DIMENSIONS

Converging Stator and Circular-Arc Rotor with Sharp Leading Edges

| ITEM | SYMBOL | STATOR | ROTOR |
|---|---|---|---|
| Number of Blades | Z | 31 | 60 |
| Blade Height (in) | h | 0.690 | 0.932 |
| Blade Width (in) | b | 0.975 | 0.750 |
| Hub Radius (in) | $R_h$ | 3.895 | 3.826 |
| Mean Radius (in) | $R_m$ | 4.240 | 4.292 |
| Tip Radius (in) | $R_t$ | 4.585 | 4.763 |
| Blade Spacing (in) | s | 0.8594 | 0.444 |
| Trailing Edge Thickness (in) | t | 0.024 | 0.020 |
| Throat Diameter (in) | a | 0.205 | 0.1313 |
| Throat Area ($in^2$) | $A_{th}$ | 4.385 | 7.348 |
| Axial Exit Area ($in^2$) | $A_{ax}$ | 18.382 | 25.134 |

## SECTION 3

## TEST INSTALLATION

The TTR installation and instrumentation has been described by Commons [2]. Therefore, the information presented here will be concerned with the salient features of the TTR only. However, modifications made to the TTR for the impulse turbine tests will be covered in more detail.

The working fluid for the TTR is air which is supplied by an Allis Chalmers VA 312 Compressor. As shown in Fig. 9, the supply air enters the turbine test cell through the inlet valve attached to tank 1 which is manually operated, and normally in the open position. The turbine inlet valve, which was originally a manually operated valve, was replaced by a remote controlled electrically operated butterfly valve. Both the turbine inlet valve and the exhauster inlet valve could then be operated simultaneously from the control room. This change reduces the time spent to set and maintain a desired pressure ratio if the TTR is operated with the exhauster.

A scale drawing of the cross-section of the TTR is shown in Fig. 10. Air enters the floating armature assembly radially from a plenum which is instrumented with total temperature and total pressure probes. Labyrinth seals, with 0.005 inch radial clearance between the armature assembly and the plenum, limit the leakage flow to about 7 per cent of the turbine flow rate. A conical screen is fitted in the armature assembly to reduce the possibility of

damage to the turbine by foreign objects. The air flows through the conical screen into the stator plenum which is instrumented with five fixed total pressure probes, one 3-hole survey probe, and two total temperature probes. In addition a so-called bullet probe is installed at the downstream end of the armature assembly, which measures total pressure and total temperature. The arrangement of these probes is shown in Fig. 11.

The closure plate assembly, also shown in Fig. 11, was completely redesigned for the impulse turbine tests. The moment on the closure plate was obtained from six equally spaced torque flexures. The flexures, which are 0.025 inch thick and extend radially from an inner support to an outer ring, are equipped with two strain gages. The strain gages are arranged to measure the bending moments on the flexures in the axial plane. The inner support is fastened to the closure plate force flexure. The force flexure consists of four webs of 0.080 inch thickness which are also instrumented with strain gages. These gages measure the bending moments applied to the flexure by the axial force acting on the closure plate. The signals from both sets of strain gages was read on a Daytronic model 700 strain gage digital indicator. Figure 12 is a photograph of the closure plate assembly which shows the force and torque flexures. The closure plate was calibrated on a specially built calibration rig by applying known forces and moments with various combinations of weights. The arrangement of the calibration rig is shown in Fig. 13. Figure 14 gives two views of the

closure plate assembly installed in the TTR.

Stator hub and tip static pressures are measured in the cavities between the stator assembly and the closure plate, and between the stator assembly and shroud, respectively. These static ports are shown in Fig. 11. The outer shroud is instrumented with seven static pressure taps, $P_{15}$ through $P_{21}$, spaced at 0.25 inch intervals from about the mid-rotor plane to the downstream end of the shroud. The last four static taps determine the shroud pressures needed in the momentum analysis of the inlet guide vanes.

There are seven shroud inserts available with different inside diameters. All inserts are cylindrical with the exception of two, one with a five degree slant and the other with a ten degree slant, for tapered rotor blade tips. Only the cylindrical shroud insert with an inside diameter of 9.546 inches was used in the present tests. The arrangement of the shroud, the shroud insert, and the seven static pressure taps is shown in Fig. 15.

Different radial tip clearances are obtained with a particular shroud insert by reducing the rotor diameter. The radial clearance used for the present tests was 0.010 inch.

The turbine rotor, shown in Fig. 11, is supported by two sets of precision ball bearings which are lubricated by oil mist. Two photographs of the rotor in the bearing stand are shown in Fig. 16. The axial clearance between the stator and rotor is varied by sliding the rotor bearing

assembly in the bearing stand. The minimum axial clearance is limited by the distance by which the closure plate extends beyond the trailing edges of the inlet guide vanes. Operating at 20,000 rpm and pressure ratios of 4 or more, the minimum axial clearance is about 0.1 inch.

The stator assembly, shown in Fig. 17, is supported by flexures which permit measuring of the reactions of the stator discharge flow by means of reluctance type force gages. One of the flexures was instrumented with strain gages for the final three runs of the impulse turbine. The results obtained with the strain gage and the reluctance capsule measurements are discussed in Section 8.

An air dynamometer capable of absorbing 200 HP at 20,000 rpm is used to measure the turbine torque. The torque is measured by a reluctance type force capsule which is attached to a 20 inch long lever arm that is fitted to the dynamometer housing. The force gage limits the angular rotation of the dynamometer housing to about 0.25 degree. Originally a so-called direct reading spring capsule, which turns by about 30 degrees at maximum torque, was used as a bearing housing for the dynamometer. At the small rotation of the dynamometer housing it was believed that the coil spring which serves as the measuring element of the capsule would not affect the readings of the reluctance gage. This assumption was proven false and it was necessary to remove the coil spring (Section 8). Similar to the rotor bearings, the dynamometer bearings are lubricated by oil mist.

All pressures are measured by mercury manometers except the pressure difference across the flow nozzle, which is read on a water U-tube manometer. All temperatures are measured with Iron-Constantan thermocouples using an ice bath as a reference. The hood temperature, to which reference is made in this study, was measured by a thermocouple located in the plastic casing of the stator torque capsule. This casing shields the thermocouple from the flow of air in the hood. The location of the thermocouple is shown in Fig. 17.

## SECTION 4

## FLOW NOZZLE CALIBRATION

The turbine flow nozzle installation and the calibration techniques used are described by Eckert [3]. Early tests by Eckert indicated that the nozzle discharge coefficient was a function of nozzle supply pressure. Further investigation by Naviaux at nozzle supply pressures of 20, 22, and 24 psia showed that the nozzle coefficient was a function of Reynolds number only [4]. The latter result was obtained with the equations used by Eckert and an expansion factor $Y_1$ for nozzles instead of sharp edge orifices in accordance with the ASME Power Test Codes [5].

Nozzle supply pressures for the turbine performance tests normally vary between 30 and 42 psia. Because of past experience with the calibration of the TTR flow nozzle it was decided to carry out additional tests at supply pressures of 24, 29, 34, 39, and 42 psia to verify the results which Naviaux obtained at lower pressures. The test data were reduced by using the IBM 360 Computer of the Naval Postgraduate School. The data reduction program was similar to that of Naviaux with the exception that the specific gravities of mercury and water in the manometer were corrected for the temperatures in the control room and that only the flange taps of the sharp edge orifice in the calibration pipe were used. The specific gravities of water and mercury as a function of temperature, and the standard conversion factors used for data reduction, were

obtained from the International Critical Tables [6]. The program description and the reduced data are given in Appendix I. In Fig. 18 the results of the nozzle calibration tests are plotted as a function of Reynolds number. Above a Reynolds number of $7(10^5)$ these results differ by less than 1 per cent from those found by Naviaux. Below a Reynolds number of $7(10^5)$ Naviaux's nozzle coefficient decreases sharply to a value of 1.002 at a Reynolds number of $4.2(10^5)$. The nozzle coefficients obtained from the present tests decrease less sharply below a Reynolds number of $7(10^5)$ resulting in differences of between 2 and 4 per cent at Reynolds numbers between $4.2(10^5)$ and $6(10^5)$. Since the present study was concerned with flows over a wider range of Reynolds numbers, considerably more data were taken at Reynolds numbers below $6(10^5)$.

An analytical expression for the nozzle discharge coefficient as a function of Reynolds number was obtained by using the method of least squares. This expression, which represents a fourth order polynomial approximation to the reduced data and is also plotted in Fig. 18, is

$$K_n = 9.32928\times10^{-1} + 4.268322\times10^{-7} R_e - 6.151495\times10^{-13} R_e^{\,2} + 3.895006\times10^{-19} R_e^{\,3} - 9.138062\times10^{-26} R_e^{\,4} \qquad (1)$$

where

$K_n$ = nozzle discharge coefficient

$R_e$ = Reynolds number referred to nozzle diameter

The maximum deviation between reduced data points and the analytical curve in the operating range of the impulse turbine between Reynolds numbers of $4(10^5)$ and $8(10^5)$ is 0.3 per cent.

## SECTION 5

## PLENUM LABYRINTH SEAL LEAK RATE

The method used for the plenum labyrinth seal leak tests and the associated instrumentation are described by Eckert [3]. Although the measuring techniques remained unchanged, the tests were carried out over a wider range of operating conditions.

The purpose of these tests was to find a simple analytical expression for the determination of the leak rate as a function of the pressure ratio across the labyrinth. This expression should cover the entire operating range of the TTR. To accomplish this goal two series of labyrinth leak tests were performed. The so-called hooded configuration of the TTR was used for both test series. Figure 9 represents a schematic of the installation of the TTR and shows the exhauster with the necessary piping for hooded operation. Labyrinth leak rates at pressure ratios between 1 and 6 were measured in both series of tests.

The first test series was performed before the impulse turbine was tested. From these tests a referred leak rate as a function of labyrinth pressure ratio was determined which was based on the actual labyrinth flow rate obtained from the square-edged orifice data for different conditions in the plenum. The referred leak rate ($in^2$) is

$$\Phi_L = \frac{\dot{W}_L}{P_{tp}\sqrt{T_{tp}\,\frac{R}{g}}} \qquad (2)$$

where

$\dot{W}_L$ = labyrinth flow rate (lbm/sec)

$P_{tp}$ = inlet plenum total pressure ($lb_f/in^2$)

$T_{tp}$ = inlet plenum total temperature ($^oR$)

R = gas constant for air ($ft\text{-}lb_f/lbm\text{-}^oR$)

g = gravitational constant ($lbm\text{-}ft/lb_f\text{-}sec^2$)

The results of the first series of labyrinth leak tests and the analytical expression derived from them are shown in Fig. 19. It can be seen that the labyrinth leak rate becomes choked at a pressure ratio of about 3. The referred labyrinth leak rate for the choked condition is equal to 0.073. This value corresponds to a flow rate between 0.06 lbm/sec and 0.1 lbm/sec, depending on inlet total conditions.

After the first twelve test runs of the impulse turbine, inconsistent values of turbine flow rates were noted. Analysis of these runs indicated that the inconsistency was probably due to errors in the labyrinth leak rate (Section 8). Re-evaluating the data from the first series of labyrinth leak tests, it was noticed that the hood temperature from run to run did not vary by more than $8^oF$ and remained practically constant during each run. However, during normal operation of the TTR with the turbine installed, the hood temperature is a function of the turbine discharge temperature and varies with turbine speed. Furthermore, the variation of hood temperature at different pressure ratios can be as much as $90^oF$. The difference in the range of hood temperatures during the first labyrinth tests and

during normal operations of the TTR made it necessary to perform a second series of leak tests. For this series a two inch pipe with a gate valve was connected from tank 1 to the TTR hood. Since the air temperature in tank 1 can be changed by about 100°F, it was possible to control the hood temperature.

Three tests were performed at hood temperatures of 59°F, 91°F and 116°F, each for the whole range of pressure ratios of the TTR. The results of these tests are given in Fig. 20, which shows the referred leak rate of Eq. (2) as a function of labyrinth pressure ratio. From this figure it is seen that the labyrinth leak rates depend on the hood temperature. Above a pressure ratio of 3 the referred leak rate varies by 12 per cent for a change in hood temperature of 57°F. Since this temperature can vary by 90°F during the turbine tests, an expression for the leak rate was empirically obtained which is independent of hood temperature and inlet plenum conditions. This expression is obtained by multiplying Eq. (2) with a correction factor which depends on the hood temperature and the inlet plenum total temperature. This so-called modified referred leak rate $\Phi_{LM}$ was found to be

$$\Phi_{LM} = \Phi_L \left[ 1 + 0.32 \left( \frac{t_{tp} - t_h}{t_{tp}} \right) \right]^{1.2} \qquad (3)$$

where

$\Phi_L$ = expression from Eq. (2)

$t_{t_p}$ = inlet plenum total temperature ($^{\circ}F$)

$t_h$ = hood temperature ($^{\circ}F$)

Figure 21 shows $\Phi_{LM}$ as a function of labyrinth pressure ratio from the tests at the three above-mentioned hood temperatures. An analytical expression for $\Phi_{LM}$ as a function of labyrinth pressure ratio was obtained from the method of least squares, by approximating the test data by a fifth order polynomial. The resulting expression is

$$\Phi_{LM} = -0.1004586 + 0.2122579r - 0.1081851r^2 + 0.0276576r^3 - 0.003489933r^4 + 0.0001726733r^5 \quad (4)$$

where

$r$ = labyrinth pressure ratio = $P_{t_p}/P_2$

$P_2$ = hood static pressure ($lb_f/in^2$)

Equation (4) is plotted in Fig. 21. The maximum deviation between the test data and the analytical curve is 4 per cent for the operating range ($1.0 < r \leq 4.0$) of the impulse turbine.

The IBM 360 Computer was used to reduce the data for both series of labyrinth leak tests. The computer program for the data reduction is presented in Appendix I together with the output for the second series of tests.

# SECTION 6

# ANALYSIS AND DATA REDUCTION

## 6.1 General

The TTR is instrumented to obtain data for a one-dimensional performance analysis of single stage axial turbines. It is assumed that steady axisymmetric flow conditions exist at the entrance and exit of the blade rows and that the flow on the mean stream surface is representative of the flow through the whole stage. The mean stream surface is assumed to exist at the mean radius $R_m$

$$R_m = \frac{R_t + R_h}{2} \tag{5}$$

where

$R_t$ = radius of stator blade tip (in)

$R_h$ = radius of stator blade hub (in)

The TTR data were analyzed on the IBM 360 Computer at the Naval Postgraduate School. The computer program is described in Appendix I, which give samples of print-outs for runs 32, 33 and 34.

## 6.2 Flow Rate Determination

The flow rate through the turbine is the difference of the flow rate through the flow nozzle and the labyrinth leak rate,

$$\dot{W} = \dot{W}_n - \dot{W}_L \tag{6}$$

where

$\dot{W}_n$ = nozzle flow rate (lbm/sec)

$\dot{W}_L$ = labyrinth leak rate (lbm/sec)

The nozzle flow rate is obtained from the nozzle flow equation given by Commons (Reference 2, p. 46). However, the nozzle discharge coefficient $K_n$ is determined from Eq. (1). Moreover, the constant in Commons' equation was found to be incorrect. The correct equation for the determination of $\dot{W}_n$ is

$$\dot{W}_n = 0.16384 D_n^2 \alpha_n K_n Y_1 \sqrt{\frac{P_{noz}\, h_w}{T_{noz}}} \tag{7}$$

where

$D_n$ = nozzle throat diameter (in)

$\alpha_n$ = coefficient of thermal expansion of the flow nozzle (dimensionless)

$K_n$ = nozzle discharge coefficient from Eq. (1) (dimensionless)

$Y_1$ = expansion factor (dimensionless)

$h_w$ = differential pressure across the pressure taps at 68° F (in $H_2O$)

$P_{noz}$ = absolute static pressure at upstream pressure tap ($lb/in^2$)

$T_{noz}$ = temperature at upstream pressure tap (°R)

The leakage flow rate through the plenum labyrinths is obtained from

$$\dot{W}_L = \frac{\Phi_{LM}\, P_{tp}}{\sqrt{T_{tp} R/g}\left[1 + 0.32\left(\frac{T_{tp} - T_n}{T_{tp}}\right)\right]^{1.2}} \tag{8}$$

where $\Phi_{LM}$ is the modified referred labyrinth leak rate obtained from Eq. (4)

## 6.3 Stator Entrance Properties

The total pressure $P_{to}$ at the stator entrance is taken as the average of the data obtained with the five fixed total pressure probes. A radial survey with the 3-hole flow probe at this location indicated a maximum variation of 0.75 per cent in total pressure from stator hub to stator tip. The results of this pressure survey are presented in Fig. 22. The total temperature $T_{to}$ is obtained from two Temperature-Kiel probes.

## 6.4 Stator Discharge Properties

The stator discharge properties can be obtained from the momentum and moment of momentum equations applied to the fluid in the stator assembly. These two fundamental equations yield the axial and peripheral velocities from which the other discharge properties can be derived. In addition, the axial velocity component can be obtained also from the equation of continuity applied to the stator exit. The equations used in the stator analysis are presented here without derivation, since they are given by Messegee [7]. From the theorem of angular mementum

$$V_{ul} = 12(M_s + M_{cl})g/\dot{N} R_{ml} \qquad (9)$$

where

$V_{ul}$ = peripheral component of absolute velocity at stator exit (ft/sec)

$M_s$ = moment acting on stator assembly, measured by a reluctance gage ($ft\text{-}lb_f$)

$M_{cl}$ = moment acting on closure plate ($ft\text{-}lb_f$)

$R_{ml}$ = mean radius at stator discharge (in)

The two values of the average axial velocity component obtained from the momentum and continuity equations are used to establish a parabolic change of the pressure at the stator discharge between the measured pressures at hub and tip such that both methods yield the same results. These calculations are carried out by an iteration procedure of the computer program. However, the resulting pressure distribution cannot be verified experimentally. The stator exit pressure distribution is first assumed to be linear between the stator hub and tip pressures. From the momentum equation

$$V_{al} = g/\dot{W}\left[F_s + F_{cl} - F_o - 2\pi \int_{R_{hl}}^{R_{tl}} P_l r dr\right] \qquad (10)$$

where

$V_{al}$ = axial velocity component at stator discharge (ft/sec)

$F_s$ = force acting on stator assembly, measured by reluctance gage ($lb_f$)

$F_{cl}$ = force acting on stator assembly by closure plate, measured by strain gages ($lb_f$)

$F_o$ = sum of pressure forces acting on stator assembly less force due to the stator discharge pressure ($lb_f$)

$P_1$ = static pressure at radius r at stator exit ($lb_f/in^2$)

The last term of Eq. (10) is then evaluated by assuming that $P_1$ varies parabolically from hub to tip. A factor $\epsilon$ is introduced so that the shape of the parabola can be changed to satisfy continuity considerations. From the derivation presented in Appendix II

$$2\pi \int_{R_{hl}}^{R_{tl}} P_1 r\,dr = \frac{\pi}{3} P_{hl}\left[(1+\epsilon)R_{tl}^2 + R_{tl}R_{hl} - (2+\epsilon)R_{hl}^2\right] + \frac{\pi}{3} P_{tl}\left[(2+\epsilon)R_{tl}^2 - R_{tl}R_{hl} - (1+\epsilon)R_{hl}^2\right] \tag{11}$$

where

$P_{hl}$ = hub static pressure at stator discharge ($lb_f/in$)

$P_{tl}$ = tip static pressure at stator discharge ($lb_f/in$)

The integral of Eq. (10) can be represented by an average stator discharge pressure $P_{lav}$, multiplied by the stator exit axial area. Using Eq. (11),

$$P_{lav} = \frac{P_{hl}}{3}\left[\frac{(1+\epsilon)R_{tl}^2 + R_{tl}R_{hl} - (2+\epsilon)R_{hl}^2}{R_{tl}^2 - R_{hl}^2}\right] + \frac{P_{tl}}{3}\left[\frac{(2+\epsilon)R_{tl}^2 - R_{tl}R_{hl} - (1+\epsilon)R_{hl}^2}{R_{tl}^2 - R_{hl}^2}\right] \tag{12}$$

From the continuity equation

$$V_{al} = \left[ C \left[ T_{to} - \frac{CA_1^2 P_{1av}^2}{R^2 \dot{W}^2} \left( -1 + \left( 1 - \frac{4\dot{W}^2 R^2}{CA_1^2 P_{1av}^2} \left( \frac{V_{ul}^2}{C} - T_{to} \right) \right)^{\frac{1}{2}} \right) \right] - V_{ul}^2 \right]^{\frac{1}{2}} \quad (13)$$

where

$A_1$ = effective axial flow area at stator exit ($in^2$)

$C$ = conversion factor, $2gJc_p$ ($ft^2/sec^2 - {}^oR$)

$c_p$ = specific heat at constant pressure (BTU/lbm-$^oR$)

The axial velocity component obtained from Eqs. (10) and (13) varies directly with the stator discharge pressure. Since this pressure is a function of the factor $\epsilon$, an increase or decrease in $\epsilon$ will increase or decrease the axial velocity, respectively. The solutions of these equations are matched by varying $\epsilon$ until the velocity calculated with Eq. (10) equals the velocity calculated from Eq. (13). This iteration is possible because the value of Eq. (10) changes more rapidly for a change in $\epsilon$ than the value of Eq. (13). The absolute velocity at the stator exit is then

$$V_1 = \left[ V_{al}^2 + V_{ul}^2 \right]^{\frac{1}{2}} \quad (14)$$

The static temperature $T_1$ at the stator exit is found from the energy equation, or

$$T_1 = T_{to} - \frac{V_1^2}{2gJc_p} \quad (15)$$

From Fig. 23, which represents a velocity diagram of a turbine stage, it can be seen that the angle of the absolute flow at the stator discharge is

$$\alpha_1 = \text{Tan}^{-1} (V_{ul}/V_{al}) \tag{16}$$

Further, the relative velocity $W_1$ at the rotor inlet has an axial component

$$W_{al} = V_{al} \tag{17}$$

and a peripheral component

$$W_{ul} = V_{ul} - U_1 \tag{18}$$

where, with N representing the rotor speed in rpm,

$$U_1 = \frac{N\pi R_{m1}}{360} \tag{19}$$

Thus, the relative velocity is

$$W_1 = [W_{al}^2 + W_{ul}^2]^{\frac{1}{2}} \tag{20}$$

The angle of the relative flow at the rotor inlet is

$$\beta_1 = \text{Tan}^{-1} (W_{ul}/W_{al}) \tag{21}$$

The speed of sound of the air at the stator exit is

$$a_1 = [\gamma g R T_1]^{\frac{1}{2}} \tag{22}$$

where $\gamma$ is the ratio of the specific heats of the working fluid. The absolute and relative Mach numbers of the flow

at the stator discharge are

$$M_1 = V_1/a_1 \tag{23}$$

$$M_{R1} = W_1/a_1 \tag{24}$$

In accordance with Fig. 24, the stator loss coefficient $\zeta_s$ is defined as

$$\zeta_s = \frac{(T_1 - T_{1is})}{\Delta T_{1is}} = \frac{(T_1 - T_{1is})}{(T_{to} - T_{1is})} \tag{25}$$

where

$$T_{1is} = T_{to}\left(\frac{P_{1av}}{P_{to}}\right)^{\frac{\gamma-1}{\gamma}} \tag{26}$$

Also, from Fig. 24,

$$\zeta_s = 1 - \frac{V_1^2}{V_{1th}^2} \tag{27}$$

where

$$V_{1th}^2 = 2gJc_p\,(T_{to} - T_{1is}) \tag{28}$$

The stator efficiency is

$$\eta_s = 1 - \zeta_s \tag{29}$$

The so-called flow function $\Phi$ is given by Vavra (Reference 8, Pt. I, p. C24) as

$$\Phi = \frac{\dot{W}}{A_{th}P_{to}}\left[T_{to}\,R/g\right]^{\frac{1}{2}} \tag{30}$$

where $A_{th}$ = stator throat area given in Table I ($in^2$).
For isentropic conditions the flow function $\Phi_{is}$ is obtained from

$$\Phi_{is} = \left[\frac{2\gamma}{\gamma-1}\left[\left(\frac{P_{th}}{P_{to}}\right)^{2/\gamma} - \left(\frac{P_{th}}{P_{to}}\right)^{\frac{\gamma+1}{\gamma}}\right]\right]^{\frac{1}{2}} \tag{31}$$

where $P_{th}$ = stator throat static pressure ($lb_f/in^2$).
The stator throat pressure is assumed to equal $P_{lav}$ until the flow through the stator becomes choked. For choked conditions the pressure ratio $P_{th}/P_{to}$ in Eq. (31) is taken as the critical pressure ratio, which for air is equal to 0.5283. A stator blockage factor can now be defined by

$$\xi = \Phi / \Phi_{is} \tag{32}$$

Therefore, $\xi$ represents that percentage of throat area which would be necessary to pass the flow if the expansion process through the stator were frictionless.

## 6.5 Rotor Discharge Properties

The rotor discharge properties are obtained by the application of the moment of momentum equation, the continuity equation, and the energy equation to the fluid passing through the rotor. The flow in the rotor will be treated with respect to a relative coordinate system. In this manner the fundamental laws, applied to the rotating row of blades, will yield discharge properties analogous to those obtained for the stator.

From the moment of momentum equation the peripheral component of the absolute discharge velocity is

$$V_{u2} = \frac{R_{m1}}{R_{m2}} V_{u1} - \frac{12 M_D g}{R_{m2} \dot{W}} \tag{33}$$

where

$M_D$ = moment acting on the dynamometer measured by a reluctance gage (ft-$lb_f$)

$R_{m2}$ = mean radius at rotor discharge (in)

The peripheral component of the relative velocity is

$$W_{u2} = V_{u2} - U_2 \tag{34}$$

with

$$U_2 = U_1 \frac{R_{m2}}{R_{m1}} \tag{35}$$

Introducing the so-called equivalent temperature $T_E$ as defined by Vavra (Reference 8, Pt. III, p. G4), the energy equation for relative flows becomes

$$T_E = T_1 + \frac{W_1^2}{2gJc_p} + \frac{U_2^2 - U_1^2}{2gJc_p} = T_2 + \frac{W_2^2}{2gJc_p} \tag{36}$$

Using the energy equation in this form with the continuity equation, the static temperature at the rotor discharge is found as

$$T_2 = \frac{\gamma}{\gamma - 1} \frac{P_2^2 A_2^2 g}{\dot{W}^2 R} \left[ \left[ 1 - \frac{2}{g} \left( \frac{\gamma - 1}{\gamma} \right) \frac{\dot{W}^2 R}{P_2^2 A_2^2} \left( \frac{W_{u2}^2}{2gJc_p} - T_E \right) \right]^{\frac{1}{2}} - 1 \right] \tag{37}$$

where

$P_2$ = hood static pressure ($lb_f/in^2$)

$A_2$ = effective axial flow area at rotor discharge ($in^2$)

From Fig. 24, the total temperature at the rotor discharge is

$$T_{t2} = T_{to} - \Delta T_W \tag{38}$$

The temperature drop $\Delta T_W$ is proportional to the work generated by the turbine stage or

$$\Delta T_W = \frac{M_D(\omega)}{\dot{W} c_p J} \tag{39}$$

where

$\omega$ = rotational speed of rotor (rad/sec).

From Euler's turbine equation, $\Delta T_W$ is also

$$\Delta T_W = \frac{U_1 V_{u1} - U_2 V_{u2}}{g J c_p} \tag{40}$$

In accordance with Fig. 24, the absolute and relative velocities at the rotor discharge are

$$V_2 = \left[(T_{t2} - T_2) 2 g J c_p\right]^{\frac{1}{2}} \tag{41}$$

$$W_2 = \left[(T_E - T_2) 2 g J c_p\right]^{\frac{1}{2}} \tag{42}$$

The axial velocity components of $V_2$ and $W_2$ are

$$V_{a2} = W_{a2} = \left[V_2^2 - V_{u2}^2\right]^{\frac{1}{2}} \tag{43}$$

From Fig. 23, the angles of the absolute and relative velocities at the rotor discharge are

$$\alpha_2 = \text{Tan}^{-1} \left(V_{u2}/V_{a2}\right) \tag{44}$$

$$\beta_2 = \text{Tan}^{-1} \left(W_{u2}/W_{a2}\right) \tag{45}$$

With the equivalent temperature of Eq. (12), the rotor loss coefficient is obtained from

$$\zeta_R = \frac{T_2 - T_{2is}}{T_E - T_{2is}} \tag{46}$$

with

$$T_{2is} = T_E\left(\frac{P_2}{P_{El}}\right)^{\frac{\gamma-1}{\gamma}} = T_1\left(\frac{P_2}{P_{1av}}\right)^{\frac{\gamma-1}{\gamma}} \tag{47}$$

where

$P_{El}$ = total equivalent pressure at the stator discharge ($lb_f/in^2$). From Fig. 24, the rotor loss coefficient of Eq. (46) is also

$$\zeta_R = 1 - \frac{W_2^2}{W_{2th}^2} \tag{48}$$

where

$$W_{2th}^2 = 2gJ_{cp}(T_1 - T_{2is}) + W_1^2 + U_2^2 - U_1^2 = 2gJc_p(T_E - T_{2is}) \tag{49}$$

The rotor efficiency is

$$\eta_R = 1 - \zeta_R \tag{50}$$

## 6.6 Performance Parameters

For the evaluating of the overall performance of a turbine stage it is advantageous to use dimensionless coefficients. The performance parameters presented in this section are those given by Vavra [9].

The overall stage efficiency is the ratio of the work generated by the turbine stage and the isentropic enthalpy drop across the turbine from the total conditions at the stator inlet to the static conditions at the rotor discharge. Therefore, the so-called total-static efficiency is obtained from

$$\eta = \frac{\Delta T_W}{\Delta T_{is}} = \frac{\frac{M_D \omega}{\dot{W} c_p J}}{\Delta T_{is}} \tag{51}$$

where, as shown by Fig. 24,

$$\Delta T_{is} = T_{to}\left[1 - \left(\frac{P_2}{P_{to}}\right)^{\frac{\gamma-1}{\gamma}}\right] \tag{52}$$

$\Delta T_{is}$ can be expressed also by

$$\Delta T_{is} = \frac{C_o^2}{2gJc_p} \tag{53}$$

where $C_o$ is the theoretical velocity obtained by an isentropic expansion from $P_{to}$ to $P_2$.

The theoretical degree of reaction r* is that fraction of the isentropic enthalpy drop of the turbine stage which is used up by the rotating row of blades. It is a measure

for the acceleration of the relative flow in the rotor. From Fig. 24

$$r^* = 1 - \frac{V_{1th}^2}{C_o^2} \tag{54}$$

Using Eqs. (26), (28), (52) and (53) the degree of reaction at the hub or the tip of the blading can be expressed by

$$r^* = \frac{\left(\frac{P'}{P_2}\right)^{\frac{\gamma-1}{\gamma}} - 1}{\left(\frac{P_{to}}{P_2}\right)^{\frac{\gamma-1}{\gamma}} - 1} \tag{55}$$

where $P' = P_{h1}$ or $P_{t1}$ ($lb_f/in^2$).

The isentropic head coefficient $K_{is}$ is used to estimate the number of stages necessary to handle a given isentropic enthalpy drop at a given speed $U_1$. It is defined as

$$K_{is} = \left(\frac{C_o}{U_1}\right)^2 \tag{56}$$

The work coefficient K is a measure of the actual work that the stage generates per unit mass of fluid at a given speed $U_1$, or

$$K = \frac{\Delta T_w}{U_1^2/2gJc_p} \tag{57}$$

The peripheral speed $U_1$ was selected to make $K_{is}$ and K dimensionless since it is usually a fixed quantity determined by rotor stress considerations.

Referred values of flow rate, rotational speed, dynamometer moment, and horsepower are obtained by using the NASA reference system. They are defined by

$$W_{REF} = \frac{\dot{W}\sqrt{\theta}}{\delta} \tag{58}$$

$$N_{REF} = N/\sqrt{\theta} \tag{59}$$

$$M_{DREF} = M_D/\delta \tag{60}$$

$$HP_{REF} = \frac{HP}{\delta\sqrt{\theta}} = \frac{M_D\,\omega}{550\,\delta\sqrt{\theta}} \tag{61}$$

with

$$\theta = T_{to}/518.4 \tag{62}$$

$$\delta = P_{to}/14.7 \tag{63}$$

## SECTION 7

## DESCRIPTION OF TURBINE TESTS

During the present study the TTR was operated for 191 hours, 84 of which were used for calibration tests with the impulse turbine installed. The initial tests consisted of the runs conducted before the second series of labyrinth leak tests, and the final tests consisted of three turbine test runs that followed these labyrinth tests.

During the first run of the impulse turbine foreign object damage to the circular-arc rotor blading was encountered. The damaged rotor, however, could be saved by cutting back the leading edge of the blade row by 0.125 inch and shaping each blade as shown in Fig. 6. Another circular-arc rotor with sharp leading edges was installed, and the tests were resumed.

The next five runs were carried out without the exhauster system at a pressure ratio of 2.0 and different axial clearance $\triangle X$ between the stator and the rotor. The turbine was tested at $\triangle X$ equal to 0.200, 0.250, 0.265, 0.300 and 0.350 inch. As stated in Section 3 the radial rotor tip clearance was 0.010 inch for all runs. Data were taken at rotor speeds between 14,000 and 20,000 rpm, where the lower speed was imposed by the maximum torque absorption of the dynamometer.

After the optimum clearance $\triangle X$ was determined, the exhauster was installed for so-called hooded operation of the TTR. Tests were conducted at turbine pressure ratios

of 1.5, 2.0, 2.5, 3.0, 3.5, and 4.0 at speeds up to 20,000 rpm. Several runs were conducted at pressure ratios of 2.0 and 3.0 to insure that consistent results could be obtained. The minimum speed possible with the presently installed dynamometer varies with pressure ratio. The minimum speeds for the above-listed pressure ratios were 9,000; 11,000; 12,500; 14,000; 15,000 and 16,900 rpm, respectively.

A particular turbine pressure ratio can be set by different combinations of stator inlet pressure and hood pressure. However, to adopt a standard procedure, the stator inlet pressure was kept at 5 inches of mercury above the atmosphere, and the pressure in the exhauster was varied to obtain the desired pressure ratio up to a value of about 2.7. For higher pressure ratios the maximum vacuum of about 17 in. Hg was maintained and the stator inlet pressure was increased.

From the initial test results, discrepancies were found in the turbine flow rates and the loss coefficients of stator and rotor. As discussed in Section 8, the second series of labyrinth leak tests was then undertaken to investigate the leakage flow problem. The unrealistic loss coefficients could be attributed to inaccurate measurement of the torque which is exserted on the stator assembly. Inaccurate stator hub and tip static pressures were thought to be a secondary cause for this discrepancy.

For the final three runs the reluctance type force capsule used for measuring the stator torque was disconnected

and one of the horizontal torque flexure shown in Fig. 17 was instrumented with strain gages to measure the torque of the stator assembly. Additionally the static taps for the measuring of the hub and tip pressures at the stator discharge were modified and static taps were arranged to determine the pressures at the hub and tip radius of the stator throat section as shown in Fig. 15.

The final tests were conducted with the hooded configuration of the TTR. For two of the three runs data were recorded at various speeds between the minimum possible and 20,000 rpm at pressure ratios of 2.0 and 2.5. The third run was carried out at a fixed speed of 13,080 rpm and a constant pressure ratio of 2.5. For this run the stator inlet total temperature was varied between 135° and 165° F. Appendix I lists the raw data that were recorded for each run.

## SECTION 8

## RESULTS AND DISCUSSION OF TURBINE TESTS

Figure 25 gives the measured total-static turbine efficiencies as a function of the referred speed at different values of the axial clearance $\Delta X$. It is seen that the maximum efficiency of 83.0 per cent was obtained for an axial clearance of 0.250 inch.

Increasing $\Delta X$ to 0.265 and 0.30 inch produced optimum efficiencies of 82.2 per cent and 82.8 per cent, respectively, indicating that the values obtained for $\Delta X = 0.265$ inch might be doubtful. At a reduced axial clearance of 0.20 inch the optimum efficiency is about 82.2 per cent, equal to that obtained for $\Delta X = 0.35$ inch.

The efficiency, as defined by Eq. (51), depends on the dynamometer torque $M_D$ and the mass flow rate $\dot{W}$, for given values of turbine pressure ratio $P_{to}/P_2$, inlet total temperature $T_{to}$, and rotational speed N. The influence of dynamometer torque can be seen by the plot of referred dynamometer moment against referred rotor speed of Fig. 26. Figure 26 shows these data for values of $\Delta X$ of 0.250, 0.265 and 0.300 inch. The graph shows that the values of referred dynamometer moment at $\Delta X = 0.250$ inch and $\Delta X = 0.300$ inch lie on the same curve, whereas the data for $\Delta X = 0.265$ inch form a curve that is parallel to but below the curve for the other clearances. Therefore, it can be concluded that the low efficiency obtained with $\Delta X = 0.265$ inch was due to low values of measured

dynamometer torque. During the tests the dynamometer seemed to be functioning normally, and no reason could be found to explain the lower readings. However, during the next several runs it was noticed that the dynamometer readings would sometimes fluctuate by 10 or more counts as the temperature of the dynamometer housing increased. It was found that the fluctuations were due to expansion and contraction with temperature of the coil spring that was located inside the capsule which served as the bearing housing of the dynamometer. After removing this spring consistent values of dynamometer torque were obtained. The results of the runs with the hood attached with $\Delta X = 0.250$ inch indicated that there were inconsistencies in the data necessary for the calculation of the efficiencies and the stator and rotor loss coefficients. These discrepancies will be discussed by comparing the data of runs 21, 23 and 24 carried out with the hood, with the data obtained from run 20 where the turbine discharged into the atmosphere. Runs 20 and 21 were carried out at a pressure ratio of 2.0, and runs 23 and 24 at a pressure ratio of 3.0.

The efficiency as a function of head coefficient $K_{is}$ for the four runs is shown in Fig. 27. It can be noted that the efficiency was different for the runs at equal pressure ratios. Moreover, the maximum efficiency was obtained at a value of $K_{is}$ of about 3.7 for runs 20, 21, and 23 whereas for run 24 the maximum efficiency occurred at $K_{is} = 4.3$.

Figure 28 shows the referred dynamometer moment as a function of referred speed. It is evident from this graph that the difference in efficiencies at a pressure ratio of 3.0 was due to the higher values of the referred dynamometer moment obtained during run 24. The non-linear shape of the referred moment curve accounts for the different value of $K_{is}$ at which the maximum efficiency for run 24 was obtained.

During later runs it was noticed that fluctuations occurred in the dynamometer moment readings. Examination of the reluctance gage showed that a lead from a cannon plug to the gage had broken within the insulation. This faulty lead may have affected the dynamometer readings during run 24.

The referred moments for runs 20 and 21 plotted against referred speed lie on the same curve. Equal referred moments for a given referred speed and pressure ratio indicate that the difference in efficiency must be due to differences in mass flow rates. Since it was believed that errors in turbine flow rate were due to wrong values of labyrinth leakage, the second series of labyrinth leak tests was undertaken as discussed in Section 5. As stated earlier it was found from these tests that the labyrinth leak rate is a function of hood temperature. However, the new labyrinth leak rates used for the reduction of the data from runs 20 and 21 did not account for the difference in efficiency of 1.7 per cent since the variation in hood temperature between the two runs was only $12^{\circ}F$. Without

further testing it is not possible to explain the differences in the efficiencies of Fig. 26.

Equation (25), (27), (46) and (48) show that the stator and rotor loss coefficients depend on the discharge properties after the rows of blades and can be obtained from the calculated velocities. These velocities are obtained with the methods explained in Section 6. The peripheral component of the absolute velocity after the stator is determined primarily from the stator torque measurements. It is about 3 to 4 times larger than the axial velocity component. Thus a variation in peripheral velocity influences the losses more than an equal percentage variation in axial velocity. Figure 29 shows the stator torque reading as a function of speed for runs 20, 21, 23, 24 and 25. All the runs clearly indicate a decrease of the order of 15 per cent in the stator moment as the speed is increased from the minimum rotor speed to 20,000 rpm. It can be shown that a 3.5 per cent variation in the stator moment will change the rotor loss coefficient by about 0.10, hence it can be concluded that the measured stator moments are responsible for the inconsistent values of the losses. Therefore, it was decided to monitor the read-out of the stator torque capsule during the second series of labyrinth leak tests to determine if a change in hood temperature would influence its reading. Since a closure plate was placed over the stator discharge during these tests, any variation of the stator torque capsule reading from its calibration setting had to occur because of different

thermal expansion of the capsule and the frame to which the capsule is attached. Figure 30 is a plot of the torque capsule readings for different hood temperatures. The latter are given in millivolts above the electrical read-out of the instrument at the calibration temperature. The calibration temperature, which changed for each run, was the hood temperature at which the capsule was set to zero. Figure 30 shows that the read-outs of the stator torque capsule are strongly affected by the hood temperature. The read-outs varied by 10 to 15 per cent of full scale read-out over a $56^{\circ}F$ temperature range. To separate the overall losses into stator and rotor losses with a sufficient degree of accuracy, the variation of the stator torque must be less than 2.5 per cent of full scale read-out. The axial stator force, which was monitored also during these tests, varied by less than 1 per cent of full scale read-out in the same temperature range. Since both reluctance capsules are identical except for their operating range, it was concluded that the large variation in the stator torque capsule read-out was due to the thermal expansion of the frame to which the capsule is fastened. This conclusion is supported by Fig. 17 since the U-shaped frame to which the capsule is attached is made of aluminum whose coefficient of thermal expansion is at least twice that of the capsule and its attachment rods.

For the final series of tests one of the horizontal torque flexures shown in Fig. 17 was instrumented with strain gages to measure the stator torque, and the

reluctance torque capsule was removed. Additionally, as shown in Fig. 15, the outer diameter of the closure plate rim was reduced by about 0.030 inch to avoid impingement of flow on the rim which could falsify the readings of the static hub pressure. This modification was necessary since the closure plate assembly could not be centered perfectly with the stator assembly. Moreover, as shown in Fig. 15, a cylindrical shim was placed behind the upstream end of the shroud insert which blocked the upper portion of the stator tip static port, reducing its radial width from 0.069 inch to about 0.025 inch, to ensure a more accurate measurement of the stator tip pressure. From Eq. (10) it is evident that correct measurements of the hub and tip pressures are necessary to obtain accurate values of the axial velocity component after the stator.

Results of tests indicated that the readings obtained by the strain gages attached to the torque flexure were influenced by the hood temperature also. Figure 31 shows the stator and rotor loss coefficients obtained from the data of a run at a constant rotor speed and constant pressure ratio. In Fig. 31 these loss coefficients are shown as functions of the measured hood temperature. It is seen that reasonable values of the loss coefficients were obtained only if the hood temperature did not differ by more than about $2^{\circ}F$ from the temperature at which the torque flexure strain gages were calibrated. During this test it was noticed also that the temperature difference along the flexure was about $70^{\circ}F$, which made it impossible

to compensate the strain gage circuit for temperature. Thus it can be concluded that accurate measurements of the stator moment are not possible with the torque flexure or the reluctance capsule as presently installed in the TTR. However, it is felt that accurate measurements can be obtained with the reluctance capsule if it is relocated as recommended in Section 9.

The change in the axial velocity due to the modifications to the stator hub and tip static pressure ports was negligible. It was found that the tip pressure decreased by about 2 per cent and that the hub pressure remained unchanged from values recorded for similar runs during earlier turbine tests.

As stated in Section 7 the stator throat was instrumented with static pressure taps at the hub and tip radii. The throat hub static pressure was found to be the same as the hub pressure measured in the gap between the closure plate and the stator hub. Whether this condition truly occurs or whether it occurs because of a leak in the measuring line can be verified only by additional tests. The throat tip pressures measured at an overall turbine pressure ratio of 2.5 were 15 per cent higher than the theoretical pressure for choked conditions. The theoretical critical pressure ratio for air is 1.89 and that obtained from the measured stator throat tip pressure was 1.60. This indicates that either the flow is not choked at the tip at a overall turbine pressure ratio of 2.5 or that

the pressure tap is located upstream of the actual stator throat. Tests at higher pressure ratios would show whether the last-mentioned condition exists.

## SECTION 9

## RECOMMENDATIONS

The rotor and stator losses cannot be separated accurately with the present instrumentation of the TTR because of the difficulties associated with the measurement of the moments that act on the stator assembly. It is felt, however, that accurate measurements of the stator torque are possible if the force capsule is arranged near the back strut of the cradle that supports the stator.

The capsule should be mounted vertically with one end connected to an arm attached to the cylindrical inlet pipe and the other end to a steel frame which is bolted to the cradle. Using steel for the frame reduces the differential thermal expansion of the frame and the capsule. To reduce temperature effects further, an enclosure should be built around the frame and the capsule into which a small amount of ambient air would be blown from the atmosphere to keep the capsule and frame at constant temperature. A similar arrangement has been successful in reducing the temperature effects on the dynamometer force capsule (Reference 2, p.33).

Further tests should be carried out at a number of turbine pressure ratios between 2.0 and 4.0 to determine whether accurate measurements of static pressure can be obtained from the stator throat hub and tip taps as presently installed, or whether these taps need to be relocated. It is suspected that the static pressure line to the stator

throat hub tap has become disconnected in the cavity between the closure plate assembly and the stator hub. This possibility should be investigated before further tests are carried out.



FIGURE 1

BLADE PROFILES
CIRCULAR – ARC ROTOR
CONVERGING STATOR

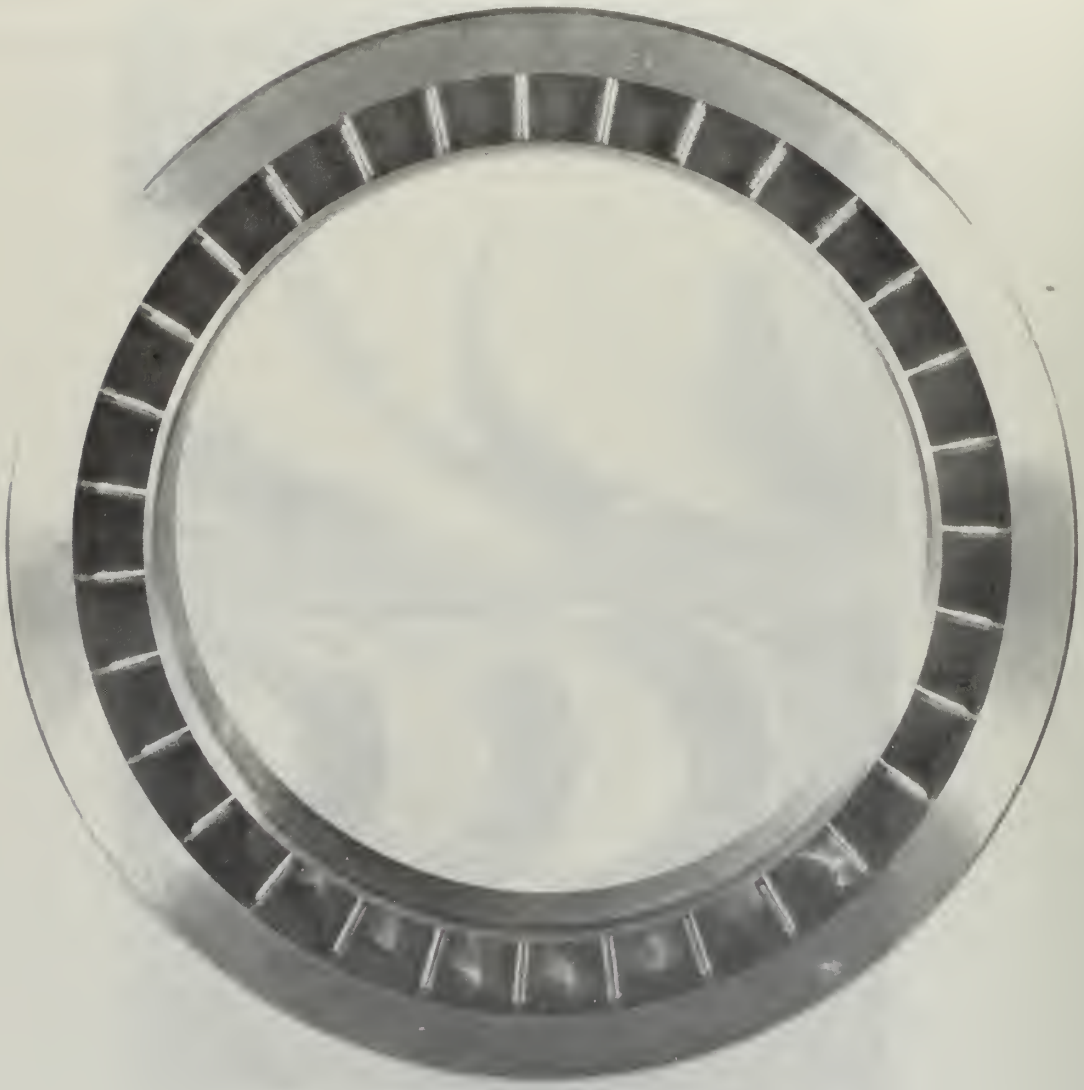


FIGURE 2

CONVERGING STATOR
(VIEW SHOWING STATOR ENTRANCE)



FIGURE 3

CIRCULAR-ARC ROTOR
(VIEW SHOWING ROTOR ENTRANCE)

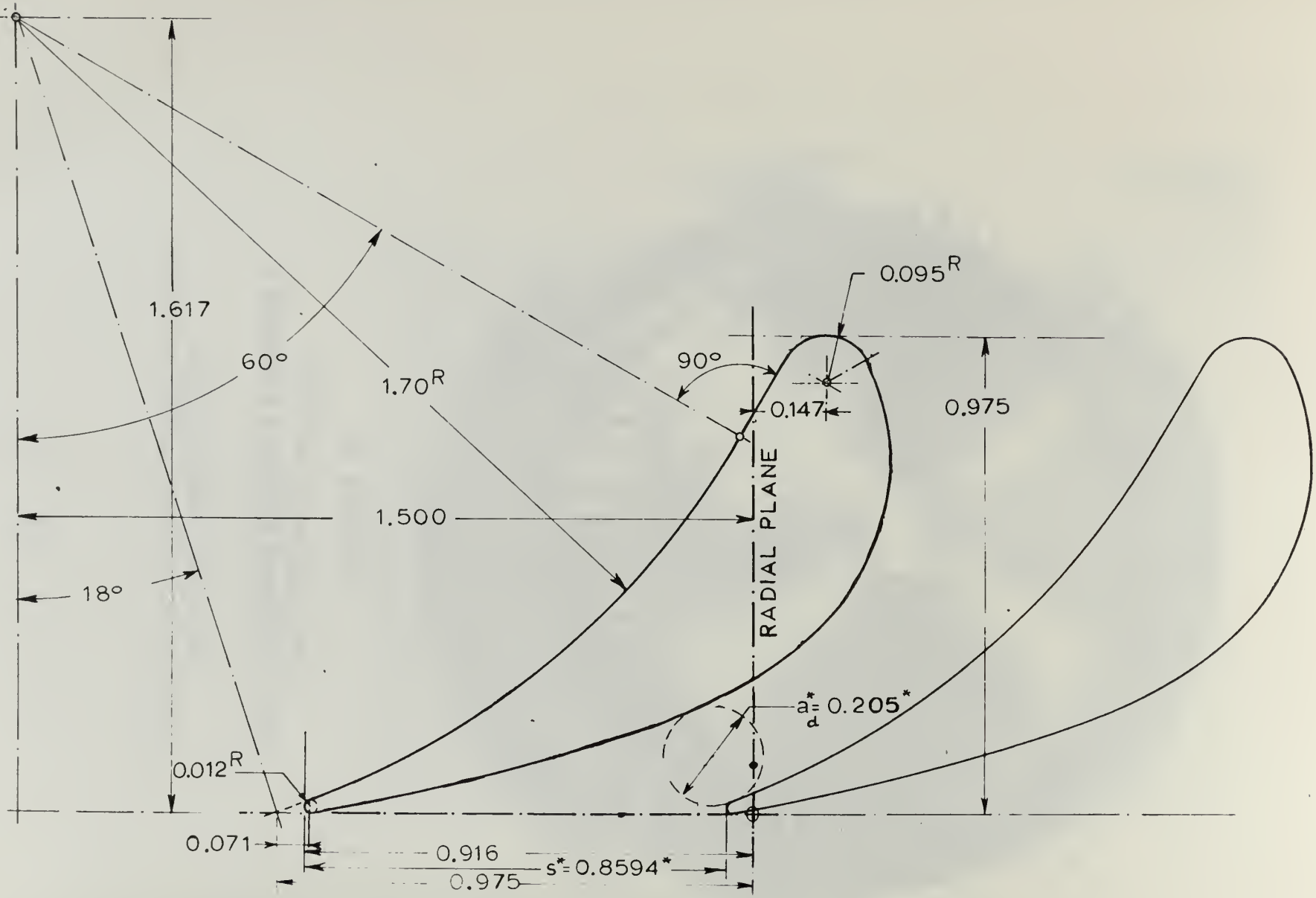



FIGURE 4

MEAN RADIUS BLADE PROFILE

CONVERGING STATOR

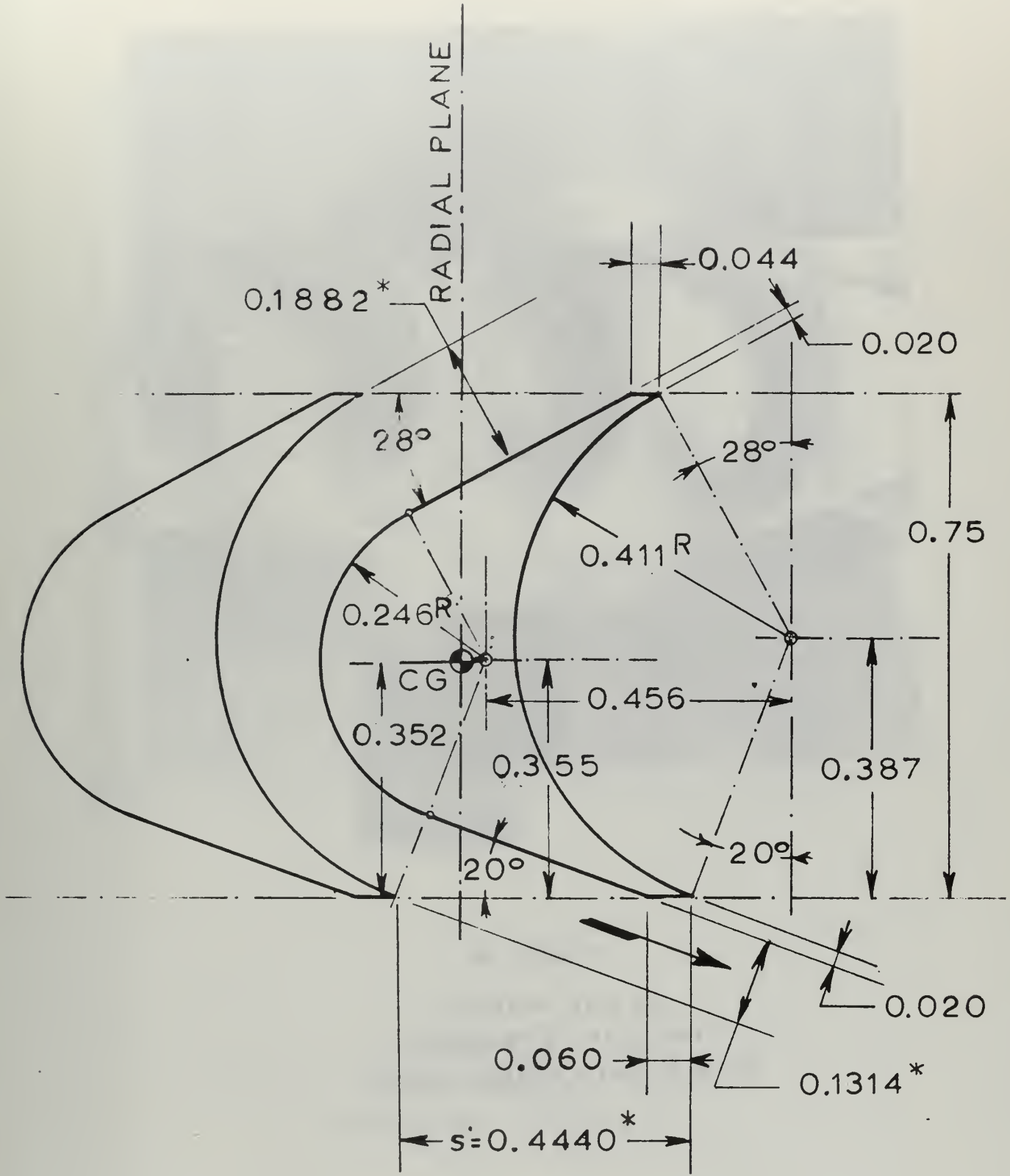



FIGURE 5

MEAN RADIUS BLADE PROFILE

CIRCULAR-ARC ROTOR WITH SHARP LEADING EDGES



FIGURE 6

BLADE PROFILE
CIRCULAR-ARC ROTOR
WITH BLUNT LEADING EDGES



FIGURE 7

BLADE PROFILE
CONTOURED ROTOR

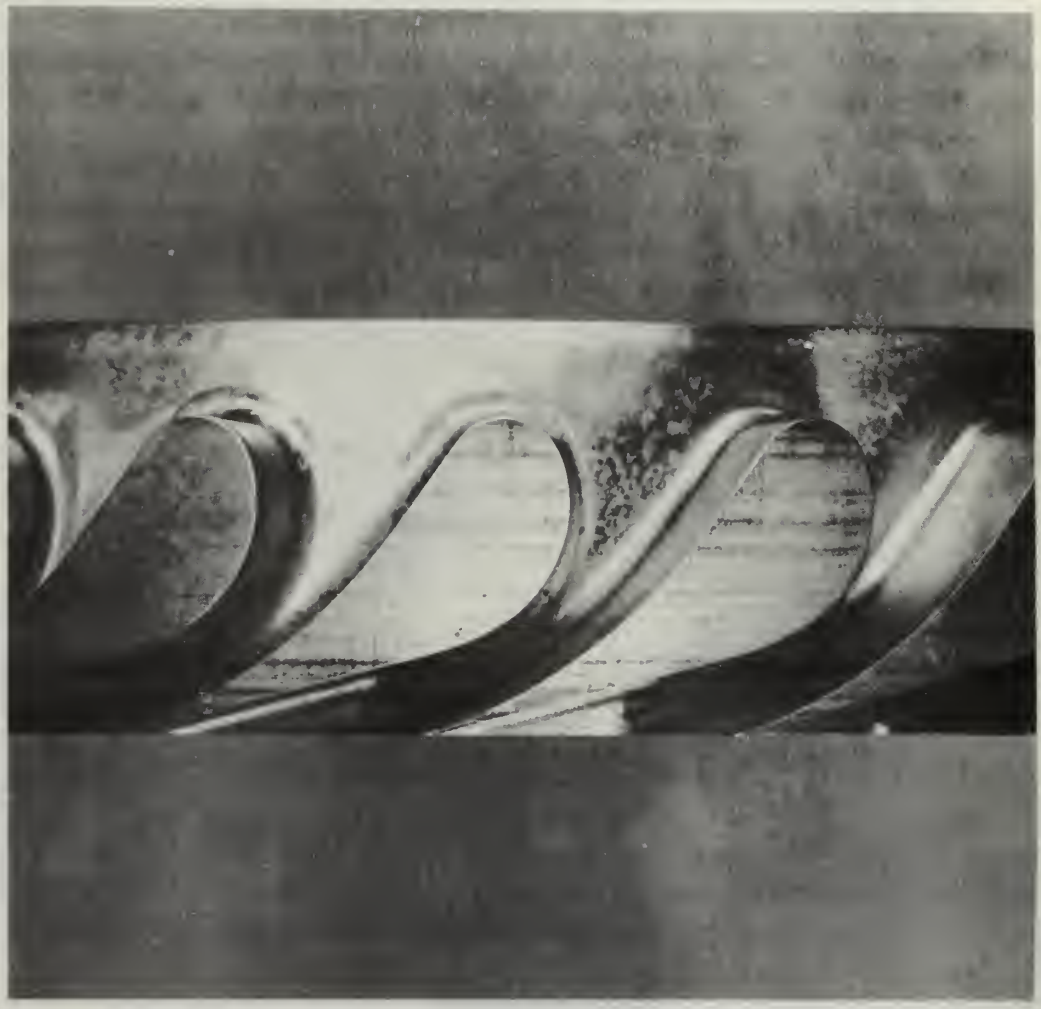


FIGURE 8

BLADE PROFILE
CONVERGING — DIVERGING STATOR

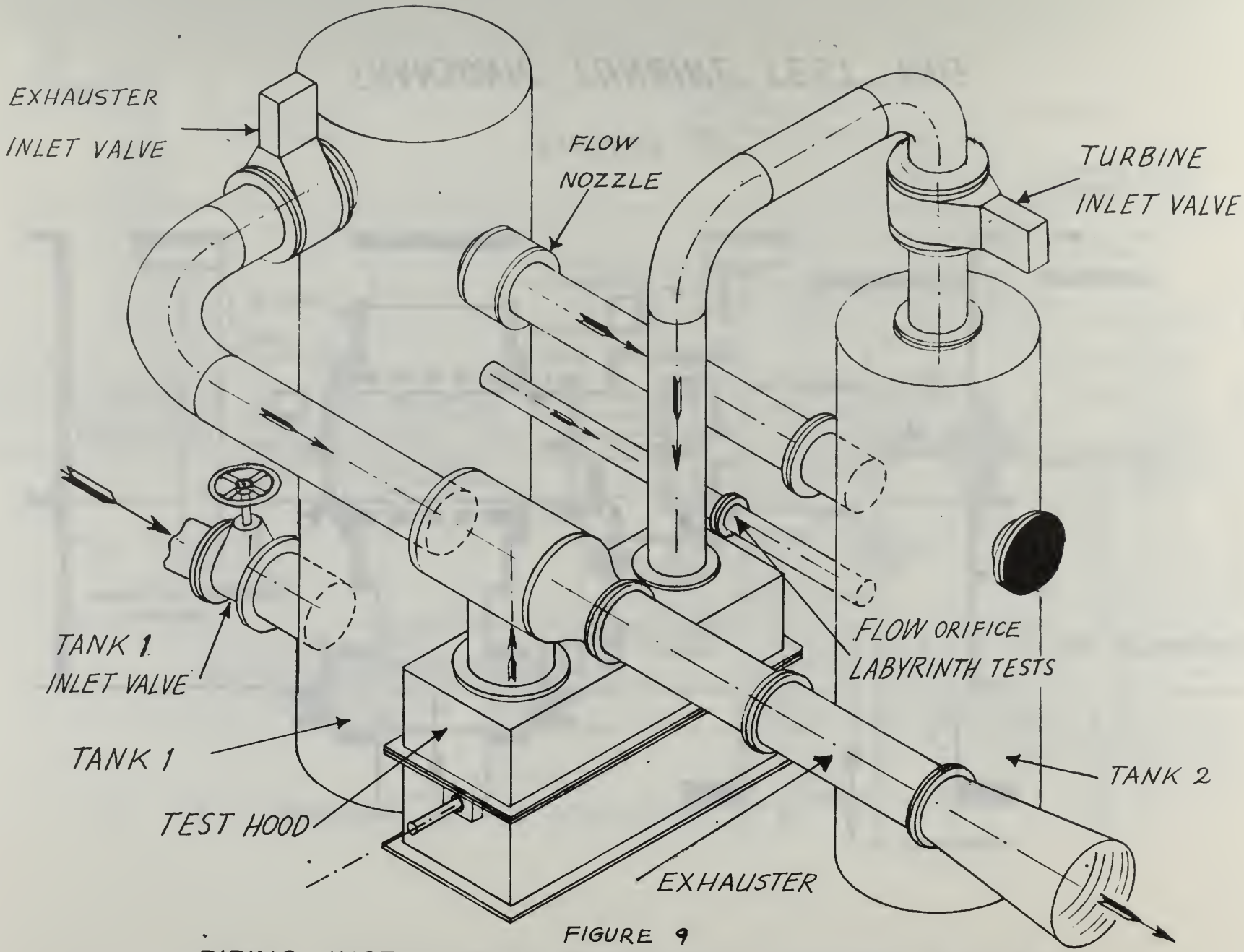



FIGURE 9

PIPING INSTALLATION, TRANSONIC TURBINE TEST RIG

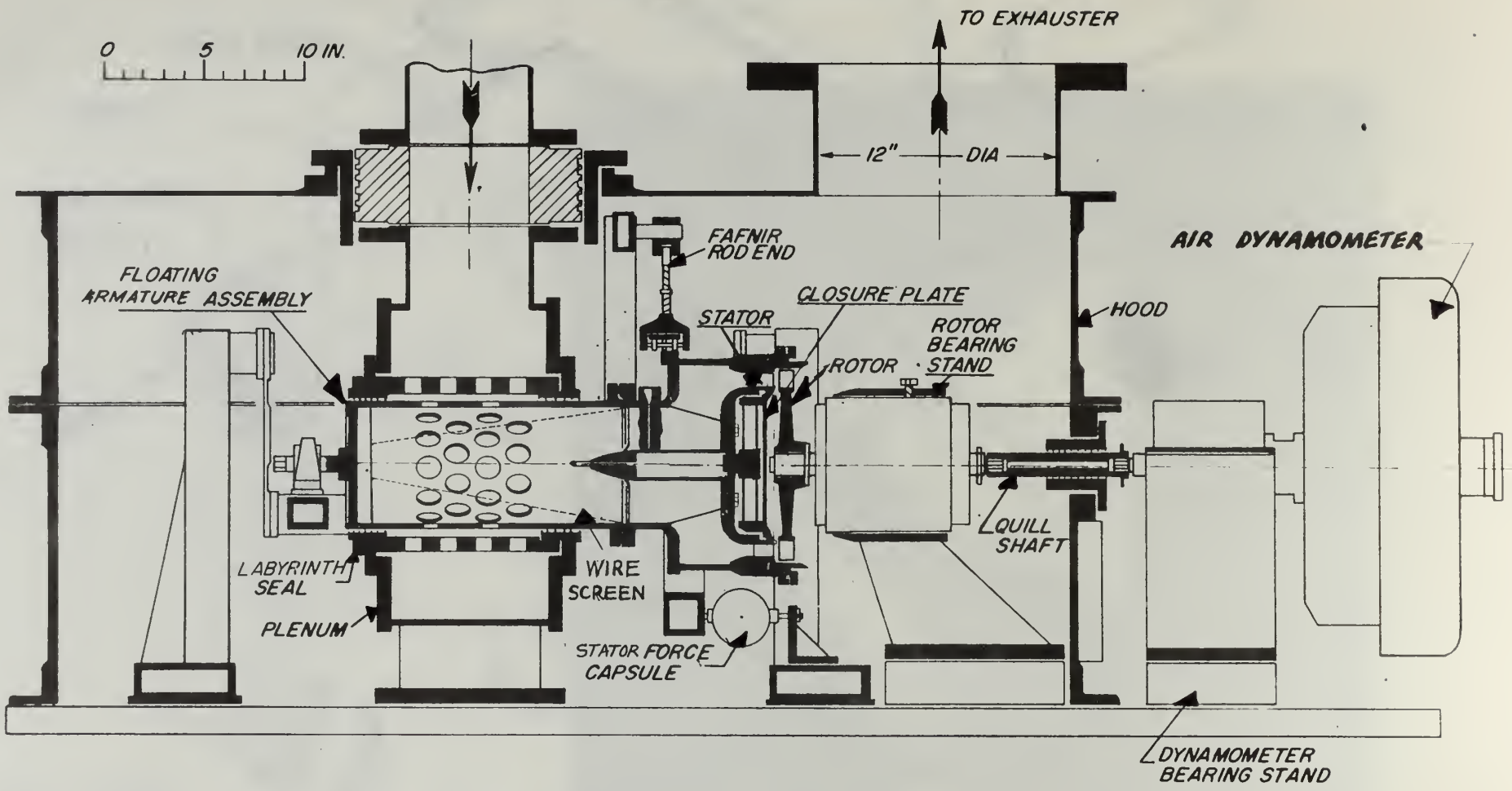



FIGURE 10

TRANSONIC TURBINE TEST RIG

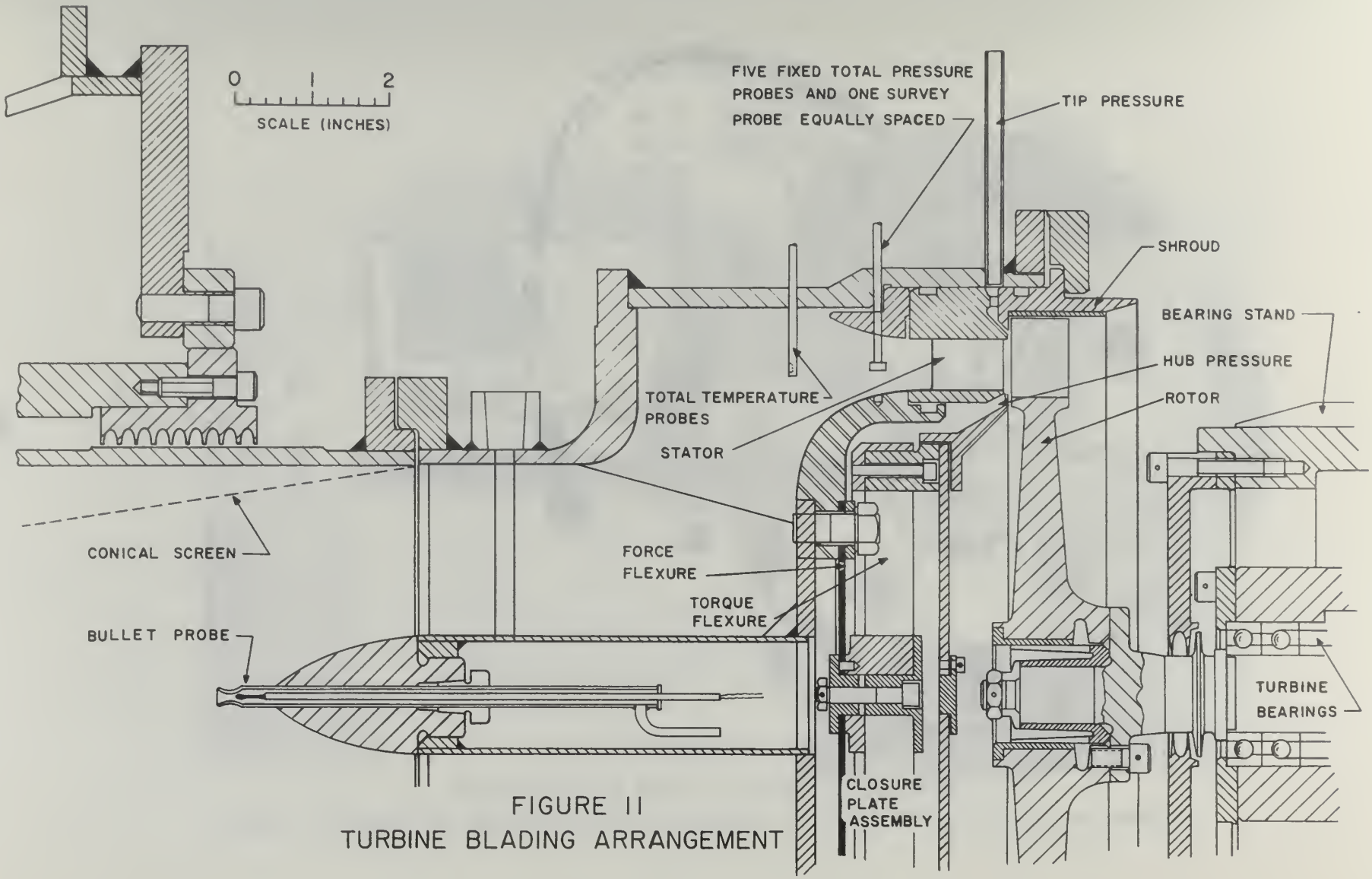



FIGURE 11
TURBINE BLADING ARRANGEMENT

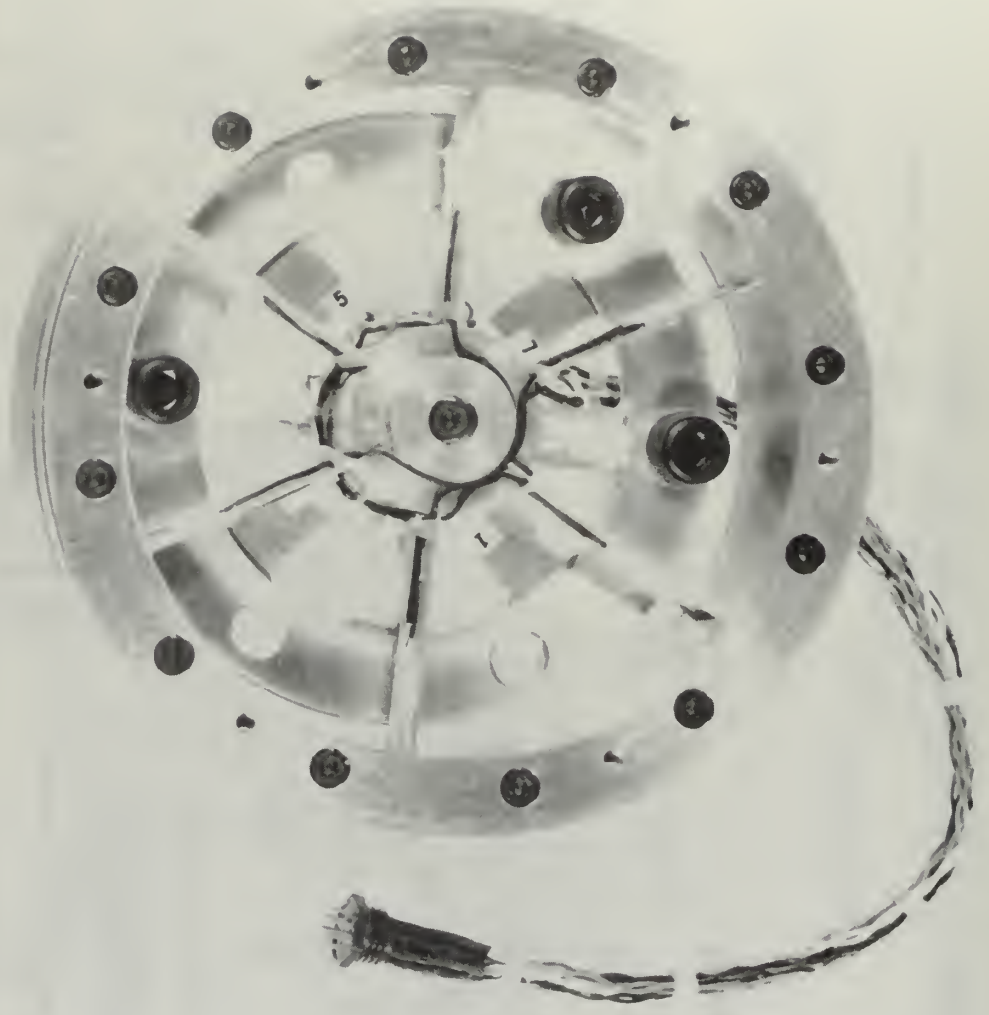


FIGURE 12

CLOSURE PLATE ASSEMBLY
TRANSONIC TURBINE TEST RIG

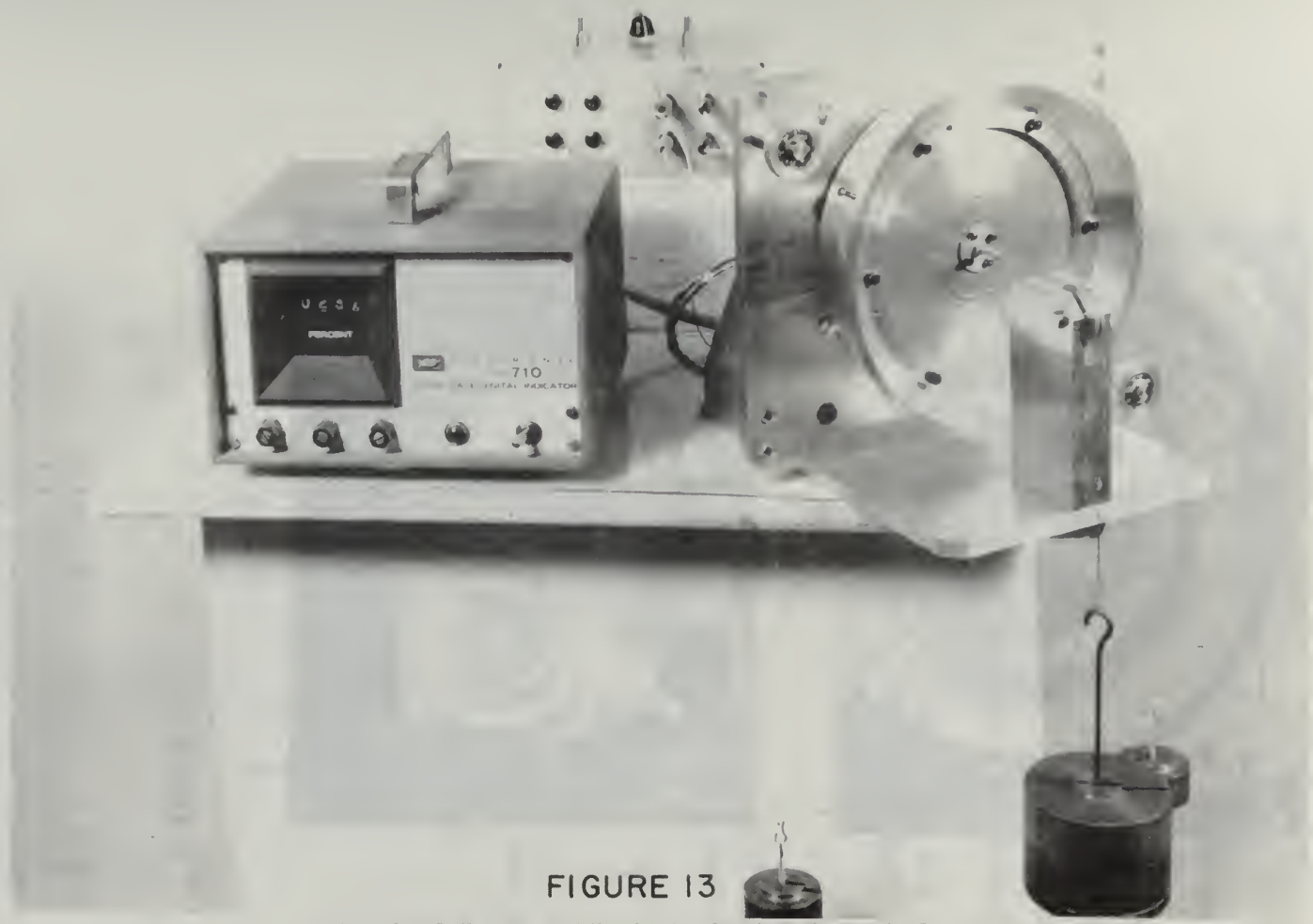
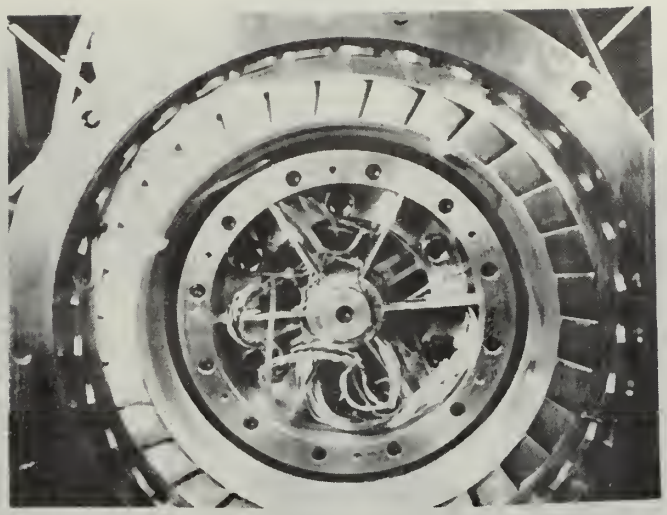


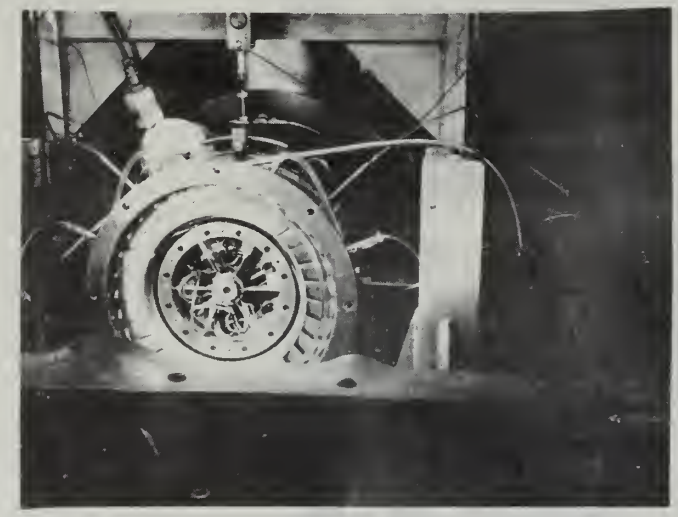

FIGURE 13

CLOSURE PLATE CALIBRATION RIG

(VIEW SHOWING CLOSURE PLATE ASSEMBLY SETUP FOR CALIBRATION RUN)



View a



View b

FIGURE 14

CLOSURE PLATE ASSEMBLY INSTALLATION
TRANSONIC TURBINE TEST RIG

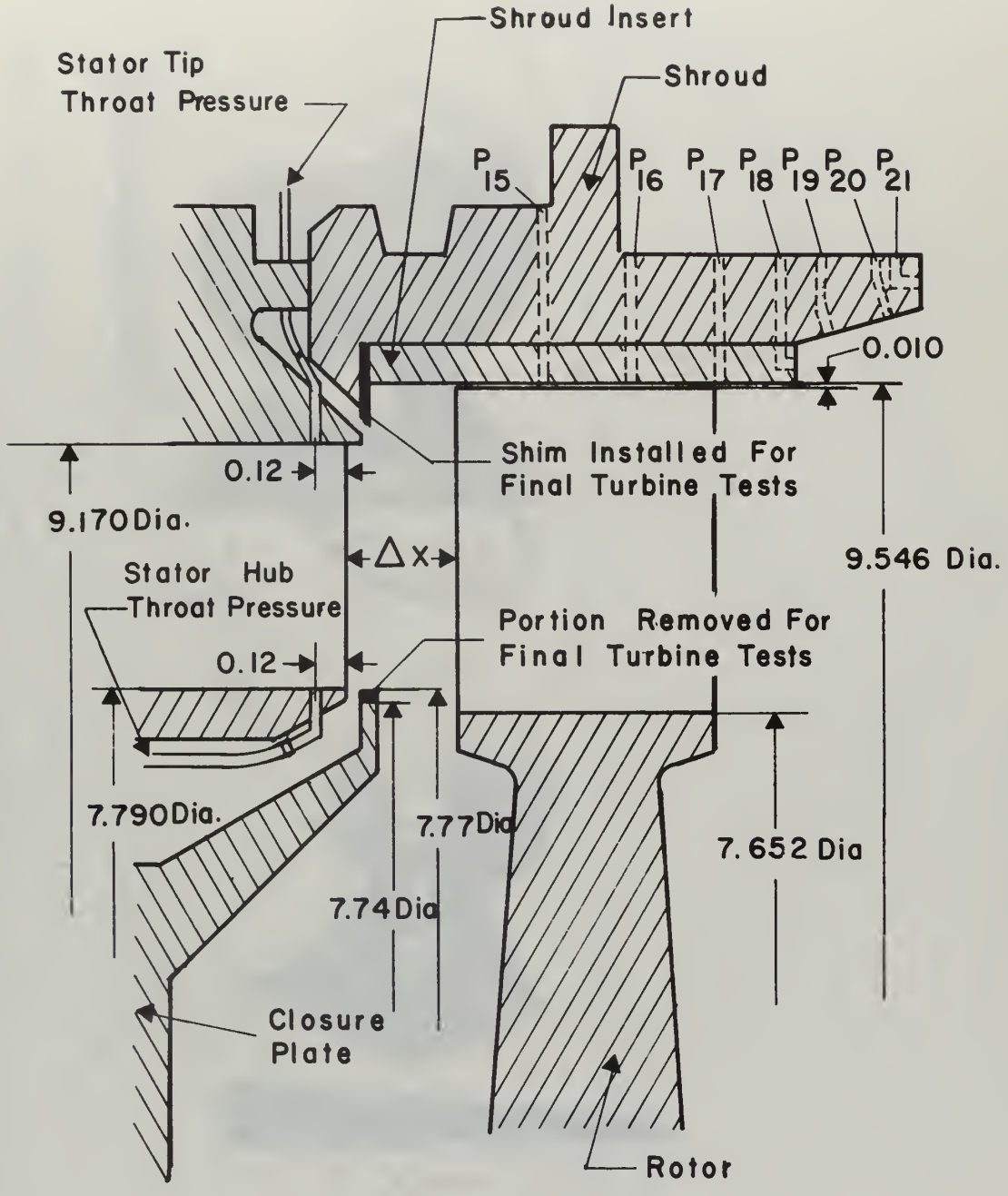
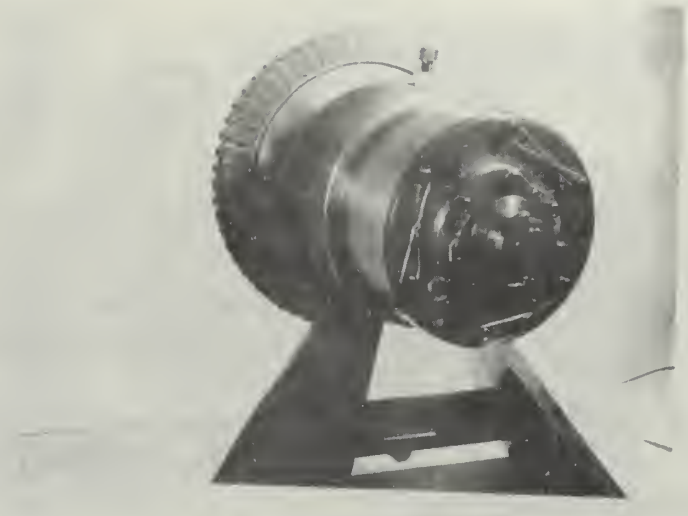



FIGURE 15

TURBINE AND SHROUD DETAILS



View a



View b

FIGURE 16

CIRCULAR-ARC ROTOR AND BEARING ASSEMBLY MOUNTED IN ROTOR BEARING STAND

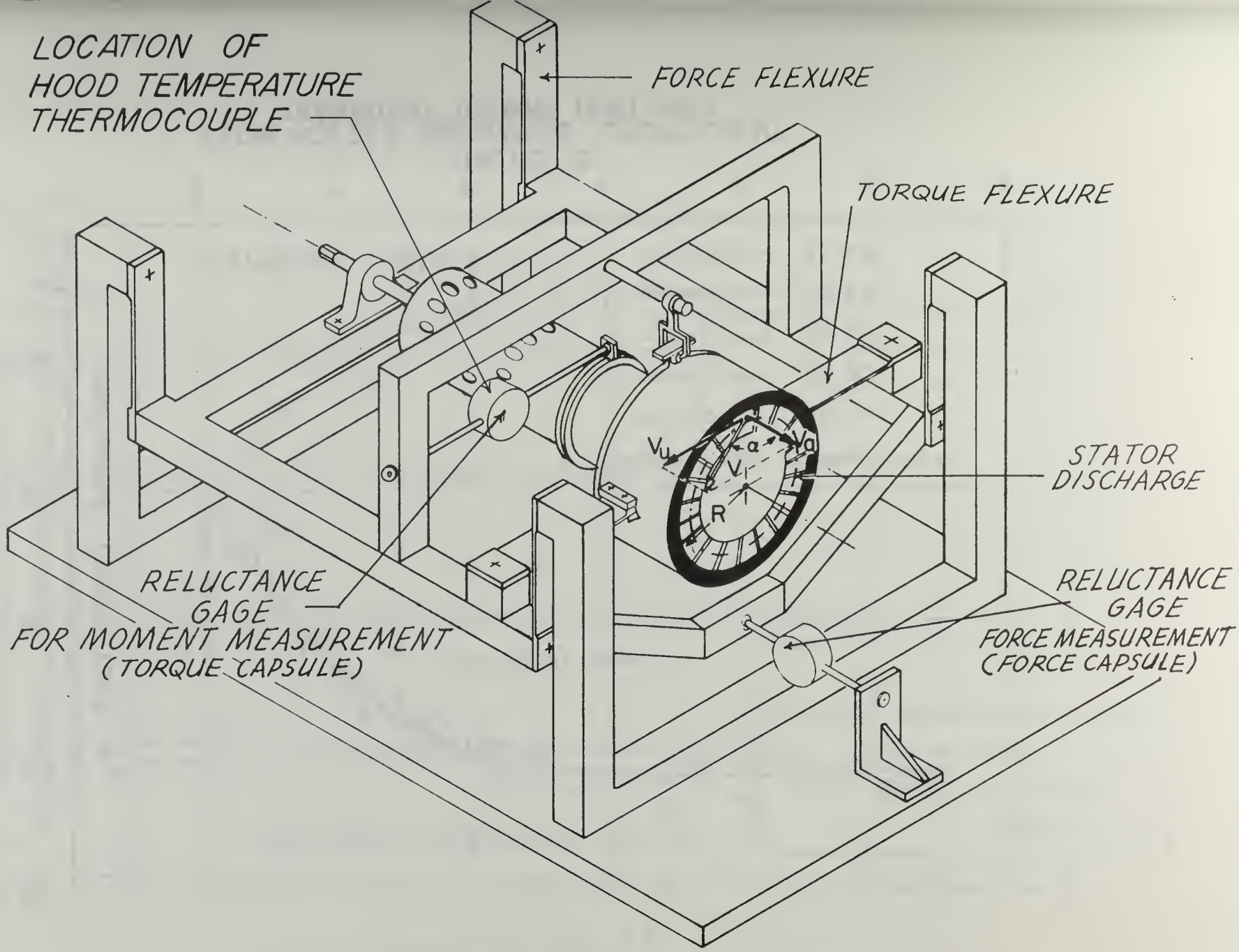



FIGURE 17
FLOATING STATOR ASSEMBLY

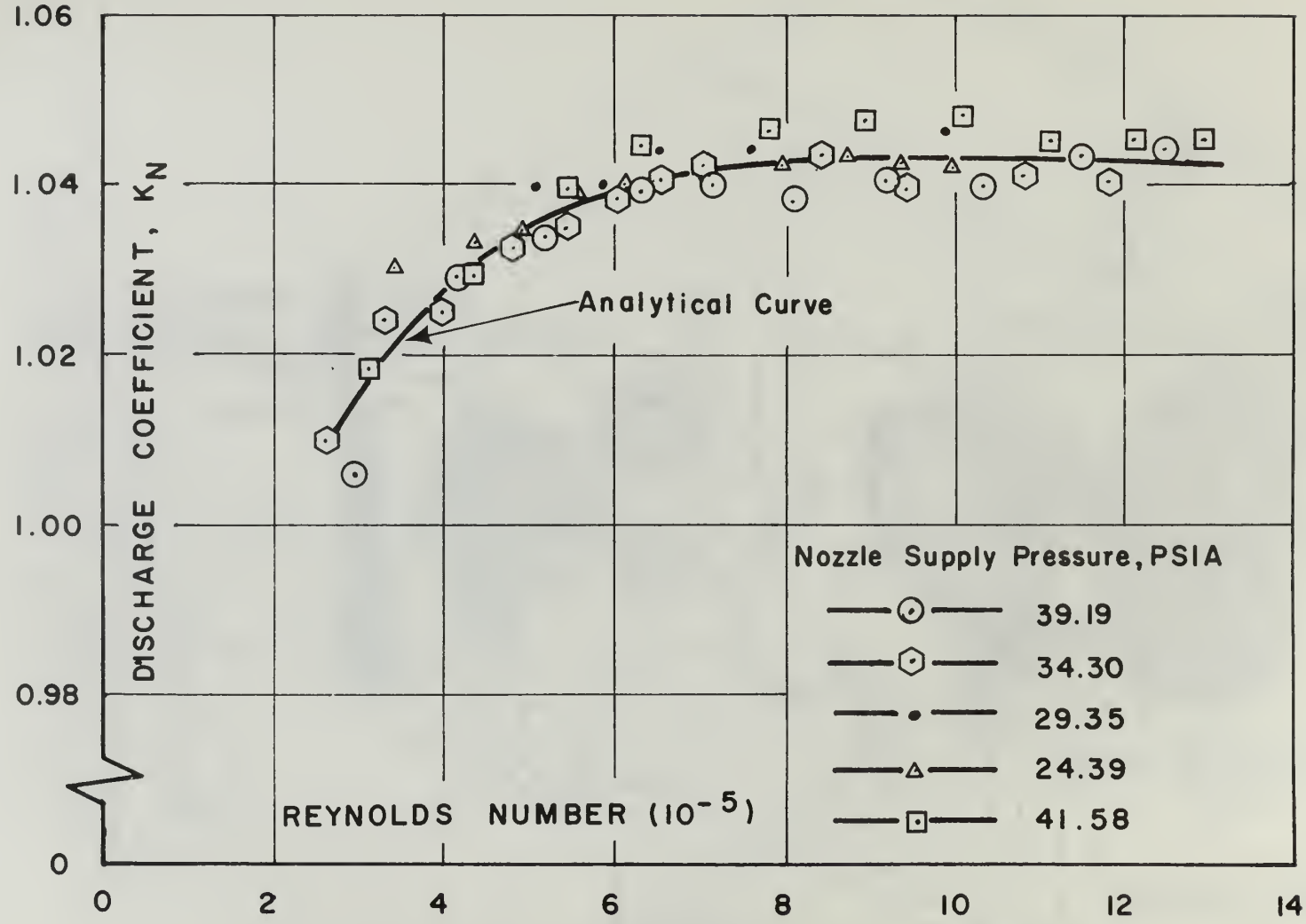



FIGURE 18
FLOW NOZZLE DISCHARGE COEFFICIENT
TRANSONIC TURBINE TEST RIG

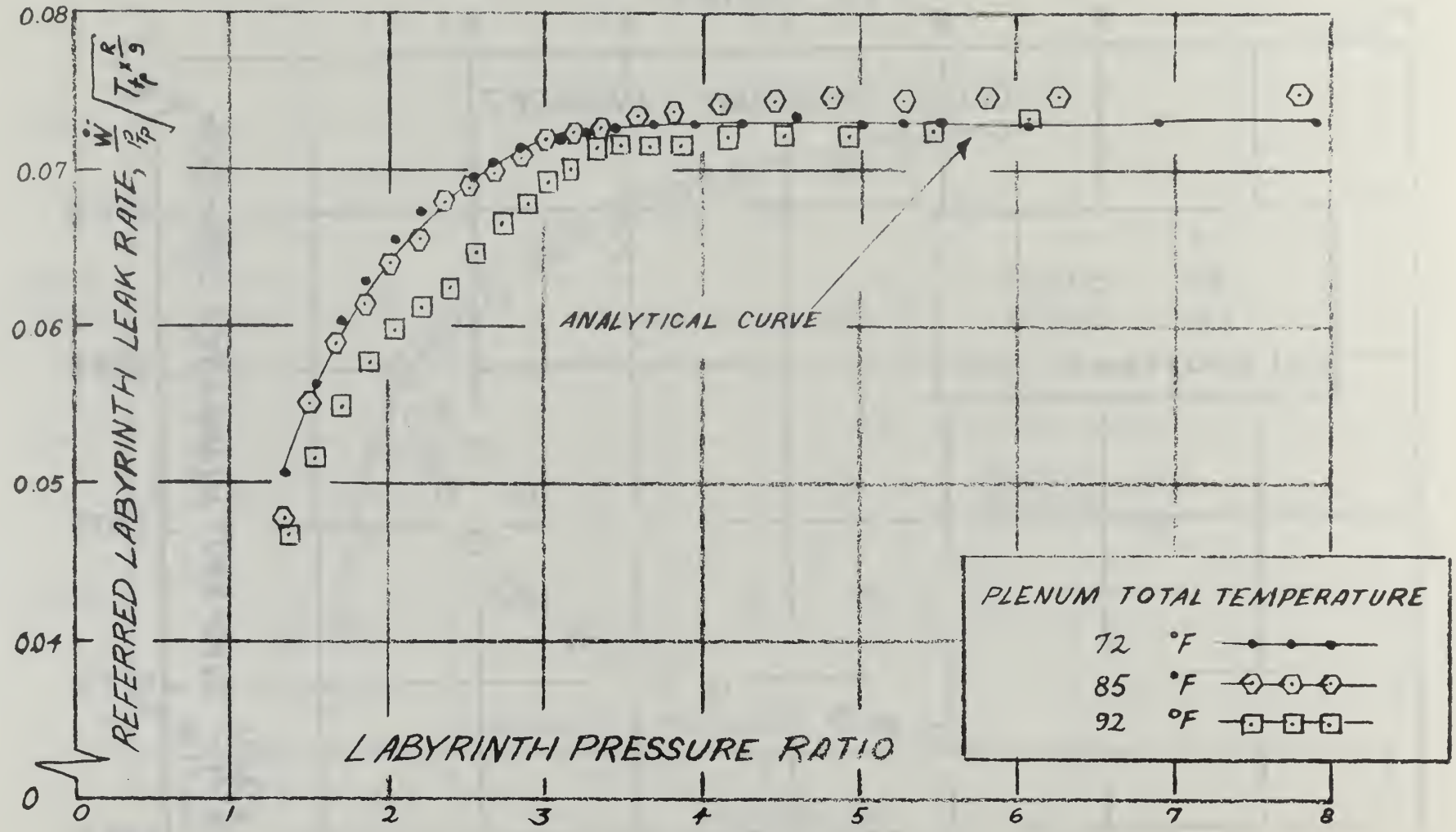



FIGURE 19
REFERRED LABYRINTH SEAL LEAK RATE
TRANSONIC TURBINE TEST RIG

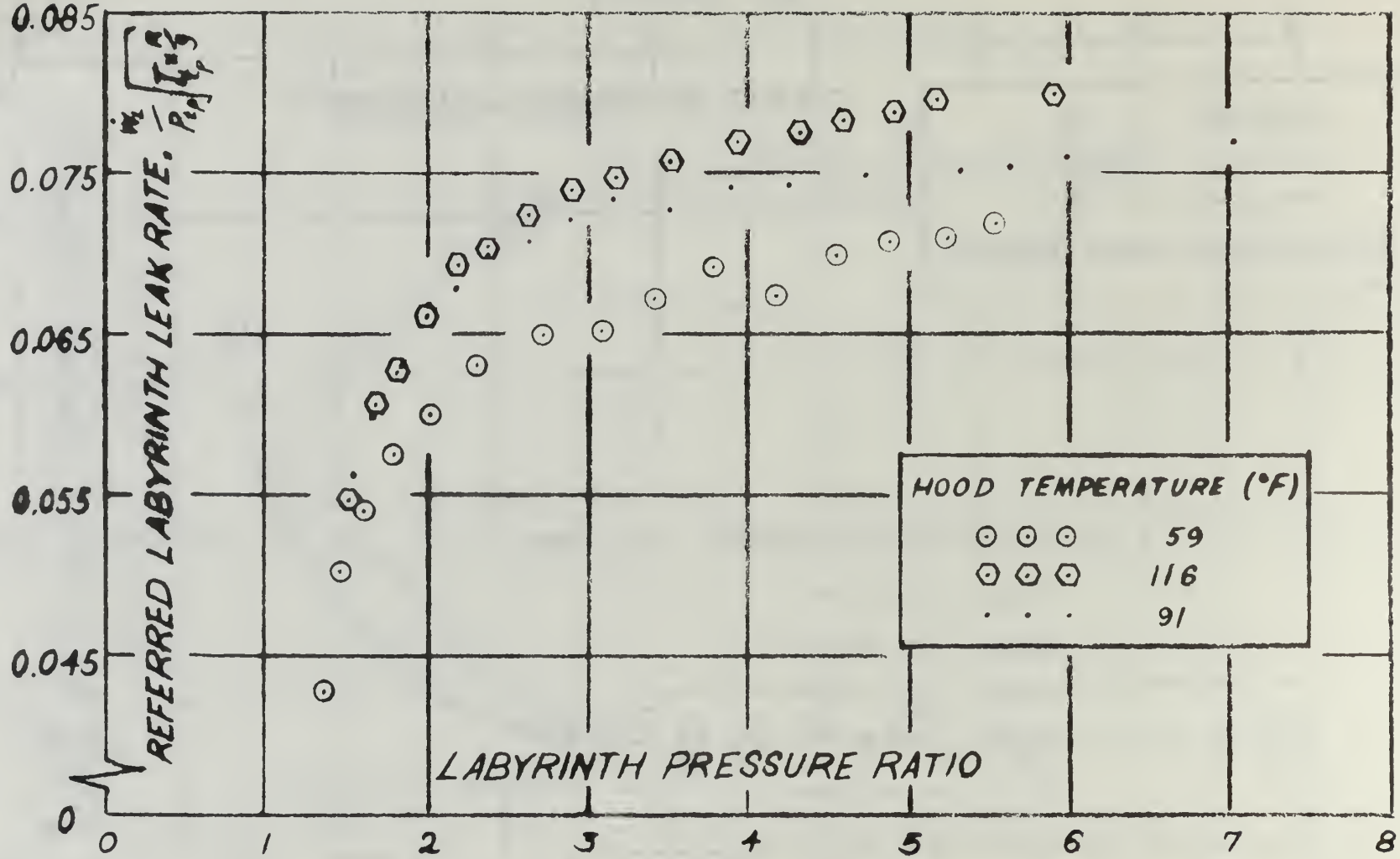



FIGURE 20
REFERRED LABYRINTH SEAL LEAK RATE
TRANSONIC TURBINE TEST RIG

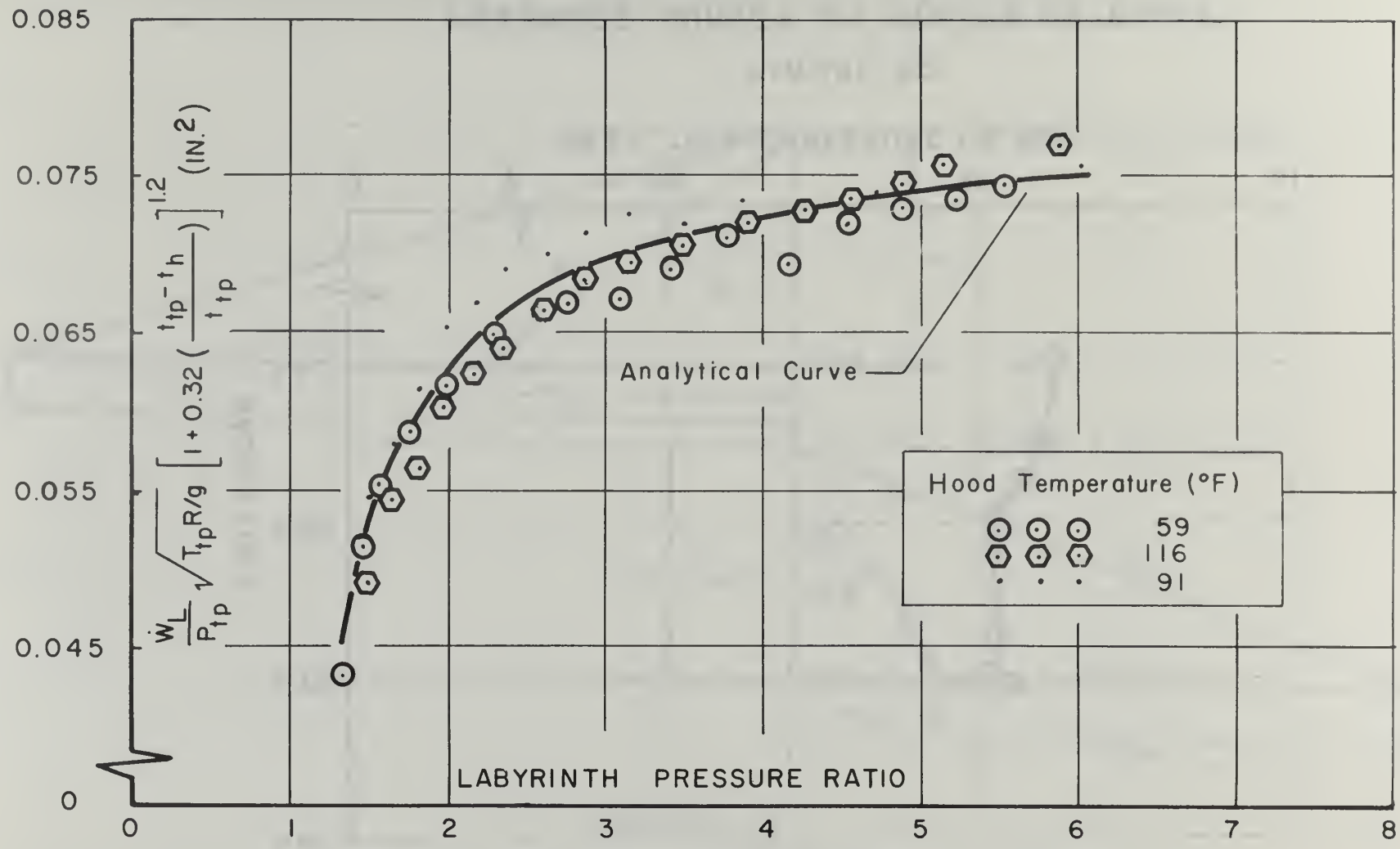



FIGURE 21

MODIFIED REFERRED LABYRINTH SEAL LEAK RATE

TRANSONIC TURBINE TEST RIG

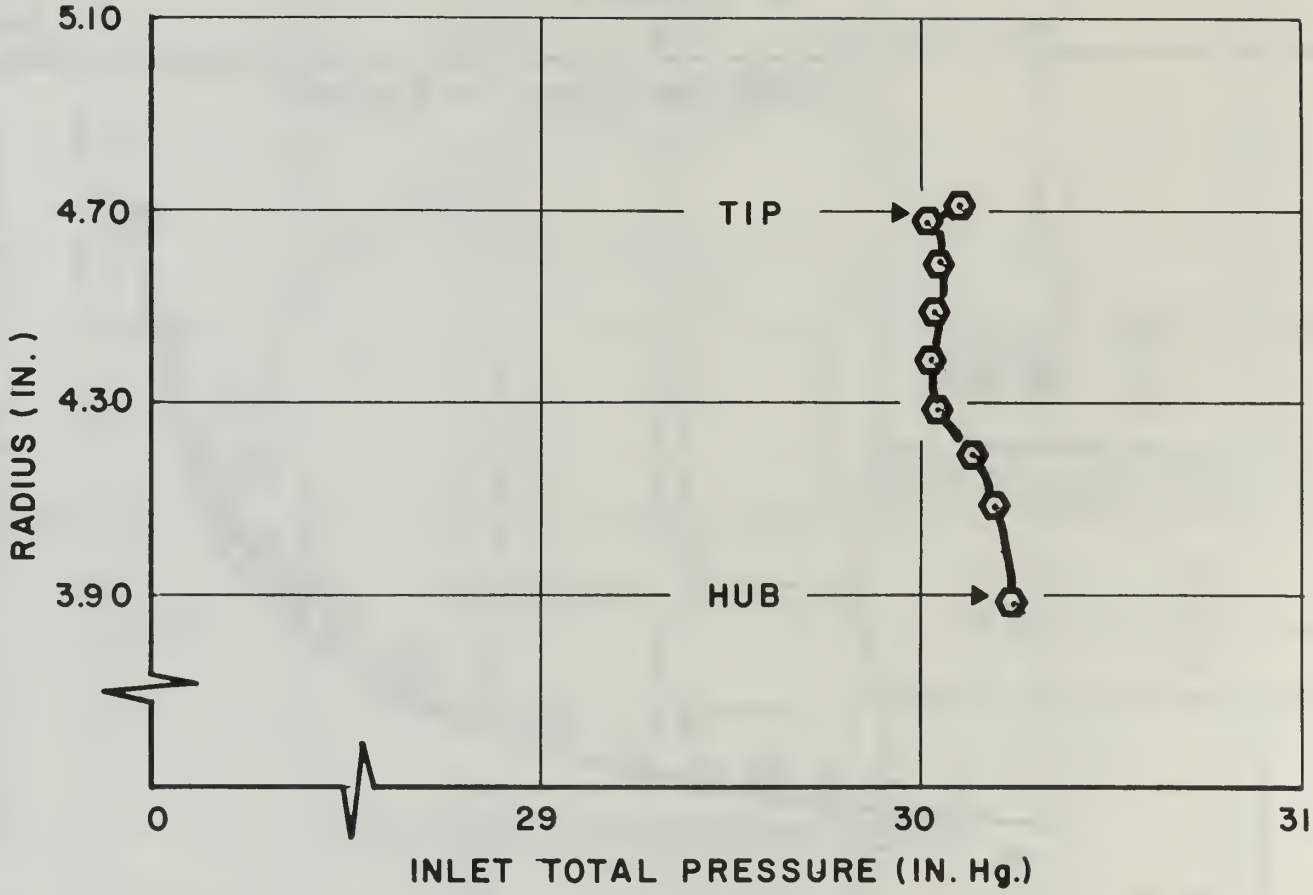



FIGURE 22

PRESSURE SURVEY AT STATOR ENTRANCE

PRESSURE RATIO = 2.0

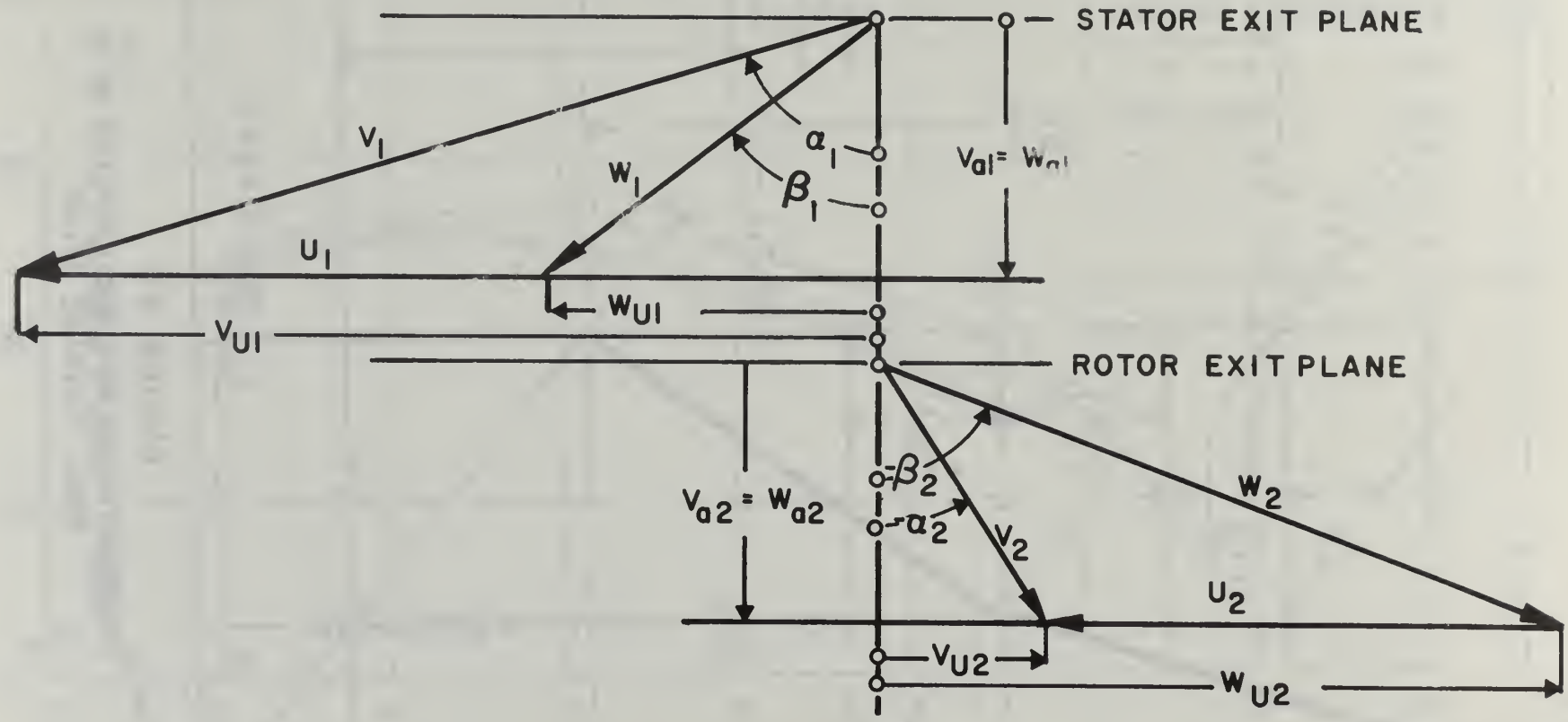



FIGURE 23

VELOCITY DIAGRAM OF TURBINE STAGE

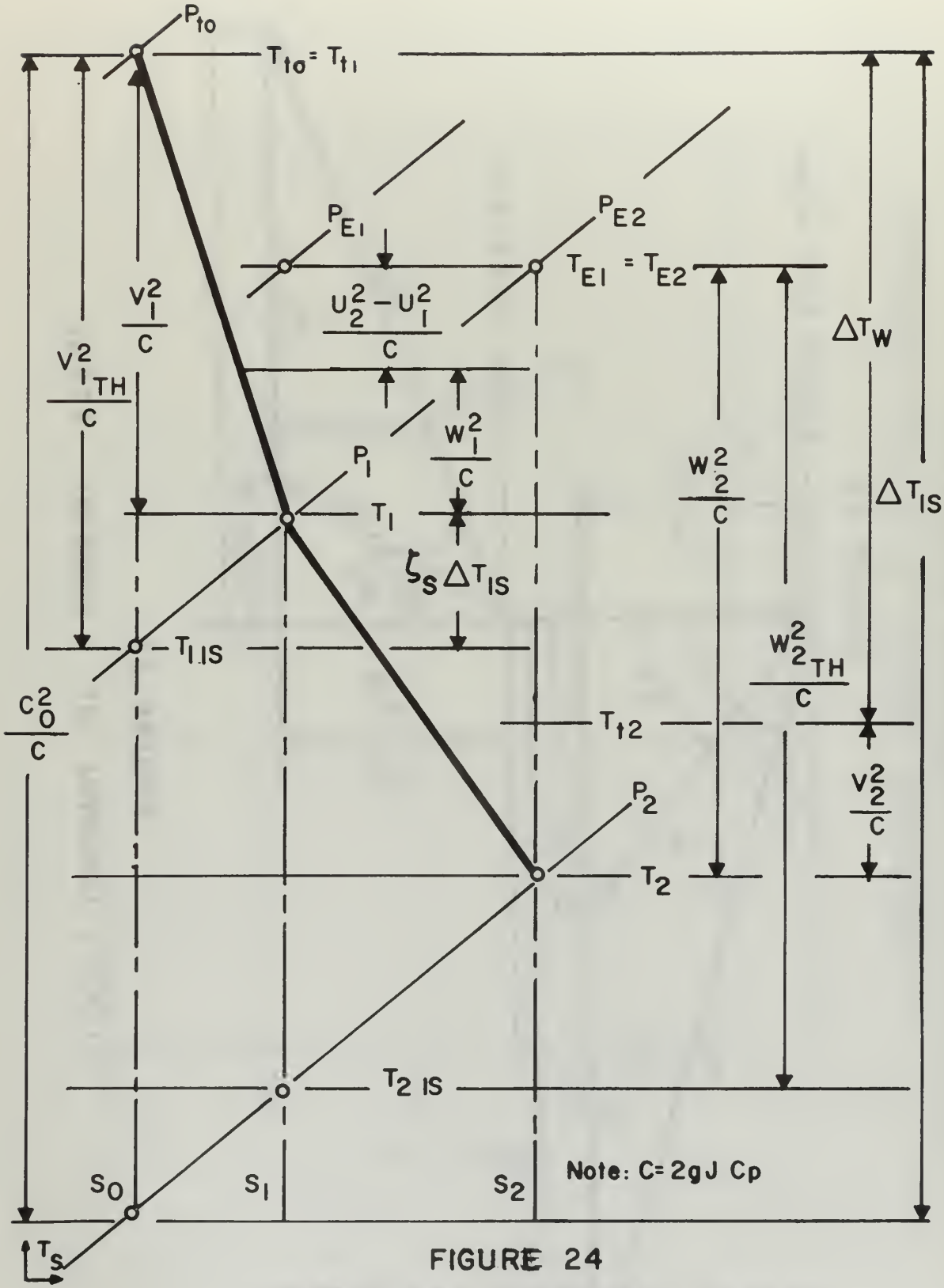



FIGURE 24

THERMODYNAMIC PROCESS OF FLUID IN AN AXIAL TURBINE STAGE

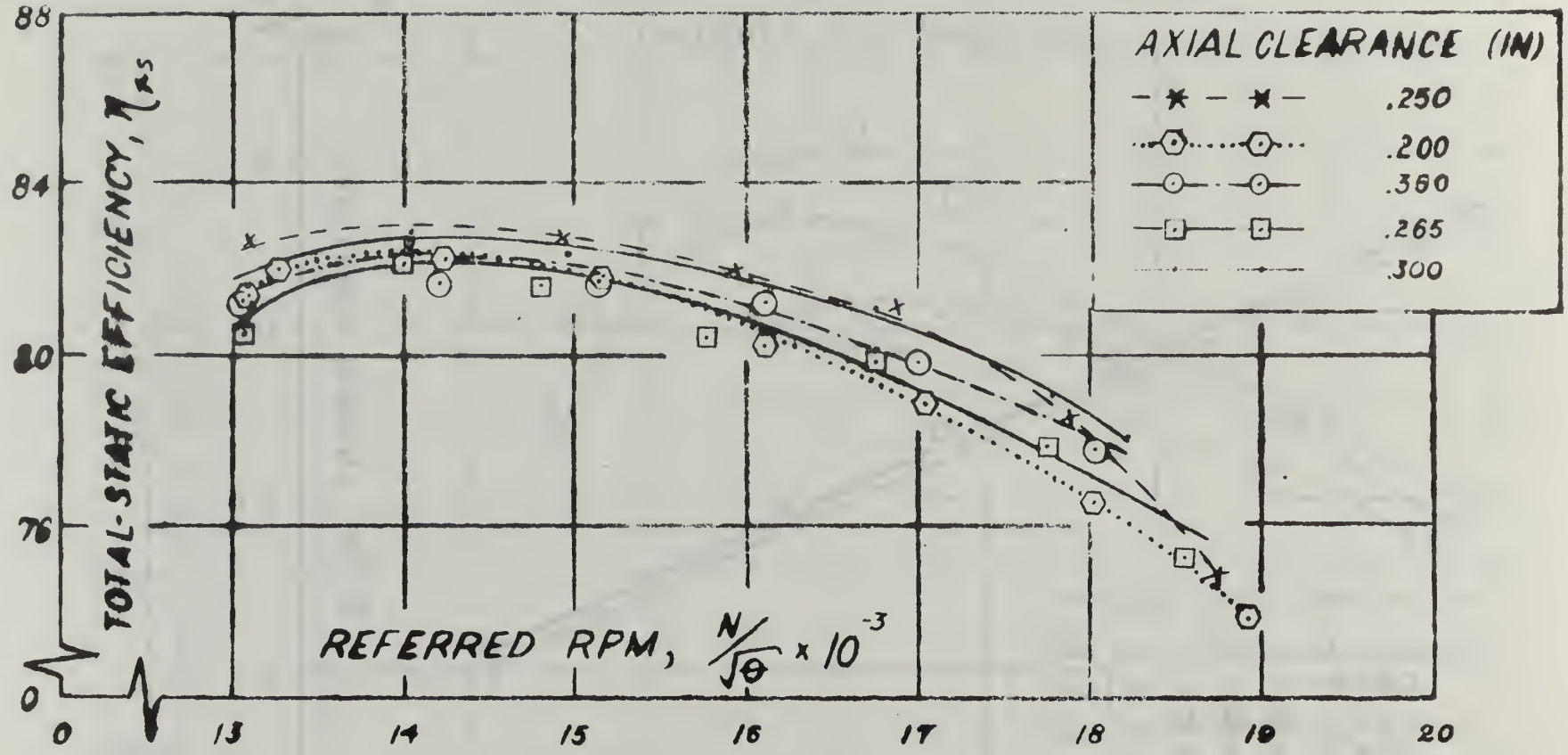



FIGURE 25

TOTAL-STATIC EFFICIENCY AT VARIOUS AXIAL CLEARANCES

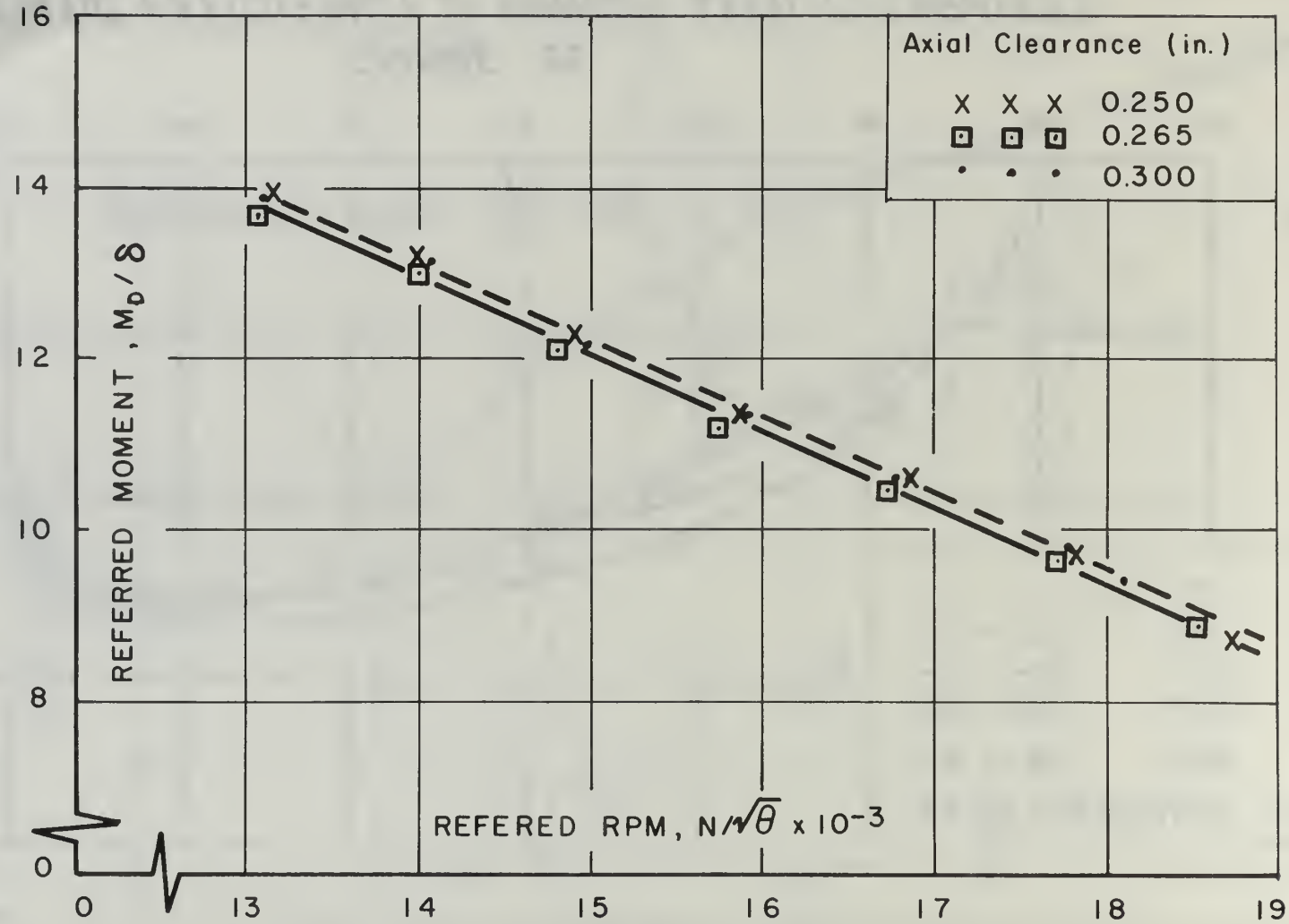



FIGURE 26
REFERRED MOMENT VERSUS REFERRED RPM
PRESSURE RATIO = 2.0

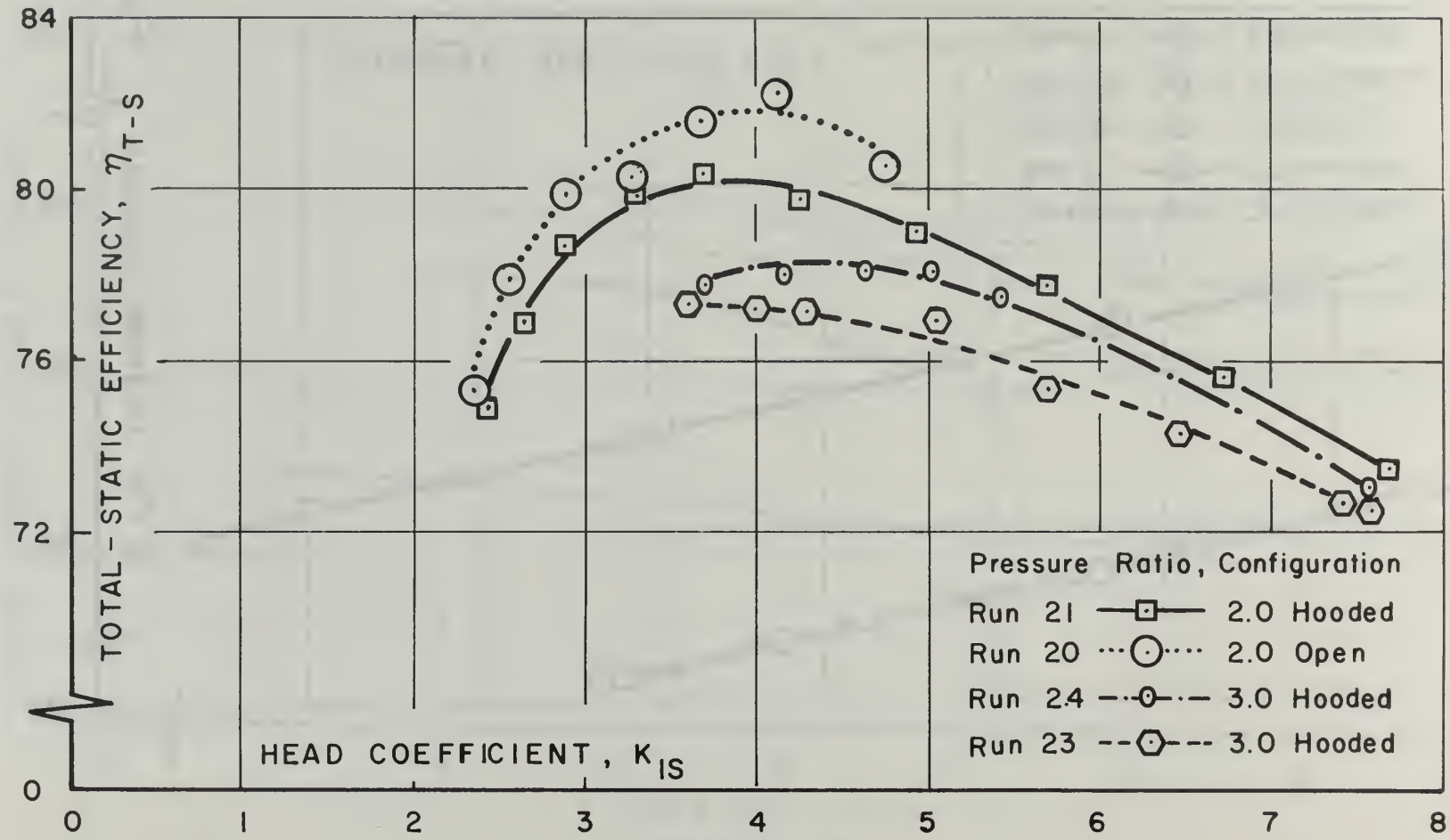



FIGURE 27

EFFICIENCY TOTAL-STATIC
INITIAL TURBINE TESTS

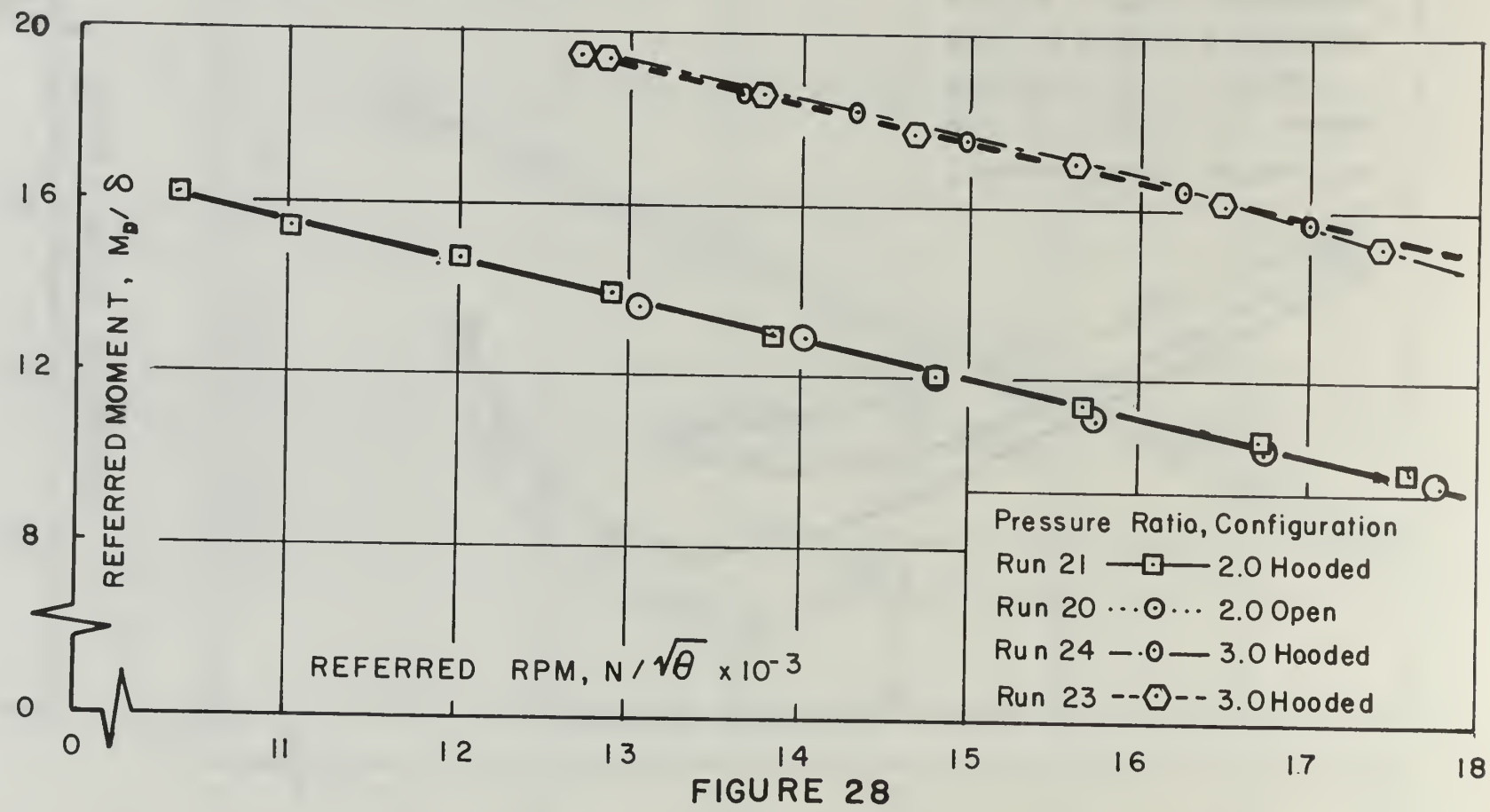



FIGURE 28

REFERRED MOMENT VERSUS REFERRED RPM
INITIAL TURBINE TESTS

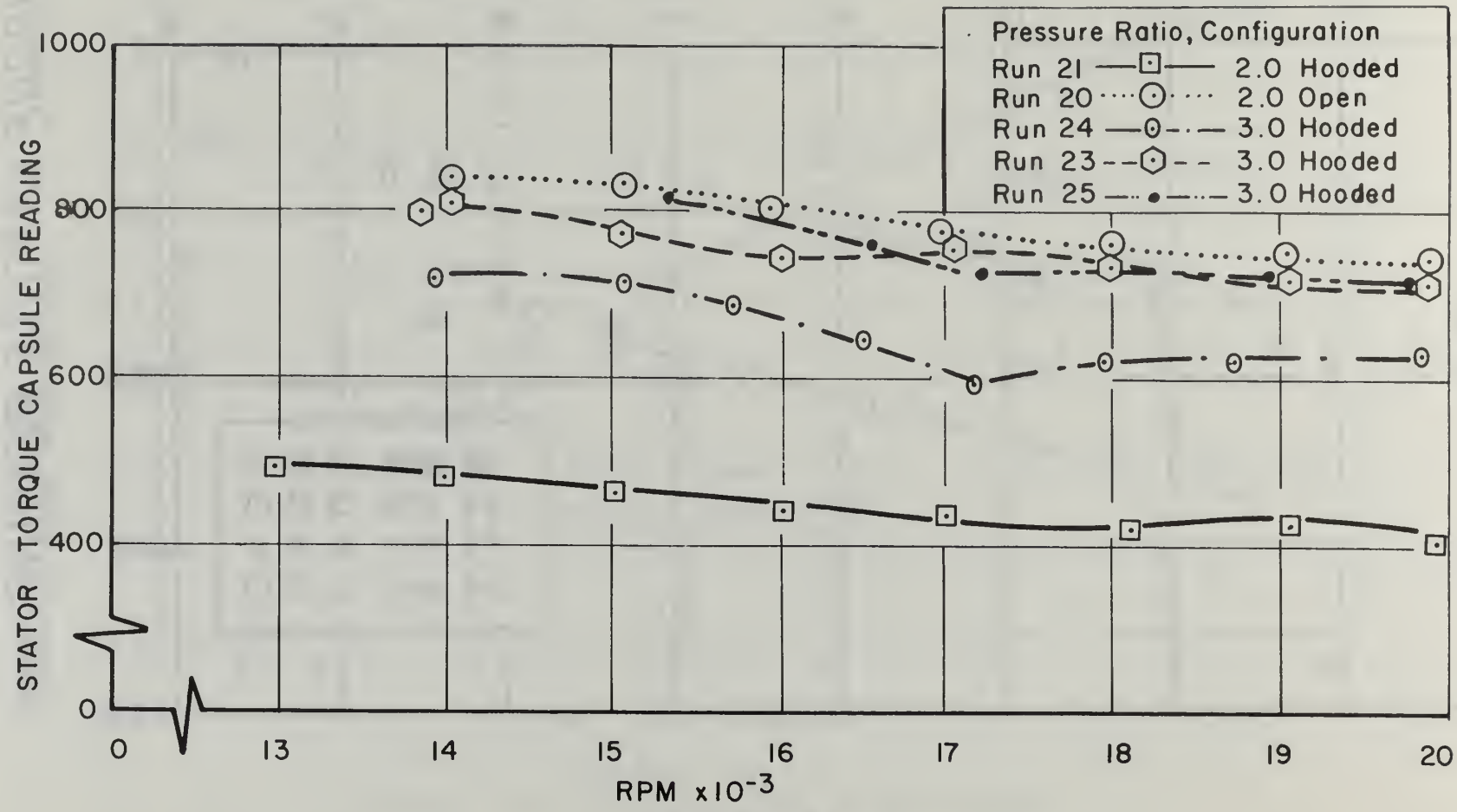



FIGURE 29

STATOR TORQUE CAPSULE VARIATION WITH RPM
TRANSONIC TURBINE TEST RIG

FIGURE 30
STATOR TORQUE CAPSULE
VARIATION WITH TEMPERATURE
TRANSONIC TURBINE TEST RIG

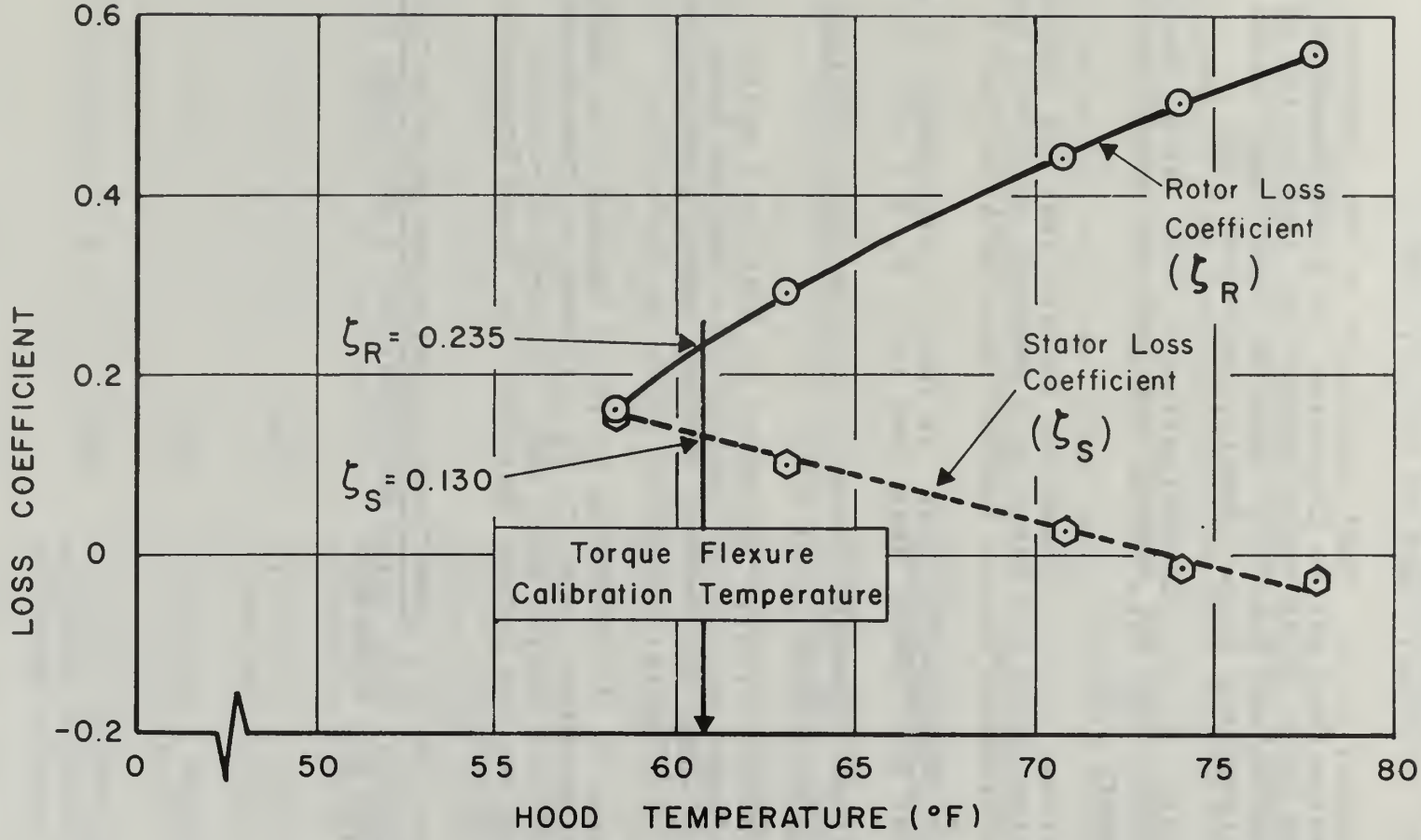



FIGURE 31
STATOR AND ROTOR LOSS COEFFICIENT
VERSUS
HOOD TEMPERATURE
AT 13080 RPM AND PRESSURE RATIO OF 2.5

## REFERENCES


1. Vanco, M. r., "Thermodynamic and Turbine Characteristics of Hydrogen-Fueled Open-Cycle Auxiliary Space Power Systems," NASA TM X-1337, 1967.

2. Commons, P. M., "Instrumentation of the Transonic Turbine Test Rig to Determine the Performance of Turbine Inlet Guide Vanes through the Application of the Momentum and Moment of Momentum Equations," Naval Postgraduate School Thesis, September 1967.

3. Eckert, R. H., "Determination of Flow Rates, Transonic Turbine Test Rig," Naval Postgraduate School TN 66T-1, January 1966.

4. Naviaux, J. C., "Transonic Turbine Test Rig Exhauster System Tests and Tests of a Reaction Turbine," Naval Postgraduate School Thesis, December 1966, p. 68.

5. Flow Measurement, Chap. 4, Part 5, Supplement to ASME Power Test Codes, ASME, New York, N. Y., 1959, p. 74.

6. National Research Council, International Critical Tables, McGraw Hill, 1928.

7. Messegee, J. A., "Influence of Axial and Radial Clearance on the Performance of a Turbine Stage with Blunt-Edge Non-Twisted Blades," Naval Postgraduate School Thesis, September 1967, pp. 112-119.

8. Vavra, M. H., Problems of Fluid Mechanics in Radial Turbomachines, Pts. I, II, III and IV, "Von Karman Institute Course Note 55a," Rhode-Saint-Genese, Belgium, Von Karman Institute for Fluid Dynamics, March 1965.

9. Vavra, M. H., Aero-Thermodynamics and Flow in Turbomachines, John Wiley and Sons, Inc., New York, N.Y., 1960, pp. 418-438.

# APPENDIX I

## COMPUTER PROGRAMS FOR FLOW RATE DETERMINATION AND TURBINE TEST DATA REDUCTION

### A. Program FLOCAL.

This program calculates the flow nozzle discharge coefficient of the Transonic Turbine Test Rig by comparing the flow through the nozzle with that through a standard ASME square-edge orifice. The inputs for this program are:

| Card No. | Format | Units | Fortran | Description |
|---|---|---|---|---|
| 1 | I3 | | L | Number of runs to be processed. |
| 2 | I3 | | N | Number of data points in a given run. Entries on cards 2 through 11 are repeated for each run. |
| 3 | 3F10.4 | in.Hg. | PBAR | Barometric pressure. |
| | | $^{o}F$ | TCL | Temperature of Hg. of barometer |
| | | $^{o}F$ | TCR | Control room temperature. |
| 4 | 8F10.4 | in.$H_2O$ | DH | Differential pressure across flow nozzle, multiple entries. |
| 5 | 8F10.4 | in.Hg. | PATM | Reference for nozzle pressure, multiple entries. |
| 6 | 8F10.4 | in.Hg. | PNOZ | Flow nozzle upstream static pressure, multiple entries. |
| 7 | 8F10.4 | m.v. | TNOZ | Flow nozzle temperature, multiple entries. |
| 8 | 8F10.4 | m.v. | TTD1 | Orifice temperature at upstream pressure tap, multiple entries. |
| 9 | 8F10.4 | in.Hg. | PFL | Orifice upstream static pressure, multiple entries. |

| | | | | |
|---|---|---|---|---|
| 10 | 8F10.4 | in.Hg. | PREF | Reference for orifice pressure, multiple entries. |
| 11 | 8F10.4 | cm.$H_2O$ | DPFL | Pressure difference across orifice with flange taps, multiple entries. |

B. Program LABLEK.

This program calculates the labyrinth leak rate of the Transonic Turbine Test Rig. The referred labyrinth leakage is computed and compared with the values obtained from the analytical expression of Section 5. The variation between these two values in percentage is included as output. The inputs for this program are:

| Card No. | Format | Units | Fortran | Description |
|---|---|---|---|---|
| 1 | I3 | | L | Number of runs to be processed. |
| 2 | F10.4 | in.Hg. | PBAR | Barometric pressure. |
| | I2 | | N | Number of data points in the given run. Entries on cards 2 through 12 are repeated for each run. |
| | I3 | | NRUN | Run number. |
| 3 | 2F10.4 | $^oF$ | TCL | Temperature of Hg. of barometer. |
| | | $^oF$ | TCR | Control room temperature |
| 4 | 8F10.4 | in.Hg. | PATM | Reference of labyrinth plenum pressure and hood pressure, multiple entries. |
| 5 | 8F10.4 | in.Hg. | PSPL | Labyrinth plenum total pressure, multiple entries. |
| 6 | 8F10.4 | in.Hg. | PHD | Hood static pressure, multiple entries. |
| 7 | 8F10.4 | m.v. | TTPLD | Labyrinth plenum total temperature, multiple entries. |

| | | | | |
|---|---|---|---|---|
| 8 | 8F10.4 | m.v. | TTD1 | Total temperature at upstream pressure tap of the flow orifice, multiple entries. |
| 9 | 8F10.4 | m.v. | THD | Hood temperature, multiple entries. |
| 10 | 8F10.4 | in.Hg. | PFL | Orifice upstream static pressure, multiple entries. |
| 11 | 8F10.4 | in.Hg. | PREF | Reference for orifice pressure, multiple entries. |
| 12 | 8F10.4 | cm.$H_2O$ | HWFL | Pressure difference across orifice with flange taps, multiple entries. |

C. Program TTRSS.

This program reduces the data obtained with the Transonic Turbine Test Rig. The program consists of an executive routine and 10 subroutines. The executive routine provides the calling sequence for the subroutines. This sequence is:

1. INPUT. This subroutine reads the input test data. The data items which have multiple entries are so indicated in the item description, all others are single entry items. Each test run may consist of a maximum of 50 data points. The input data consists of the following items:

| Card No. | Format | Units | Fortran | Description |
|---|---|---|---|---|
| 1 | I10 | | MM | Number of runs to be processed |
| 2 | I10 | | NRUN | Run number. Entries on cards 2 through 37 are repeated for each run. |
| 3 | 2F10.4 | in. | AXCLR | Axial clearance. |

| | | | | |
|---|---|---|---|---|
| | | in. | RADCR | Radial clearance. |
| 4 | F10.4 | in.Hg. | PBAR | Barometric pressure. |
| 5 | I10 | | N | Number of data points in the given run. |
| 6 | 2F10.4 | $^{o}F$ | TCL | Temperature of Hg of barometer. |
| | | $^{o}F$ | TCR | Control room temperature |
| 7 | 8F10.4 | in.Hg. | PREF2 | Reference for stator plenum pressure and shroud pressures, multiple entries. |
| 8 | 8F10.4 | in.Hg. | PTPL | Stator plenum total pressure, multiple entries. |
| 9-15 | 8F10.4 | in.Hg. | P15-P21 | Shroud pressures, multiple entries. |
| 16 | 8F10.4 | in.$H_2O$ | DH | Differential pressure across the flow nozzle, multiple entries. |
| 17 | 8F10.4 | in.Hg. | PATM | Reference for the nozzle pressure, labyrinth plenum pressure, stator hub and tip pressures and the hood pressure, multiple entries. |
| 18 | 8F10.4 | in.Hg. | PNOZ | Flow nozzle upstream static pressure, multiple entries. |
| 19 | 8F10.4 | in.Hg. | PSPL | Labyrinth plenum total pressure, multiple entries. |
| 20 | 8F10.4 | in.Hg. | PHUB | Stator hub static pressure, multiple entries. |
| 21 | 8F10.4 | in.Hg. | PTIP | Stator tip static pressure, multiple entries. |
| 22 | 8F10.4 | in.Hg. | PHD | Hood static pressure, multiple entries. |

| | | | | |
|---|---|---|---|---|
| 23 | 8F10.4 | m.v. | TNOZ | Flow nozzle temperature, multiple entries. |
| 24 | 8F10.4 | m.v. | TTPLD | Labyrinth plenum total temperature, multiple entries. |
| 25 | 8F10.4 | m.v. | TTPL | Stator plenum total temperature, multiple entries. |
| 26 | 8F10.4 | m.v. | THD | Hood temperature, multiple entries. |
| 27 | 8F10.4 | RPM | RPM | Turbine rotational speed, multiple entries. |
| 28 | 8F10.4 | counts | AXIL | Stator assembly axial force, multiple entries. |
| 29 | 8F10.4 | counts | TORQR | Stator assembly torque, multiple entries. |
| 30 | 8F10.4 | counts | DYNAR | Dynamometer torque, multiple entries. |
| 31 | 8F10.4 | counts | CLAXIL | Closure plate force, multiple entries. |
| 32 | 8F10.4 | counts | CLTRQR | Closure plate torque, multiple entries. |
| 33 | 10X,4A2 | | DATE | Month/Day/Year. |
| 34 | 15X,3A2 | | TTYPEB | I (circular-arc rotor with sharp leading edges) or II (circular-arc rotor with blunt leading edges). |
| | | | STATOR | I (converging stator) or II (converging-diverging stator). |
| | | | METHOD | MF ($V_{a1}$ determined using momentum and continuity) or CF ($V_{a1}$ determined using continuity alone). |
| 35 | F5.3 | in. | RMEAN | Stator mean radius. |
| 36 | I1 | | J | Number of pressure ratios tested in given run. |

| | | | |
|---|---|---|---|
| 37 | 8(2I5) | NPTS(K) | First data point at particular pressure ratio. |
| | | NPTSS(K) | Last data point at particular pressure ratio. These two entries repeat in pairs, one pair for each pressure ratio tested in given run. |

2. SETCON. This subroutine consists of all the constant factors used in the data reduction calculations.

3. CONVERT. This subroutine converts the units of the input data into a single system compatible with the equations of Section 6.

4. FLORAT. This subroutine computes the turbine flow rate using the equations of Subsection 6.2.

5. STATOR. This subroutine uses the equation of Subsection 6.4 to calculate the stator discharge properties. Subroutine MOMENT is called from STATOR when using momentum and continuity to compute the axial velocity component.

6. MOMENT. This subroutine determines the axial component of absolute velocity by the application of the momentum equation to the fluid within the stator assembly.

7. ROTOR. This subroutine computes the rotor discharge properties using the equations of Subsection 6.5.

8. PERFRM. This subroutine computes the performance parameters and the referred quantities of Subsection 6.6.

9. OUTPTA. This subroutine gives a detailed printed output consising of the stator and rotor discharge properties and the performance parameters.

10. OUTPUT. This subroutine prints the turbine performance parameters in report form.

```
      DIMENSION TNOZ(100),TTD1(100),DH(100),PNOZ(100),PATM(100),PFL(100)
     1,PREF(100),DPFL(100),RE(100),W(100),FLOCO(100),TTD1R(100),TNOZR(10
     20)
CTHIS PROGRAM CALCULATES THE DISCHARGE COEFFICIENT OF THE TRANSONIC
CTURBINE TEST RIG FLOW RATE NOZZLE BY MATCHING THE FLOW THROUGH THE
CNOZZLE WITH THAT OF A STANDARD SHARP EDGE ORIFICE. INPUT DATA DH(IN.
CH2O),PATM(IN HG),PNOZ(IN HG),PFL(IN HG),PREF(IN HG),DPFL(CM H2O),TCR
C(DEGREES F),TCL(DEGREES F),TNOZ(MV),TTD1(MV),PBAR(IN HG),L(NUMBER OF
CDATA SETS),N(NUMBER OF DATA POINTS WITHIN EACH SET)
      WRITE(6,101)
      READ(5,99)L
      DO 90 M=1,L
      READ(5,99)N
      READ(5,100)PBAR,TCL,TCR
      READ(5,100) (DH(I),I=1,N)
      READ(5,100) (PATM(I),I=1,N)
      READ(5,100) (PNOZ(I),I=1,N)
      READ(5,100) (TNOZ(I),I=1,N)
      READ(5,100) (TTD1(I),I=1,N)
      READ(5,100) (PFL(I),I=1,N)
      READ(5,100) (PREF(I),I=1,N)
      READ(5,100) (DPFL(I),I=1,N)
      D1O=6.065
      D1N=7.975
      D2O=4.2425
      D2N=4.25
      BO=D2O/D1O
      BN=D2N/D1N
      B=BN**4
      GAM=1.4
      EX1=GAM/(GAM-1.)
      EX2=(GAM-1.)/GAM
      EX3=2./GAM
      QKINF=0.689556
      A=D2O*(830.-5000.*BO+9000.*BO**2-4200.*BO**3+530./SQRT(D1O))
      GHGCL=13.63905-.0013630303*TCL
      GHGRM=13.63905-.0013630303*TCR
      CHGC=0.4891585*GHGCL/13.54
      CHGCR=0.4891585*GHGRM/13.54
      GW68=0.99837633+1.0605756*68./10000.-1.5931861*68.**2/1000000.
      GWRM=0.99837633+1.0605756*TCR/10000.-1.5931861*TCR**2/1000000.
      RATGW=GWRM/GW68
      PAMB=PBAR
      PAMB=PAMB*CHGC
      DO 50 I=1,N
```

```
      QDH=DH(I)
      QDPFL=DPFL(I)
      TTD1(I)=32.+35.98*TTD1(I)-.425*TTD1(I)**2
      TTD1R(I)=TTD1(I)+459.7
      TNOZ(I)=32.+35.98*TNOZ(I)-.425*TNOZ(I)**2
      TNOZR(I)=TNOZ(I)+459.7
      ALPHO=1.+0.00193*((TTD1(I)-68.)/100.)
      ALPHN=1.+0.00252*((TNOZ(I)-68.)/100.)
      DPFL(I)=QDPFL/2.54*GWRM*62.42732/1728.
      PFL(I)=CHGCR*(PREF(I)-PFL(I))+PAMB
      YO=1.-(.41+.35*BO**4)*DPFL(I)/(GAM*PFL(I))
      DH(I)=QDH*GWRM/12.*62.42732/144.
      PNOZ(I)=CHGCR*(PATM(I)-PNOZ(I))+PAMB
      XR=1.-(DH(I)/PNOZ(I))
      YN=SQRT(XR**EX3*EX1*((1.-XR**EX2)/(1.-XR))*((1.-B)/(1.-B*XR**EX3))
     1)
      HW68=QDPFL/2.54*RATGW
      Z=0.019+0.0024*(TTD1(I)/100.-1.)
      WPART=0.163842658*D2O**2*ALPHO*YO*SQRT(PFL(I)*HW68/TTD1R(I))
      C1=WPART*QKINF
      C2=C1*A*Z/5359.48144
      W(I)=C1/2.+SQRT((C1**2/4.)+C2)
      HW68N=QDH*RATGW
      FLOCO(I)=6.1034166*W(I)/(D2N**2*YN*ALPHN)*SQRT(TNOZR(I)/(HW68N*PNO
     1Z(I)))
      RE(I)=5359.48144*W(I)/Z
   50 CONTINUE
      WRITE(6,102)
      WRITE(6,103)M,PNOZ(1)
      WRITE(6,104)
      WRITE(6,105)PAMB,N,GAM
      WRITE(6,106)
      DO 90 I=1,N
      WRITE(6,107)I,W(I),FLOCO(I),RE(I)
   90 CONTINUE
   99 FORMAT(I3)
  100 FORMAT(8F10.4)
  101 FORMAT(1H1///32X,58HFLOW NOZZLE CALIBRATION FOR THE TRANSONIC TURB
     1INE TEST RIG)
  102 FORMAT (////32X,11HTEST SERIES25X,22HNOZZLE SUPPLY PRESSURE)
  103 FORMAT(/35X,I3,38X,F5.2)
  104 FORMAT(/32X,13HATMOS. PRESS.11X,11HDATA POINTS11X,5HGAMMA)
  105 FORMAT(/35X,F6.3,19X,I2,17X,F3.1)
  106 FORMAT(//34X,5HPOINT8X,9HFLOW RATE8X,9HDISCHARGE8X,8HREYNOLDS/47X,
     19H(LBM/SEC)7X,11HCOEFFICIENT8X,6HNUMBER//)
```

```
107 FORMAT(36X,I2,9X,F8.4,8X,F9.5,7X,F11.2)
    STOP
    END
```

FLOW NOZZLE CALIBRATION FOR THE TRANSONIC TURBINE TEST RIG

| TEST SERIES | | NOZZLE SUPPLY PRESSURE |
|---|---|---|
| 1 | | 39.19 |
| ATMOS. PRESS. | DATA POINTS | GAMMA |
| 14.766 | 10 | 1.4 |

| POINT | FLOW RATE (LBM/SEC) | DISCHARGE COEFFICIENT | REYNOLDS NUMBER |
|---|---|---|---|
| 1 | 4.5470 | 1.04389 | 1249496.00 |
| 2 | 4.1810 | 1.04332 | 1150119.00 |
| 3 | 3.7625 | 1.03974 | 1036495.37 |
| 4 | 3.3435 | 1.04034 | 921833.00 |
| 5 | 2.9460 | 1.03806 | 812751.44 |
| 6 | 2.6033 | 1.04049 | 718826.87 |
| 7 | 2.2851 | 1.03916 | 631762.94 |
| 8 | 1.8747 | 1.03327 | 519366.69 |
| 9 | 1.4961 | 1.02885 | 415375.44 |
| 10 | 1.0637 | 1.00591 | 295950.94 |

| TEST SERIES | | NOZZLE SUPPLY PRESSURE |
|---|---|---|
| 2 | | 41.95 |
| ATMOS. PRESS. | DATA POINTS | GAMMA |
| 14.767 | 10 | 1.4 |

| POINT | FLOW RATE (LBM/SEC) | DISCHARGE COEFFICIENT | REYNOLDS NUMBER |
|---|---|---|---|
| 1 | 4.6679 | 1.03796 | 1284592.00 |
| 2 | 4.2442 | 1.03850 | 1167508.00 |
| 3 | 3.8877 | 1.03734 | 1069204.00 |
| 4 | 3.4127 | 1.04024 | 939151.62 |
| 5 | 2.8829 | 1.03816 | 793691.87 |
| 6 | 2.5549 | 1.03302 | 703979.37 |
| 7 | 2.2868 | 1.03217 | 630379.37 |
| 8 | 1.9506 | 1.02720 | 538148.44 |
| 9 | 1.5451 | 1.01220 | 426719.87 |
| 10 | 1.0399 | 0.98741 | 287806.31 |

| TEST SERIES | | NOZZLE SUPPLY PRESSURE |
|---|---|---|
| 3 | | 34.30 |
| ATMOS. PRESS. | DATA POINTS | GAMMA |
| 14.735 | 2 | 1.4 |

| POINT | FLOW RATE (LBM/SEC) | DISCHARGE COEFFICIENT | REYNOLDS NUMBER |
|---|---|---|---|
| 1 | 4.2561 | 1.04044 | 1182130.00 |
| 2 | 3.9094 | 1.04132 | 1085137.00 |

| TEST SERIES | | NOZZLE SUPPLY PRESSURE |
|---|---|---|
| 4 | | 34.25 |
| ATMOS. PRESS. | DATA POINTS | GAMMA |
| 14.700 | 10 | 1.4 |

| POINT | FLOW RATE (LBM/SEC) | DISCHARGE COEFFICIENT | REYNOLDS NUMBER |
|---|---|---|---|
| 1 | 3.4087 | 1.03932 | 944578.00 |
| 2 | 3.0387 | 1.04327 | 842217.06 |
| 3 | 2.5675 | 1.04209 | 711613.37 |
| 4 | 2.3839 | 1.04038 | 660725.44 |
| 5 | 2.1594 | 1.03792 | 598632.69 |
| 6 | 1.9635 | 1.03493 | 544912.75 |
| 7 | 1.7285 | 1.03260 | 479896.50 |
| 8 | 1.4205 | 1.02484 | 395303.19 |
| 9 | 1.1926 | 1.02393 | 332649.62 |
| 10 | 0.9363 | 1.00979 | 261676.87 |

| TEST SERIES | | NOZZLE SUPPLY PRESSURE |
|---|---|---|
| 5 | | 29.35 |
| ATMOS. PRESS. | DATA POINTS | GAMMA |
| 14.682 | 9 | 1.4 |

| POINT | FLOW RATE (LBM/SEC) | DISCHARGE COEFFICIENT | REYNOLDS NUMBER |
|---|---|---|---|
| 1 | 3.9243 | 1.04078 | 1094621.00 |
| 2 | 3.5504 | 1.04636 | 990741.62 |
| 3 | 3.1456 | 1.04380 | 878523.81 |
| 4 | 2.7296 | 1.04415 | 762850.12 |
| 5 | 2.3435 | 1.04390 | 655627.62 |
| 6 | 2.0941 | 1.04002 | 586375.50 |
| 7 | 1.8079 | 1.03963 | 506764.06 |
| 8 | 1.4423 | 1.02582 | 404797.87 |
| 9 | 0.9900 | 1.02611 | 278830.06 |

TEST SERIES 6

NOZZLE SUPPLY PRESSURE 24.39

ATMOS. PRESS. 14.603

DATA POINTS 4

GAMMA 1.4

| POINT | FLOW RATE (LBM/SEC) | DISCHARGE COEFFICIENT | REYNOLDS NUMBER |
|---|---|---|---|
| 1 | 3.5521 | 1.04187 | 994823.81 |
| 2 | 3.3403 | 1.04228 | 935497.94 |
| 3 | 3.1144 | 1.04286 | 872236.44 |
| 4 | 2.8472 | 1.04237 | 796562.81 |

TEST SERIES 7

NOZZLE SUPPLY PRESSURE 24.32

ATMOS. PRESS. 14.574

DATA POINTS 6

GAMMA 1.4

| POINT | FLOW RATE (LBM/SEC) | DISCHARGE COEFFICIENT | REYNOLDS NUMBER |
|---|---|---|---|
| 1 | 2.5438 | 1.04131 | 711068.44 |
| 2 | 2.2157 | 1.03960 | 619473.12 |
| 3 | 1.9886 | 1.03860 | 556218.69 |
| 4 | 1.7660 | 1.03475 | 493973.37 |
| 5 | 1.5451 | 1.03297 | 432556.75 |
| 6 | 1.2198 | 1.03049 | 342052.44 |

TEST SERIES 8

NOZZLE SUPPLY PRESSURE 41.58

ATMOS. PRESS. 14.654

DATA POINTS 11

GAMMA 1.4

| POINT | FLOW RATE (LBM/SEC) | DISCHARGE COEFFICIENT | REYNOLDS NUMBER |
|---|---|---|---|
| 1 | 4.6614 | 1.04521 | 1294436.00 |
| 2 | 4.3785 | 1.04539 | 1216127.00 |
| 3 | 4.0059 | 1.04457 | 1112648.00 |
| 4 | 3.6474 | 1.04790 | 1013286.12 |
| 5 | 3.2227 | 1.04723 | 896041.56 |
| 6 | 2.8031 | 1.04634 | 779872.37 |
| 7 | 2.5465 | 1.04855 | 708955.31 |
| 8 | 2.2738 | 1.04442 | 633425.87 |
| 9 | 1.9652 | 1.03927 | 547810.06 |
| 10 | 1.5387 | 1.02991 | 429389.37 |
| 11 | 1.1206 | 1.01809 | 313372.31 |

# PROGRAM LABLEK

```
      DIMENSION PATM(80),PSPL(80),PHD(80),TTPLD(80),ERROR(80),TTD1(80),
     1PEL(80),HWEL(80),WREET(80),          WLABR(80),WREE(80),PE(80),PR(80)
     2,PREE(80),THD(80)
CTHIS PROGRAM CALCULATES THE LABYRINTH LEAK RATE OF THE TRANSONIC TURBIN
CRIG. INPUT DATA PATM(IN.HG.),PSPL(IN.HG.),PHD(IN.HG.),TTPLD(MV),THD(MV)
CTTD1(MV),PEL(IN.HG.),              HWEL(CM.H2O),              PBAR(IN.HG.)
CTCL(DEGREES F.),TCR(DEGREES F.),PREE(IN.HG.)
      A1=-1.004586E-01
      A2=2.122579E-01
      A3=-1.081851E-01
      A4=2.767576E-02
      A5=-3.489933E-03
      A6=1.726733E-04
      READ(5,99)L
      DO 50 M=1,L
      READ(5,100)PBAR,N,NRUN
      WRITE (6,199)NRUN
      WRITE(6,200)
      READ(5,101)TCL,TCR
      READ(5,101) (PATM(I),I=1,N)
      READ(5,101) (PSPL(I),I=1,N)
      READ(5,101) (PHD(I),I=1,N)
      READ(5,101) (TTPLD(I),I=1,N)
      READ(5,101) (TTD1(I),I=1,N)
      READ(5,101) (THD(I),I=1,N)
      READ(5,101) (PEL(I),I=1,N)
      READ(5,101) (PREE(I),I=1,N)
      READ(5,101) (HWEL(I),I=1,N)
      EN(1)=1.0
      EN(2)=1.1
      EN(3)=1.2
      EN(4)=1.3
      EN(5)=1.4
      D1= 2.067
      D2= 0.825
      B= D2/D1
      QKINE=0.608913
      A=D2*(830.-5000.*B+9000.*B**2-4200.*B**3+530./SQRT(D1))
      GAM=1.4
      GHGRM=13.63905-.0013630303*TCR
      GHGCL=13.63905-.0013630303*TCL
      CHGC=0.4891585*GHGCL/13.54
      CHGCR=0.4891585*GHGRM/13.54
      GW68=0.99837633+1.0605756*68./10000.-1.593186*68.**2/1000000.
      GWRM=0.99837633+1.0605756*TCR/10000.-1.593186*TCR**2/1000000.
```

```
      RATGW=GWRM/GW68
      PAMB=PBAR
      PAMB=PAMB*CHGC
      R=53.3448
      G=32.174
      DO 49 I=1,N
      OPATM=PATM(I)
      OPSPL=PSPL(I)
      OPHD=PHD(I)
      OTTPLD=TTPLD(I)
      OTTD1=TTD1(I)
      OPEL=PEL(I)
      OPREF=PREF(I)
      OHWEL=HWEL(I)
      THD(I)=32.+35.98*THD(I)-.435*THD(I)**2
      TTPLD(I)=32.+35.98*OTTPLD-.435*OTTPLD**2
      OTTD1=32.+35.98*OTTD1-.435*OTTD1**2
      ALPH=1.+.00193*((OTTD1-68.)/100.)
      DPEL=OHWEL/2.54*GWRM/12.*62.42732/144.
      OPEL=CHGCR*(OPREF-OPEL)+PAMB
      Y=1.-(0.41+0.35*B**4)*DPEL/(GAM*OPEL)
      HW68=OHWEL/2.54*RATGW
      TTD1R=OTTD1+459.7
      WPART=0.1115154*ALPH*Y*SQRT(OPEL*HW68/TTD1R)
      Z=0.019+0.0024*(OTTD1/100.-1.)
      C1=WPART*OKINE
      C2=C1*A*7/27560.727
      WLABR(I)=C1/2.+SQRT((C1**2/4.)+C2)
      RE(I)=27560.727*WLABR(I)/7
      OPSPL=CHGCR*(OPATM-OPSPL)+PAMB
      OPHD=CHGCR*(OPATM-OPHD)+PAMB
      PR(I)=OPSPL/OPHD
      TTPLDR=TTPLD(I)+459.7
      PHI=WLABR(I)/OPSPL*SQRT(TTPLDR*R/G)
      CORR=(1.0+.32*((TTPLD(I)-THD(I))/TTPLD(I)))
        WREF(I)=PHI*CORR**1.2
  504 WREFR=A1+A2*PR(I)+A3*PR(I)**2+A4*PR(I)**3+A5*PR(I)**4+A6*PR(I)**5
      WREFT(I)=WREFR
      IF(WREFT(I)-WREF(I))20,20,30
   20 ERROR(I)=-(WREF(I)-WREFT(I))/WREF(I)*100.
      GO TO 51
   30 ERROR(I)=(WREFT(I)-WREF(I))/WREFT(I)*100.
   51 WRITE(6,201)I,WLABR(I),PR(I),TTPLD(I),RE(I),WREF(I),WREFT(I),ERROR
     1(I),THD(I)
   49 CONTINUE
```

```
 50 CONTINUE
 99 FORMAT(I3)
100 FORMAT(F10.4,I2,I3)
101 FORMAT(8F10.4)
199 FORMAT (1H1//54X,16HTTRSS RUN NUMBER3X,I3)
200 FORMAT (    ///39X,53HLABYRINTH LEAK RATE OF THE TRANSONIC TURBINE
   1TEST RIG//2X,5HPOINT6X,9HLABYRINTH7X,9HLABYRINTH4X,12HPLENUM TOTAL
   26X,8HREYNOLDS 9X,8HREFERRED8X,11HANALYTICAL 6X,7HPERCENT9X,4HHOOD/
   313X,9HLEAK RATE7X,8HPRESSURE5X,11HTEMPERATURE8X,6HNUMBER10X,9HLEAK
   4 RATE8X,8HREFERRED9X,5HERROR5X,11HTEMPERATURE/13X,9H(LBM/SEC)9X,5H
   5RATIO8X,7H(DEG F)27X,7H(SQ IN)9X,9HLEAK RATE21X,7H(DEG F)//)
201 FORMAT(3X,I2,8X,F8.6,8X,F7.4,8X,F7.3,8X,F10.2,7X,F9.5, 9X,F8.6,7X,
   1F8.4,7X,F7.3)
    STOP
    END
```

TTRSS RUN NUMBER 27

LABYRINTH LEAK RATE OF THE TRANSONIC TURBINE TEST RIG

| POINT | LABYRINTH LEAK RATE (LBM/SEC) | LABYRINTH PRESSURE RATIO | PLENUM TOTAL TEMPERATURE (DEG F) | REYNOLDS NUMBER | REFERRED LEAK RATE (SQ IN) | ANALYTICAL REFERRED LEAK RATE | PERCENT ERROR | HOOP TEMPERATURE (DEG F) |
|---|---|---|---|---|---|---|---|---|
| 1 | 0.084465 | 5.5690 | 107.005 | 109630.50 | 0.077182 | 0.074548 | -3.4135 | 115.864 |
| 2 | 0.085082 | 5.4678 | 111.093 | 111805.52 | 0.078407 | 0.074400 | -5.0939 | 118.217 |
| 3 | 0.085526 | 5.3559 | 109.391 | 114077.25 | 0.078310 | 0.074303 | -5.7305 | 116.524 |
| 4 | 0.086093 | 5.4566 | 107.858 | 115708.56 | 0.078304 | 0.074395 | -5.7145 | 113.811 |
| 5 | 0.086881 | 5.4628 | 104.956 | 118244.31 | 0.078340 | 0.074402 | -5.2232 | 110.072 |
| 6 | 0.085693 | 5.3829 | 101.364 | 117920.44 | 0.078370 | 0.074324 | -5.1527 | 105.081 |
| 7 | 0.085647 | 5.4171 | 97.590 | 119213.56 | 0.078365 | 0.074355 | -5.1180 | 101.706 |
| 8 | 0.086158 | 5.4059 | 95.699 | 121205.87 | 0.078509 | 0.074346 | -5.4241 | 99.135 |
| 9 | 0.086213 | 5.3674 | 92.771 | 123121.12 | 0.078215 | 0.074311 | -4.9999 | 96.043 |
| 10 | 0.085482 | 5.3376 | 88.454 | 123918.19 | 0.077360 | 0.074288 | -3.9834 | 91.219 |
| 11 | 0.085284 | 5.3551 | 84.124 | 125485.44 | 0.077194 | 0.074301 | -3.7480 | 85.685 |
| 12 | 0.083399 | 5.3962 | 80.824 | 123203.31 | 0.075873 | 0.074336 | -2.0253 | 81.867 |
| 13 | 0.082868 | 5.3913 | 78.039 | 122473.37 | 0.075522 | 0.074333 | -1.5741 | 77.965 |
| 14 | 0.068396 | 3.2336 | 74.200 | 101152.37 | 0.062417 | 0.060027 | -4.7532 | 72.277 |
| 15 | 0.067472 | 3.2175 | 74.550 | 98774.94 | 0.062402 | 0.060081 | -3.4825 | 73.326 |
| 16 | 0.067640 | 3.2334 | 76.121 | 97631.50 | 0.062388 | 0.060030 | -3.6133 | 75.248 |
| 17 | 0.067689 | 3.2164 | 79.084 | 96251.00 | 0.061366 | 0.060076 | -2.0870 | 80.000 |
| 18 | 0.068397 | 3.2312 | 84.471 | 95023.56 | 0.062264 | 0.060024 | -3.2330 | 88.800 |
| 19 | 0.068580 | 3.2192 | 87.070 | 96161.69 | 0.062606 | 0.060085 | -1.0214 | 96.730 |

TTRSS RUN NUMBER 28

LABYRINTH LEAK RATE OF THE TRANSONIC TURBINE TEST RIG

| POINT | LABYRINTH LEAK RATE (LBM/SEC) | LABYRINTH PRESSURE RATIO | PLENUM TOTAL TEMPERATURE (DEG F) | REYNOLDS NUMBER | PREDICTED LEAK RATE (SQ IN) | ANALYTICAL PREDICTED LEAK RATE | PERCENT ERROR | HOOP TEMPERATURE (DEG F) |
|---|---|---|---|---|---|---|---|---|
| 1 | 0.021826 | 1.3314 | 61.123 | 32578.10 | 0.043589 | 0.045445 | 4.0859 | 59.740 |
| 2 | 0.025725 | 1.4502 | 61.299 | 38363.04 | 0.051375 | 0.049017 | -3.3389 | 59.554 |
| 3 | 0.027210 | 1.5885 | 61.564 | 40503.99 | 0.055252 | 0.054195 | -1.0393 | 59.544 |
| 4 | 0.028948 | 1.7786 | 61.828 | 43033.96 | 0.058863 | 0.058605 | -0.3959 | 59.740 |
| 5 | 0.030337 | 2.0187 | 62.092 | 45067.64 | 0.061507 | 0.062663 | 1.7006 | 59.544 |
| 6 | 0.031957 | 2.3155 | 62.357 | 47452.64 | 0.064824 | 0.065743 | 1.3973 | 59.740 |
| 7 | 0.033083 | 2.7261 | 62.709 | 49113.49 | 0.066714 | 0.068133 | 2.0817 | 59.740 |
| 8 | 0.037032 | 3.1010 | 63.061 | 54939.91 | 0.073049 | 0.075507 | 3.3352 | 59.917 |
| 9 | 0.042354 | 3.4257 | 63.414 | 62778.99 | 0.080137 | 0.080520 | 1.9026 | 59.934 |
| 10 | 0.048026 | 3.7731 | 63.766 | 71170.50 | 0.087130 | 0.086022 | -0.5622 | 59.279 |
| 11 | 0.051290 | 4.1759 | 64.118 | 75972.62 | 0.090340 | 0.092720 | 4.4594 | 59.447 |
| 12 | 0.058159 | 4.5450 | 64.557 | 86127.87 | 0.097033 | 0.093531 | -3.0357 | 59.800 |
| 13 | 0.063139 | 4.8767 | 65.085 | 93481.63 | 0.102017 | 0.103060 | 1.0234 | 59.976 |
| 14 | 0.068072 | 5.2587 | 65.788 | 100786.62 | 0.107402 | 0.104235 | -2.9136 | 60.153 |
| 15 | 0.073451 | 5.5364 | 66.491 | 108725.06 | 0.114466 | 0.114497 | 0.0411 | 60.506 |
| 16 | 0.071527 | 5.4391 | 68.861 | 104049.37 | 0.114589 | 0.114376 | -0.4184 | 61.564 |
| 17 | 0.073983 | 5.6582 | 70.526 | 105991.75 | 0.115503 | 0.114730 | -1.0358 | 62.269 |
| 18 | 0.073608 | 5.5273 | 73.501 | 103679.44 | 0.116063 | 0.114483 | -2.0756 | 63.679 |
| 19 | 0.073249 | 5.5528 | 78.300 | 101545.25 | 0.117049 | 0.114533 | -3.2773 | 66.316 |
| 20 | 0.073991 | 5.5957 | 81.172 | 101495.94 | 0.117667 | 0.114594 | -3.0558 | 67.896 |
| 21 | 0.074626 | 5.5415 | 82.996 | 101963.75 | 0.118477 | 0.114595 | -5.0515 | 68.940 |
| 22 | 0.073963 | 5.5279 | 87.070 | 100251.94 | 0.115874 | 0.114485 | -1.8335 | 81.519 |
| 23 | 0.075382 | 5.6280 | 92.426 | 99242.12 | 0.116623 | 0.114655 | -2.5819 | 87.762 |
| 24 | 0.075741 | 5.5308 | 95.699 | 99335.75 | 0.116865 | 0.114490 | -3.2158 | 92.254 |
| 25 | 0.075677 | 5.5054 | 100.164 | 100111.25 | 0.115702 | 0.114454 | -1.6473 | 102.229 |
| 26 | 0.076396 | 5.4655 | 104.956 | 100837.13 | 0.116641 | 0.114406 | -2.3153 | 114.151 |
| 27 | 0.078033 | 5.2217 | 108.028 | 103093.75 | 0.116590 | 0.116211 | -0.5089 | 120.004 |

TTRSS RUN NUMBER 22

LABYRINTH LEAK RATE OF THE TRANSONIC TURBINE TEST 216

| POINT | LABYRINTH LEAK RATE (LBM/SEC) | LABYRINTH PRESSURE RATIO | PLENUM TOTAL TEMPERATURE (DEG F) | REYNOLDS NUMBER | CORRECTED LEAK RATE (SQ IN) | ANALYTICAL CORRECTED LEAK RATE | PERCENT ERROR | WORK TEMPERATURE (DEG F) |
|---|---|---|---|---|---|---|---|---|
| 1 | 0.033354 | 1.4001 | 85.944 | 45456.91 | 0.048082 | 0.051243 | 6.2141 | 105.221 |
| 2 | 0.039216 | 1.6586 | 87.742 | 53278.64 | 0.054357 | 0.056014 | 2.9534 | 111.243 |
| 3 | 0.042311 | 1.8030 | 89.146 | 57360.87 | 0.056265 | 0.058175 | 4.0184 | 113.649 |
| 4 | 0.047126 | 1.9774 | 91.132 | 63013.36 | 0.059085 | 0.061000 | 3.2318 | 114.208 |
| 5 | 0.051266 | 2.1702 | 91.823 | 69653.81 | 0.062503 | 0.064434 | 2.8572 | 115.677 |
| 6 | 0.054204 | 2.3658 | 93.288 | 73728.25 | 0.064019 | 0.066124 | 3.1949 | 115.846 |
| 7 | 0.058356 | 2.6177 | 95.255 | 79297.37 | 0.066442 | 0.067632 | 1.7411 | 116.602 |
| 8 | 0.061834 | 2.8781 | 97.419 | 84024.12 | 0.068336 | 0.069737 | 2.0833 | 117.022 |
| 9 | 0.065040 | 3.1677 | 97.932 | 88571.00 | 0.069269 | 0.069722 | 0.6046 | 116.602 |
| 10 | 0.068253 | 3.4081 | 98.534 | 93018.94 | 0.070533 | 0.070752 | 0.3243 | 116.185 |
| 11 | 0.071632 | 3.9077 | 99.564 | 97129.75 | 0.071819 | 0.071991 | 0.2386 | 116.863 |
| 12 | 0.074619 | 4.2892 | 101.364 | 100306.62 | 0.072701 | 0.073007 | 0.3967 | 118.248 |
| 13 | 0.080311 | 4.5743 | 101.702 | 108067.75 | 0.073575 | 0.073570 | 0.0050 | 117.709 |
| 14 | 0.086070 | 4.8939 | 102.562 | 117185.81 | 0.074529 | 0.073987 | -0.7277 | 117.232 |
| 15 | 0.091794 | 5.1605 | 103.418 | 124979.64 | 0.075713 | 0.074176 | -2.0305 | 116.602 |
| 16 | 0.099423 | 5.9089 | 105.640 | 135438.81 | 0.076834 | 0.075611 | -1.7861 | 116.185 |

TTRSS RUN NUMBER 30

LABYRINTH LEAK RATE OF THE TRANSONIC TURBINE TEST SIG

| POINT | LABYRINTH LEAK RATE (LBM/SEC) | LABYRINTH PRESSURE RATIO | PLENUM TOTAL TEMPERATURE (DEG F) | REYNOLDS NUMBER | REFERRED LEAK RATE (SQ IN) | ANALYTICAL REFERRED LEAK RATE | PERCENT ERROR | HOOD TEMPERATURE (DEG F) |
|---|---|---|---|---|---|---|---|---|
| 1 | 0.034971 | 1.5151 | 85.511 | 48596.26 | 0.054604 | 0.052035 | -4.7049 | 93.288 |
| 2 | 0.038855 | 1.6533 | 85.858 | 54115.61 | 0.058001 | 0.055883 | -3.6527 | 93.288 |
| 3 | 0.043203 | 1.8195 | 86.551 | 60220.97 | 0.061528 | 0.059630 | -3.1124 | 93.590 |
| 4 | 0.047854 | 1.9881 | 86.897 | 66744.00 | 0.065422 | 0.062744 | -4.0575 | 93.256 |
| 5 | 0.050789 | 2.1750 | 87.416 | 71069.06 | 0.066702 | 0.064483 | -3.4570 | 91.736 |
| 6 | 0.054682 | 2.3702 | 87.935 | 76800.25 | 0.069124 | 0.066156 | -4.2979 | 91.736 |
| 7 | 0.057763 | 2.6285 | 88.281 | 81295.00 | 0.070003 | 0.067696 | -3.3111 | 91.564 |
| 8 | 0.061205 | 2.8761 | 88.627 | 86621.56 | 0.071436 | 0.068730 | -3.7876 | 91.564 |
| 9 | 0.064549 | 3.1589 | 88.108 | 92105.31 | 0.072462 | 0.069693 | -3.8295 | 91.219 |
| 10 | 0.066266 | 3.4865 | 87.935 | 94574.69 | 0.071703 | 0.070717 | -1.5099 | 90.873 |
| 11 | 0.070279 | 3.8718 | 87.762 | 100195.94 | 0.073326 | 0.071985 | -1.8651 | 90.873 |
| 12 | 0.072579 | 4.2467 | 87.762 | 103496.81 | 0.073382 | 0.072906 | -0.6433 | 90.873 |
| 13 | 0.075610 | 4.7290 | 87.762 | 107932.62 | 0.073869 | 0.073806 | -0.0859 | 91.044 |
| 14 | 0.078390 | 5.3212 | 87.762 | 111760.44 | 0.074150 | 0.074276 | 0.1632 | 90.873 |
| 15 | 0.083899 | 5.6315 | 87.940 | 119715.44 | 0.074592 | 0.074664 | 0.0965 | 90.873 |
| 16 | 0.090341 | 6.0351 | 88.281 | 128907.44 | 0.075311 | 0.076289 | 1.4113 | 90.873 |

```
C       PROGRAM TTRSS
C       COMPUTES EXPERIMENTAL PERFORMANCE CHARACTERISTICS OF THE
C       TURBINE TEST RIG
C       INPUT DATA DH(IN H20),PNOZ(IN HG),TNOZ(MV),PTPL(IN HG),PHUB(IN HG)
C       PTIP(IN HG),          ,TTPL(MV),PATM(IN HG),RPM(RPM),TORQR(COUNTS)
C       AXIL(COUNTS),DYNAR(COUNTS),PHD(IN HG),          ,PSPL(IN HG),
C       CLAXIL(COUNTS),CLTROR(COUNTS),PRE2(IN HG),THD(MV),P15 TH2U P21
C       (IN HG),TCL(DEGREES F),TCR(DEGREES F).
        DIMENSION DH(50),PNOZ(50),TNOZ(50),PTPL(50),PHUB(50),PTIP(50),
       1        TTPL(50),PATM(50),RPM(50),TORQR(50),AXIL(50),DYNAR(50),
       2PHD(50),        PSPL(50),CLAXIL(50), CLTROR(50),PRE2(50)
       3,P18(50),P15(50),P16(50),P17(50),P19(50),P20(50),TTPLD(50),
       4HW68(50),P21(50),THD(50)
        DIMENSION FLOWT(50),PR(50),HP(50),XKTS(50),COEFL(50),COEFM(50),
       1COEFP(50),COEFS(50),V1(50),V2(50),W1(50),W2(50),U1(50),U2(50),
       2T1(50),T2(50),T2IS(50),TT2(50),ALPH1(50),ALPH2(50),BETA1(50),
       3BETA2(50),DBETA(50),ETA(50),ETAT(50),ZETAP(50),ZETAS(50),ZETA(50),
       4REACHB (50),REACMN(50),REACTP (50),VM1(50),WM1(50),PHI(50),
       5        XI(50),PRS(50)
        COMMON G,R,C2,EX2,RM1,RM2,AAX,ATH,QFLOWT,QTTPL,T1IS,QT1,QPTPL,
       1QPTIP,QPHUB,P1AV,QP18,QP15,QP16,QP17,QPRS,TORQ,CLTORQ,QV1,VA1,VU1,
       2QZETAS,QPHI,QXI,GAM,QALPH1,QBETA1,QRPM,QU1,QW1,QVM1,QWM1,QPHD,
       3 CLEAX,EAX,RTIP1,RHUB1,SKT,PAMB,QP19,QP20,EX3,QP21,EX1
        READ 20,MM
   20 FORMAT(I10)
        CALL CANCEL (2)
        DO 99 M=1,MM
        CALL INPUT(NRUN,AXCLR,RADCLR,PBAR,N,TCL,TCR,DH,PNOZ,TNOZ,PTPL,
       1PHUB,PTIP,     TTPL,PATM,RPM,TORQR,AXIL,DYNAR,PHD,      PSPL,
       2CLAXIL,CLTROR,PRE2,P18,P15,P16,P17,P19,P20,P21,TTPLD,THD)
        CALL SETCON(BETA,D1,D2,AAXR,AAX,ATH,R,GAM,G,CP,CJ,C1,C2,EX2,EX1,
       1RTIP1,RHUB1,RTIP2,RHUB2,RM1,RM2,RADCLR,SKT,PKT,B,EX3,A,B1,B2,B3,B4
       2,B5,A1,A2,A3,A4,A5,A6,CL1,CL2,CL3,CL4,CE1,CE2,CE3,CE4)
        DO 90 I=1,N
        QDH=DH(I)
        QPNOZ=PNOZ(I)
        QTNOZ=TNOZ(I)
        QPTPL=PTPL(I)
        QPHUB=PHUB(I)
        QPTIP=PTIP(I)
        QTTPL=TTPL(I)
        QTTPLD=TTPLD(I)
        QTHD=THD(I)
        QPATM=PATM(I)
        QRPM=RPM(I)
```

```
      QTORQR=TORQR(I)
      QAXIL=AXIL(I)
      QDYNAR=DYNAR(I)
      QPHD=PHD(I)
      QPSPL=PSPL(I)
      QCLXIL=CLAXIL(I)
      QLTRQR=CLTRQR(I)
      QPRF2=PRF2(I)
      QP18=P18(I)
      QP15=P15(I)
      QP16=P16(I)
      QP17=P17(I)
      QP19=P19(I)
      QP20=P20(I)
      QP21=P21(I)
      CALL  CNVERT(QDH,QPNOZ,QTNOZ,QPTPL,QPHUB,QPTIP,QTTPLD,QTTPL,QPATM,
     1QRPM,QTORQR,QAXIL,QDYNAR,QPHD,QTHD, QPSPL, QLTRQR, QCLXIL,P1AV,P2,
     2QP18,QP15,QP16,QP17,TORQ,CLTORQ,FAX,CLFAX,DYNA,PRAR,QPRF2,TCL,
     3TCR,   PAMB,QP19,QP20,QHW6R,QP21,CL1,CL2,CL3,CL4,CF1,CF2,CF3,CF4)
      CALL FLORAT(A,R,D2,BETA,EX1,EX2,EX3,R,G,GAM,QPNOZ,QPSPL,QTNOZ,
     1QTTPLD,QPHD,QDH,QHW6R,NRUN,B1,B2,B3,B4,B5,A1,A2,A3,A4,A5,A6,
     2QFLOWT,QTHD,I)
      CALL STATOR
      CALL ROTOR(G,R,CP,CJ,C2,EX2,RM1,RM2,AAXR,QFLOWT,QTTPL,QRPM,DYNA,
     1QDP,P1AV,P2,QT1,QT2,QTT2,QT2IS,VA1,VU1,QV2,QW1,QW2,QU1,QU2,QALPH2,
     2QBETA1,QBETA2,EX1,RKT)
      CALL  PERFM(G,R,CP,C1,C2,EX2,GAM,QTTPL,QPTPL,QPHUB,QPTIP,QPHD,
     1QRPM,QFLOWT,DYNA,QDP,P2,T1IS,QT1,QT2IS,QPR,QETA,QXKIS,QCOEFL,
     2QCOEFM,QCOEFP,QCOEFS, QEACMN,QEACHB ,QEACTP ,QZETAR,QALPH1,QALPH2,
     3QBETA1,QBETA2,QDBETA,QHP,QU2,QW1,QW2,EX1,QTT2,QT2,QETAT,QU1)
      FLOWT(I)=QFLOWT
      PR(I)=QPR
      HP(I)=QHP
      XKIS(I)=QXKIS
      COEFL(I)=QCOEFL
      COEFM(I)=QCOEFM
      COEFP(I)=QCOEFP
      COEFS(I)=QCOEFS
      V1(I)=QV1
      V2(I)=QV2
      W1(I)=QW1
      W2(I)=QW2
      U1(I)=QU1
      U2(I)=QU2
      TTPL(I)=QTTPL
```

```
      T1(I)=QT1
      T2(I)=QT2
      T2IS(I)=QT2IS
      TT2(I)=QTT2
      ALPH1(I)=QALPH1
      ALPH2(I)=QALPH2
      BETA1(I)=QBETA1
      BETA2(I)=QBETA2
      QBETA(I)=QQBETA
      ETA(I)=QETA
      ETAT(I)=QETAT
      ZETAR(I)=QZETAR
      ZETAS(I)=QZETAS
      REACHB (I)=QREACHB
      REACMN(I)= QREACMN
      REACTP (I)=QREACTP
      VM1(I)=QVM1
      WM1(I)=QWM1
      PHI(I)=QPHI
      XI(I)=QXI
      PRS(I)=QPRS
      PTPL(I)=QPTPL
   90 CONTINUE
      CALL OUTPTA (NRUN,AXCLR,RADCLR,FLOWT,N ,HP,XKIS,COEFL,COEFM,COEFD,
     1COEFS,V1,V2,W1,W2,U1,U2,T1,T2,T2IS,TT2,ALPH1,ALPH2,BETA1,BETA2,
     2DBETA,ETA,ETAT,ZETAR,ZETAS,     REACHB ,REACMN,REACTP ,VM1,WM1,
     3PHI,     XI,PRS,RPM,TTPL,PR)
      CALL OUTPUT(NRUN,AXCLR,RADCLR,N,PR,XKIS,ETA,COEFL,COEFM,COEFD,
     1COEFS,REACHB ,REACTP ,PTPL)
   99 CONTINUE
      STOP
      END



      SUBROUTINE INPUT(NRUN,AXCLR,RADCLR,PRAR,N,TCL,TCP,DH,PNOZ,TNOZ,
     1PTPL,PHUB,PTIP,     TTPL,PATM,RPM,TORQR,AXIL,DYNAR,PHD,     PSPL,
     2CLAXIL, CLTRQR,PRE2,P18,P15,P16,P17,P19,P20,P21,TTPLD,THD)
      DIMENSION DH(50),PNOZ(50),TNOZ(50),PTPL(50),PHUB(50),PTIP(50),
     1 TTPLD(50)       ,PATM(50),RPM(50),TORQR(50),AXIL(50),DYNAR(50),
     2PHD(50),TTPL(50),PSPL(50),CLAXIL(50), CLTRQR(50),PRE2(50),
     3P18(50),P15(50),P16(50),P17(50),P19(50),P20(50),P21(50),THD(50)
      READ (5,101)NRUN
```

```
      READ (5,102)AXCLR,RADCLR
      READ (5,102)PBAR
      READ (5,101)N
      READ (5,102)TCL,TCR
      READ (5,102)(PRE2(I),I=1,N)
      READ (5,102)(PTPL(I),I=1,N)
      READ (5,102)(P15 (I),I=1,N)
      READ (5,102)(P16 (I),I=1,N)
      READ (5,102)(P17 (I),I=1,N)
      READ (5,102)(P18 (I),I=1,N)
      READ (5,102)(P19 (I),I=1,N)
      READ (5,102)(P20 (I),I=1,N)
      READ (5,102)(P21(I),I=1,N)
      READ (5,102)(DH(I),I=1,N)
      READ (5,102)(PATM(I),I=1,N)
      READ (5,102)(PNOZ(I),I=1,N)
      READ (5,102)(PSPL(I),I=1,N)
      READ (5,102)(PHUB(I),I=1,N)
      READ (5,102)(PTIP(I),I=1,N)
      READ (5,102)(PHD (I),I=1,N)
      READ (5,102)(TNOZ(I),I=1,N)
      READ (5,102)(TTPLD(I),I=1,N)
      READ (5,102)(TTPL(I),I=1,N)
      READ (5,102)(THD(I),I=1,N)
      READ (5,102)(RPM(I),I=1,N)
      READ (5,102)(AXIL(I),I=1,N)
      READ (5,102)(TORQR(I),I=1,N)
      READ (5,102)(DYNAR(I),I=1,N)
      READ (5,102)(CLAXIL(I),I=1,N)
      READ (5,102)(CLTRQR(I),I=1,N)
      WRITE(6,105)NRUN,PBAR
      WRITE(6,107)(PRE2(I),I=1,N)
      WRITE(6,107)(PTPL(I),I=1,N)
      WRITE(6,107)(P15(I),I=1,N)
      WRITE(6,107)(P16(I),I=1,N)
      WRITE(6,107)(P17(I),I=1,N)
      WRITE(6,107)(P18(I),I=1,N)
      WRITE(6,107)(P19(I),I=1,N)
      WRITE(6,107)(P20(I),I=1,N)
      WRITE(6,107)(P21(I),I=1,N)
      WRITE(6,107)(DH(I),I=1,N)
      WRITE(6,107)(PATM(I),I=1,N)
      WRITE(6,107)(PNOZ(I),I=1,N)
      WRITE(6,107)(PSPL(I),I=1,N)
      WRITE(6,107)(PHUB(I),I=1,N)
```

```
      WRITE(6,107)(PTIP(I),I=1,N)
      WRITE(6,107)(PHD(I),I=1,N)
      WRITE(6,107)(TNO7(I),I=1,N)
      WRITE(6,107)(TTPLO(I),I=1,N)
      WRITE(6,107)(TTPL(I),I=1,N)
      WRITE(6,107)(THD(I),I=1,N)
      WRITE(6,107)(RPM(I),I=1,N)
      WRITE(6,107)(AXIL(I),I=1,N)
      WRITE(6,107)(TORQR(I),I=1,N)
      WRITE(6,107)(DYNAR(I),I=1,N)
      WRITE(6,107)(CLAXIL(I),I=1,N)
      WRITE(6,107)(CLTRQR(I),I=1,N)
101   FORMAT(I10)
102   FORMAT(8E10.4)
105   FORMAT(1H1,//5X,11H RUN NUMBER,I5,//5X,40H INPUT DATA, CARD IMAGE,
     1 1 LINE = 1 CARD //,5X,6H PRAR=,F6.3/)
107   FORMAT(8E15.5)
      RETURN
      END


      SUBROUTINE SETCON(BETA,D1,D2,AAXR,AAX,ATH,R,GAM,G,CP,CJ,C1,C2,EX2,
     1EX1,RTIP1,RHUB1,RTIP2,RHUB2,RM1,RM2,RADCLR,SKT,BKT,B,EX3,A,B1,B2,
     2B3,B4,B5,A1,A2,A3,A4,A5,A6,CL1,CL2,CL3,CL4,CE1,CE2,CE3,CE4)
      BETA=0.163842658
      D1=7.975
      D2=4.250
      R=53.3448
      GAM=1.4
      G=32.174
      CP=0.24
      CJ=778.16
      C1=2.*G*CJ
      C2=2.*G*CJ*CP
      EX1=GAM/(GAM-1.)
      EX2=(GAM-1.)/GAM
      PI=3.14159
      ZN1=31.
      ASTAT=0.205
      SSTAT=0.8594
      THKS=0.024
      AROTR=0.1314
```

```
      SROTR=0.4440
      THKR=0.020
      RTIP1=4.584
      RHUB1=3.896
      RTIP2=9.516/2.
      RHUB2=7.652/2.
      AAX=PI*((RTIP1)**2-(RHUB1)**2)
      AAXR=PI*((RTIP2)**2-(RHUB2)**2)
      ATH=ASTAT*(RTIP1-RHUB1)*ZN1
      RM1=(RTIP1+RHUB1)/2.
      RM2=(RTIP2+RHUB2)/2.
      SKT=1.-(2.7/1000.)*(THKS/SSTAT*100.)**3.3*ASTAT/SSTAT
      RKT=(1.-(2.7/1000.)*(THKR/SROTR*100.)**3.3*AROTR/SROTR)*((AAXR+
     13.14159*RADCLR*(RTIP2+RADCLR/2.))/AAXR)
      B=(D2/D1)**4
      EX3=2./GAM
      A=6.316*3600./D2
      B1=0.93292874
      B2=4.268322E-07
      B3=-6.151495E-13
      B4=3.895006E-19
      B5=-9.138062E-26
      A1=-1.004586E-01
      A2=2.122579E-01
      A3=-1.081851E-01
      A4=2.767576E-02
      A5=-3.489933E-03
      A6=1.726733E-04
      CL1=-4.901048E-02
      CL2=7.376791E-03
      CL3=-4.121890E-06
      CL4=1.661981E-08
      CE1=-2.631117E-01
      CE2=3.890573E-02
      CE3=-2.068711E-06
      CE4=2.281905E-09
      RETURN
      END



      SUBROUTINE CNVERT(DH,PNOZ,TNOZ,PTPL,PHUB,PTIP,TTPLD,TTPL,PATM,PDM,
     1TORQR,AXIL,DYNAR,PHD,THD, PSPL, CLTROR,CLAXIL,P1AV,P2,P18,P15,P16,
```

```
2P17,TORQ,CLTORQ,FAX,CLFAX,DYNA,PBAR,PRE2,TCL,TCR,   PAMB,P1R,P2C,
3HW68,P21,CL1,CL2,CL3,CL4,CF1,CF2,CF3,CF4)
 TEMP(X)=32.+35.98*X-.435*X**2
 GWRM=0.99837633+1.0605756*TCR/10000.-1.5931861*TCR**2/10000000.
 GW68=0.99837633+1.0605756*68./10000.-1.5931861*68.**2/10000000.
 RATGW=GWRM/GW68
 GHGCL=13.63905-0.0013630303*TCL
 GHGCR=13.63905-0.0013630303*TCR
 CHGC =0.4891585*GHGCL/13.54
 CHGCR=0.4891585*GHGCR/13.54
 PAMB=PBAR
 PAMB=PAMB*CHGC
 HW68=DH*RATGW
 DH=DH*GWRM/12.*62.42732/144.
 PNOZ=CHGCR*(PATM-PNOZ)+PAMB
 PTPL=CHGCR*(PRE2-PTPL)+PAMB
 PHUB=CHGCR*(PATM-PHUB)+PAMB
 PTIP=CHGCR*(PATM-PTIP)+PAMB
 P15=CHGCR*(PRE2-P15)+PAMB
 P16=CHGCR*(PRE2-P16)+PAMB
 P17=CHGCR*(PRE2-P17)+PAMB
 P18=CHGCR*(PRE2-P18)+PAMB
 P19=CHGCR*(PRE2-P19)+PAMB
 P20=CHGCR*(PRE2-P20)+PAMB
 P21=CHGCR*(PRE2-P21)+PAMB
 PSPL=CHGCR*(PATM-PSPL)+PAMB
 PHD=CHGCR*(PATM-PHD)+PAMB
 P2=PHD
 TTPL= TEMP(TTPL)+459.7
 TNOZ=TEMP(TNOZ)
 TTPLD=TEMP(TTPLD)
 THD=TEMP(THD)
 ST1=-4.955933E-01
 ST2=4.451445E-01
 ST3=-4.259542E-05
 ST4=4.823251E-08
 TORQ=(ST1+ST2*TORQR+ST3*TORQR**2+ST4*TORQR**3)/12.
 CLTORQ=(CL1+CL2*CLTRQR+CL3*CLTRQR**2+CL4*CLTRQR**3)/12.
 FAX=0.1*AXIL
 CLFAX=CF1+CF2*CLAXIL+CF3*CLAXIL**2+CF4*CLAXIL**3
 DYNA=DYNAR/30.
 RETURN
 END
```

```
      SUBROUTINE FLORAT (A,B,D2,BETA,EX1,EX2,EX3,R,G,GAM,PNOZ,PSPL,TNOZ,
     1TTPLD,PHD,DH,HW68,NRUN,B1,B2,B3,B4,B5,A1,A2,A3,A4,A5,A6,FLOWT,THD,
     2I)
      ALPHN=1.+0.00252*(TNOZ-68.)/100.
      XR=1.-(DH/PNOZ)
      YN=SQRT(XR**EX3*EX1*((1.-XR**EX2)/(1.-XR))*((1.-B)/(1.-B*XR**EX3))
     1)
      Z=0.019+0.0024*(TNOZ/100.-1.)
      TNOZR=TNOZ+459.7
      EPS=0.0
   48 WG=1.0+EPS
      RE=A*WG/7
      IF(RE.GT.1300000.)GO TO 52
      CN=B1+B2*RE+B3*RE**2+B4*RE**3+B5*RE**4
      W=BETA*D2**2*ALPHN*YN*CN*SQRT(PNOZ*HW68/TNOZR)
      WD=W-WG
      IF(WD.LT..0001)GO TO 50
      EPS=EPS+0.88*WD
      GO TO 48
   52 WRITE(6,100)NRUN,I
  100 FORMAT  (/33X,I4,7X,I2,7X,36HFLOW RATE TOO HIGH, CHECK INPUT DATA/
     1)
   50 FLOW=W
      PR=PSPL/PHD
      WREF=A1+A2*PR+A3*PR**2+A4*PR**3+A5*PR**4+A6*PR**5
      CORR=(1.0+0.32*((TTPLD-THD)/TTPLD))**1.2
      TTPLDR=TTPLD+459.7
      WLAB=WREF*PSPL/SQRT(TTPLDR*R/G)/CORR
      FLOWT=FLOW-WLAB
      RETURN
      END



      SUBROUTINE STATOR
      COMMON G,R,C2,EX2,RM1,RM2,AAX,ATH, FLOWT, TTPL,TITS, T1, PTPL,
     1PTIP,PHUB,P14V,P18,P15,P16,P17,PRS,TORQ,CLTORQ,V1,VA1,VU1,
     2 ZETAS, PHI, XI,GAM, ALPHI, BETA1, RPM, U1, W1, VM1, WM1, PHD,
     3 CLEAX,EAX,RTIP1,RHUB1,SKT,PAMB,P19,P20,EX3,P21,EX1
      RR=0.0
```

911

```
      WRITE (6,55) SKT
   55 FORMAT (///10X,6HKTE =  ,F7.5//9X,3HEPS8X,4HP1AV9X,3HT1M10X,3HT1C9X,
     14HVA1M9X,4HVA1C10X,4HVM1M9X,4HVM1C7X,8HALPHA 1M5X,8HALPHA 1C//)
   97 EPS=RR
      P1AV=PHUB/3.*(((1.+EPS)*(2.*RTIP1)**2+(2.*RHUB1)*(2.*RTIP1)-(2.+
     1EPS)*(2.*RHUB1)**2)/((2.*RTIP1)**2-(2.*RHUB1)**2))+PTIP/3.*(((2.+
     2EPS)*(2.*RTIP1)**2-(2.*RHUB1)*(2.*RTIP1)-(1.+EPS)*(2.*RHUB1)**2)/
     3((2.*RTIP1)**2-(2.*RHUB1)**2))
      CALL MOMENT(G,C2,AAX,RM1,PHD,PTIP,P1AV,PHUB,P18,P15,P16,P17,
     1FLOWT,TORQ,CLEAX,EAX,TTPL,VU1,VA1,V1,ALPH1,T1,RTIP1,RHUB1,CPTORQ,
     2RADCLR,PBAR,DELP1,EX2,SKT,R,EPS,P19,P20,P21)
      T1C=EX1*G*(P1AV*AAX*SKT)**2/(R*FLOWT**2)*(SQRT(1.-2.*EX2*R*FLOWT**
     12/(G*(P1AV*AAX*SKT)**2)*(VU1**2/C2-TTPL))-1.)
      V1C=SQRT((TTPL-T1C)*C2)
      VA1C=SQRT(V1C**2-VU1**2)
      ALPH1C=ATAN(VU1/VA1C)
      AL1C=ALPH1C*57.295779
      AL1M=ALPH1*57.295779
      VM1C=V1C/SQRT(GAM*G*R*T1C)
      VM1M=V1/SQRT(GAM*G*R*T1)
      WRITE (6,58)EPS,P1AV,T1,T1C,VA1,VA1C,VM1M,VM1C,AL1M,AL1C
   58 FORMAT (10F13.5)
      DIFF=ABS(T1C-T1)
      IF (DIFF-0.02)98,98,50
   50 IF (T1C.LT.T1) GO TO 47
      RR=RR+DIFF/250.
      GO TO 97
   47 RR=RR-DIFF/250.
      GO TO 97
   98 PRS=P1AV/PTPL
      T1IS=TTPL*PRS**EX2
      ZETAS=(T1-T1IS)/(TTPL-T1IS)
      PHI=FLOWT/PTPL/ATH *SQRT (TTPL* R/G)
      PRST=PRS
      IF (PRST.LT.0.52828) PRST=0.52828
      XI=PHI/SQRT(2./EX2*(PRST**EX2-  PRST**((GAM+1.)/GAM)))
      RAD=.10471967*RPM
      U1=RM1*RAD/12.
      WU1=VU1-U1
      WA1=VA1
      BETA1=ATAN (WU1/WA1)
      W1=WA1/COS (BETA1)
      VM1=V1/SQRT (GAM*G* R*T1)
      WM1=W1/SQRT (GAM*G* R*T1)
      RETURN
```

```
      END


      SUBROUTINE MOMENT(G,C2,AAX,RM1,PHD,PTIP,P1AV,PHUB,P18,P15,P16,P17,
     1FLOWT,TORQ,CLEAX,FAX,TTPL,VU1,VA1,V1,ALPH1,T1,RTIP1,RHUB1,CLTORQ,
     2RADCLR,PBAR,DELP1,EX2,SKT,R,EPS,P19,P20,P21)
      VU1=(TORQ+CLTORQ)*G/FLOWT/RM1*12.
      PI=3.14159
      A1=PI*(5.125)**2
      A2=PI*((5.125)**2-(5.003)**2)
      A3=PI*(5.003**2-4.901**2)
      A3A=PI*(4.901**2-4.773**2)
      A4=PI*(4.773**2-RTIP1**2)
      A5=PI*(RTIP1**2-RHUB1**2)
      A6=PI*RHUB1**2
      F1=A1*PHD
      F2=A2*P21
      F3=A3*((P20+P19)/2.)
      F3A=A3A*P18
      F4=A4*PTIP
      F5=A5*P1AV
      F6=A6*PHUB
      FNET=F1+FAX+CLEAX-F2-F3-F4-F5-F6-F3A
       VA1=G*FNET/FLOWT
      ALPH1=ATAN (VU1/VA1)
      V1=SQRT (VA1**2+VU1**2)
      T1=TTPL-V1**2/C2
      RETURN
      END



      SUBROUTINE ROTOR(G,R,CP,CJ,C2,EX2,RM1,RM2,AAXR,FLOWT,TTPL,RPM,
     1DYNA,DP,P1AV,P2,T1,T2,TT2,T2IS,VA1,VU1,V2,W1,W2,U1,U2,ALPH2,BETA1,
     2BETA2,EX1,RKT)
      RAD=.104719667*RPM
      DP=DYNA*RAD/CJ
      VU2=RM1/RM2*VU1-DYNA*G/RM2/FLOWT*12.
      TT2=TTPL-DP/CP/FLOWT
      T2IS=T1*(P2/P1AV)**EX2
```

```
      U2=RM2*RAD/12.
      WU2=VU2-U2
      TE=T1+(W1**2.-U1**2.+U2**2.)/C2
      T2=EX1*G*(P2*AAXR*RKT)**2/(R*FLOWT**2)*(SQRT(1.-2.*EX2*R*FLOWT**2
     1/(G*(P2*AAXR*RKT)**2)*(WU2**2/C2-TE))-1.)
      V2=SQRT ((TT2-T2)*C2)
      VA2=SQRT(V2**2-VU2**2)
  615 WA2=VA2
      W2=SQRT (WA2**2+WU2**2)
      ALPH2=ATAN (VU2/VA2)
      BETA2=ATAN (WU2/WA2)
      RETURN
      END
```

```
      SUBROUTINE PERFRM  (G,R,CP,C1,C2,EX2,GAM,TTPL,PTPL,PHUB,PTIP,PHD,
     1RPM,FLOWT,DYNA,DP,P2,T1IS,T1,T2IS,PR,ETA,XKIS,COEFL,COEFM,COEFP,
     2COEFS,REACMN,REACHB ,REACTP ,ZETAR,ALPH1,ALPH2,BETA1,BETA2,DBETA,
     3HP,U2,W1,W2,EX1,TT2,T2,ETAT,U1)
      PR=PTPL/P2
      T2TH=TTPL*(PHD/PTPL)**EX2
      DHIS=CP*(TTPL-T2TH)
      ETA=DP/DHIS/FLOWT
      PT2=P2*(TT2/T2)**EX1
      TT2IS=TTPL*(PT2/PTPL)**EX2
      ETAT=DP/(CP*(TTPL-TT2IS))/FLOWT
      XKIS=DHIS*C1/U1**2
      DEL=PTPL/14.69
      THETA=SQRT (GAM* R*TTPL)/196.8107
      COEFL=FLOWT*THETA/DEL
      COEFM=DYNA/DEL
      HP=3600./2545.*DP
      COEFP=HP/(DEL*THETA)
      COEFS=RPM/THETA
      REACMN=1.0-CP*(TTPL-T1IS)/DHIS
      REACHB=((PHUB/PHD)**EX2-1.)/((PTPL/PHD)**EX2-1.)
      REACTP=((PTIP/PHD)**EX2-1.)/((PTPL/PHD)**EX2-1.)
      SQW2TH=C2*(T1-T2IS)+W1**2+(U2**2-U1**2)
      ZETAR=1.-W2**2/SQW2TH
      ALPH1=ALPH1*57.295779
      ALPH2=ALPH2*57.295779
      BETA1=BETA1*57.295779
```

```
      BETA2=BETA2*57.295779
      DBETA=BETA1-BETA2
      RETURN
      END



      SUBROUTINE OUTPTA (NRUN,AXCLR,RADCLR,FLOWT,N ,HP,XKIS,COEFL,COEFM,
     1COEFP,COEFS,V1,V2,W1,W2,U1,U2,T1,T2,T2IS,TT2,ALPH1,ALPH2,BETA1,
     2BETA2,DBETA,ETA,ETAT,ZETAR,ZETAS,     REACHR ,REACMN,REACTP ,
     3VM1,WM1,PHI,     XI,PRS,RPM,TTPL,PR)
      DIMENSION FLOWT(50),PR(50),HP(50),XKIS(50),COEFL(50),COEFM(50),
     1COEFP(50),COEFS(50),V1(50),V2(50),W1(50),W2(50),U1(50),U2(50),
     2T1(50),T2(50),T2IS(50),TT2(50),ALPH1(50),ALPH2(50),BETA1(50),
     3BETA2(50),DBETA(50),ETA(50),ETAT(50),ZETAR(50),ZETAS(50),ZETA(50),
     4REACHR (50),REACMN(50),REACTP (50),VM1(50),WM1(50),PHI(50),
     5          XI(50),PRS(50),RPM(50),TTPL(50)
      WRITE(6,805)
  805 FORMAT(1H1//24H TURBINE CIRCULAR ARC  T //10H STATOR  T //)
      WRITE(6,806)NRUN,AXCLR,RADCLR
  806 FORMAT(11H RUN NUMBER I3,8H SPACING F10.3,11H TIP CLEAR. F10.3//)
      WRITE(6,807)
  807 FORMAT (5X,6H POINT  6X,10H FLOW RATE  9X,4H RPM
     1 5X,15H PRESSURE RATIO   5X,11H HORSEPOWER  /)
      DO 808 I=1,N
  808 WRITE(6,809)I,FLOWT(I),RPM(I),PR(I),HP(I)
  809 FORMAT (I5,12X,4(F10.4,5X))
      WRITE(6,810)
  810 FORMAT(///20X,37H DIMENSIONLESS PERFORMANCE PARAMETERS //
     15X, 6H POINT 11X, 2H K 10X, 9H REFERRED  8X, 9H REFERRED
     27X,9H REFERRED  7X,9H REFERRED  6X,      /
     317X,11H ISENTROPIC  5X,10H FLOW RATE  8X, 7H TORQUE
     4 9X, 6H POWER 10X, 6H SPEED  9X,/)
      DO 811 I=1,N
  811 WRITE(6,812)     I,XKIS(I),COEFL(I),COEFM(I),COEFP(I),COEFS(I)
  812 FORMAT ( I5,12X,6(F10.4,6X))
      WRITE(6,813)NRUN
  813 FORMAT(1H1/////5X,16H GENERAL RESULTS //20X,20H VELOCITIES (FT/SEC
     1)//,20X,11H RUN NUMBER   I5/
     2//5X, 6H POINT 10X, 3H V1 12X, 3H V2 12X,3H W1 12X,3H W2
     312X,3H U1 12X,3H U2  /  )
      DO 814 I=1,N
  814 WRITE(6,815)   I,V1(I),V2(I),W1(I),W2(I),U1(I),U2(I)
```

```
815 FORMAT ( I5,12X, 6(F10.5,5X))
    WRITE(6,816)
816 FORMAT (       /20X,23H TEMPERATURES (DEG R )  //
   1 5X, 6H POINT    8X, 7H PLENUM  6X, 7H STATOR  9X, 6H ROTOR
   2 9X,11H ISENTROPIC   4X, 6H TOTAL  /19X, 6H TOTAL   7X,
   310H DISCHARGE  5X,10H DISCHARGE  5X, 8H FROM T1   7X,
   410H DISCHARGE / )
    DO 817 I = 1,N
817 WRITE(6,818)       I, TTPL(I), T1(I), T2(I), T2IS(I), TT2(I)
818 FORMAT ( I5,12X, 5(F10.5,5X))
    WRITE(6,819)NRUN
819 FORMAT(1H1/////20X,33H FLOW ANGLES (DEGREES FROM AXIAL)  //
   120X,11H RUN NUMBER    I5///
   2 5X, 6H POINT    7X, 8H ALPHA 1  8X, 8H ALPHA 2  7X, 7H BETA 1
   3 8X, 7H BETA 2   6X,12H DELTA BETA  / )
    DO 820 I=1,N
820 WRITE(6,821) I, ALPH1(I),ALPH2(I),BETA1(I),BETA2(I),DBETA(I)
821 FORMAT ( I5,12X, 5(F10.5,5X))
    WRITE(6,822)
822 FORMAT (       ///20X,24H EFFICIENCIES AND LOSSES     //
   12X,6H POINT 10X, 11H EFFICIENCY 14X, 11H EFFICIENCY 17X, 5H ZETA
   220X, 5H ZETA/ 17X, 13H TOTAL STATIC 13X, 12H TOTAL TOTAL 16X, 6H R
   3OTOR 18X, 7H STATOR/)
    DO 823 I=1,N
823 WRITE(6,824)   I,ETA(I),ETAT(I),ZETAR(I),ZETAS(I)
824 FORMAT (I5,12X,4(F10.5,15X))
    WRITE(6,825)NRUN
825 FORMAT  (1H1,36H MACH NUMBERS AND DEGREE OF REACTION   //
   120X,11H RUN NUMBER    I5///
   25X,6H POINT  8X,9H REACTION  6X,9H REACTION  7X,9H REACTION
   37X,9H ABSOLUTE  7X,9H RELATIVE  / 23X,4H HUB  9X,5H MEAN  11X,
   44H TIP  12X,7H MACH 1  9X,7H MACH 1   //)
    DO 826 I=1,N
826 WRITE(6,827) I,REACHB (I),REACMN(I),REACTP (I),VM1(I),WM1(I)
827 FORMAT  (I5,12X,5(F10.4,6X))
    WRITE(6,828)
828 FORMAT (//49H STATOR PRESSURE RATIO AND THROAT BLOCKAGE FACTOR//
   12X,6H POINT 11X,9H PRESSURE 17X,9H BLOCKAGE /
   221X,6H RATIO 19X,7H FACTOR /)
    DO 829 I=1,N
829 WRITE(6,830) I,PRS(I),XI(I)
830 FORMAT(I5,12X,2(F10.5,15X))
    RETURN
    END
```

```
      SUBROUTINE OUTPUT(NRUN,AXCLR,RADCLR,N,PR,XKIS,EFF,COEFL,COEFM,
     1                  COEFP,COEFS,REACHB ,REACTP ,PTPL)
      DIMENSION PR(50),XKIS(50),EFF(50),COEFL(50),COEFM(50),COEFP(50),
     1          COEFS(50),REACHB (50),REACTP (50),PTPL(50),NPTS(8),
     2          NPTSS(8),ICOEFS(50)
      READ(5,905)D,A,T,E
      READ(5,906)                                TTYPER,STATOR,METHOD
      READ(5,907)RMEAN
      READ(5,908)J
      READ(5,909)  (NPTS(K),NPTSS(K),K=1,8)
      DO 919 I=1,N
  919 EFF(I)=100.*EFF(I)
      DO 950 JJ=1,2
      IF (N+3*J-43) 920,920,921
  920 NPP=1
      NXX=N
      GO TO 922
  921 NPP=2
      NXX=43
  922 NP=1
      NX=1
      K=1
  923 WRITE(6,900)                          NP,NPP,       TTYPER,STATOR,RADCLR,
     1           AXCLR,NRUN,D,A,T,E,METHOD
      WRITE(6,901)RMEAN
      DO 940 I=NX,NXX
      ICOEFS(I)=COEFS(I)
      II=I
      WRITE(6,902)  I,PR(I),XKIS(I),EFF(I),COEFL(I),COEFM(I),COEFP(I),
     1           ICOEFS(I),REACHB (I),REACTP (I)
      IF (J-K) 940,924,924
  924 IF (I-NPTSS(K)) 940,925,940
  925 LL=NPTS(K)
      LLL=NPTSS(K)
      INTGER =LLL-LL+1
      AVG=INTGER
      AVGATM=0.0
      AVGPR=0.0
      DO 926 L=LL,LLL
      AVGATM=AVGATM+PTPL(L)/14.69 /AVG
  926 AVGPR=AVGPR+PR(L)/AVG
```

```
      LLL=LLL-1
      COMPAR =PR(LL)
      DO 931 L=LL,LLL
      IF (COMPAR -PR(L+1)) 930,931,931
  930 COMPAR =PR(L+1)
  931 CONTINUE
      DEVHI  =100.*(COMPAR -AVGPR)/AVGPR
      COMPAR =PR(LL)
      DO 934 L=LL,LLL
      IF (COMPAR -PR(L+1)) 934,934,933
  933 COMPAR =PR(L+1)
  934 CONTINUE
      DEVLOW=100.*(AVGPR-COMPAR )/AVGPR
      WRITE(6,903)  NPTS(K),NPTSS(K),AVGPR,DEVHI  ,DEVLOW,AVGATM
      IF (NPTSS(K+1)+3*(K+1)-43) 935,936,935
  935 IF (NP-2) 944,936,944
  936 K=K+1
  940 CONTINUE
  944 IF (N-II) 950,950,945
  945 K=K+1
      NP=2
      NX=II+1
      NXX=N
      WRITE(6,904)NP
      GO TO 923
  900 FORMAT(1H1,/ ,9X,7H REPORT,12X      ,77X,6H SHEET,1X,I1,3H OF,1X,I1
     1,//,33X,53H TURBO PROPULSION LABORATORY USNPGS, MONTEREY, CALIF. ,
     2///,21X,79H REDUCED PERFORMANCE DATA OF TURBINE FROM TESTS WITH TR
     3ANSONIC TURBINE TEST RIG // ,27H TURBINE TYPE CIRCULAR-ARC A2,8H S
     4TATOR 1X, A2,4X,25H RADIAL ROTOR TIP CLEAR.=,2X,F6.3,3H IN.  AXIA
     5L CLEAR. STATOR-ROTOR=,1X,F5.3,4H IN./ ,24X,13H TEST RUN NO.,1X,I2
     6,3X,13H DATE OF TEST1X,4A2,2X,22H DATA REDUCTION METHOD,2X,A2 // )
  901 FORMAT(7X,105H POINT  PRESSURE  ISENTROPIC  EFFICIENCY  REFERRED
     1   REFERRED  REFERRED  REFERRED  DEGREE OF  DEGREE OF / ,15X, 94H
     2RATIO     HEAD COEFF.  TOT-STATIC  FLOW RATE   TORQUE     POWER
     3 SPEED    REACTION   REACTION / ,24X, 4H (R=,   F5.3,7H IN.)  PER
     4CENT     LBM/SEC     FT-LB       HP          RPM       (HUB)      (TIP)
     5  //)
  902 FORMAT(9X,I2,5X,F6.4,5X,F6.4,8X,F5.2,6X,F6.4,5X,F6.3,4X,F6.3,4X,
     1I5,4X,F6.4,6X,F5.4 )
  903 FORMAT(/5X,12H FOR POINTS , I2,3H TO,1X,I2,21H AVG. PRESSURE RATIO
     1=,1X,F6.4,18H , MAX.DEVIATION +,   F5.3,7H PCT. -,   F5.3,10H PCT.
     2, PAVG./PATMO=,1X,F6.4 /)
  904 FORMAT(/45X,16H CONTD. ON SHEET,1X,I1,/)
  905 FORMAT(10X,4A2)
```

```
906 FORMAT(15X,3A2)
907 FORMAT(F5.3)
908 FORMAT(I1)
909 FORMAT(8(2I5))
950 CONTINUE
    RETURN
    END
```

TURBINE CIRCULAR ARC I
STATOR I

RUN NUMBER 32 SPACING 0.250 TIP CLEAR. 0.009

| POINT | FLOW RATE | RPM | PRESSURE RATIO | HORSEPOWER |
|---|---|---|---|---|
| 1 | 1.4920 | 11320.0000 | 2.0276 | 40.7987 |
| 2 | 1.4894 | 12000.0000 | 2.0258 | 41.8028 |
| 3 | 1.4833 | 12980.0000 | 2.0305 | 42.8282 |
| 4 | 1.4760 | 14010.0000 | 2.0265 | 42.5820 |
| 5 | 1.4745 | 15030.0000 | 2.0318 | 43.7748 |
| 6 | 1.4724 | 15900.0000 | 2.0265 | 44.0891 |
| 7 | 1.4714 | 17000.0000 | 2.0247 | 43.1480 |
| 8 | 1.4685 | 17930.0000 | 2.0300 | 42.6642 |
| 9 | 1.4710 | 19080.0000 | 2.0212 | 40.8000 |

DIMENSIONLESS PERFORMANCE PARAMETERS

| POINT | K ISENTROPIC | REFERRED FLOW RATE | REFERRED TORQUE | REFERRED POWER | REFERRED SPEED |
|---|---|---|---|---|---|
| 1 | 7.4668 | 1.3702 | 16.2194 | 32.6023 | 10559.4414 |
| 2 | 6.6408 | 1.3662 | 15.6545 | 33.3479 | 11190.6172 |
| 3 | 5.6990 | 1.3614 | 14.8276 | 34.1468 | 12097.7617 |
| 4 | 4.8795 | 1.3597 | 13.7092 | 34.0765 | 13057.7539 |
| 5 | 4.2537 | 1.3564 | 13.1181 | 34.9811 | 14008.4258 |
| 6 | 3.7862 | 1.3537 | 12.4858 | 35.2321 | 14823.4297 |
| 7 | 3.3047 | 1.3517 | 11.4254 | 34.4895 | 15857.8203 |
| 8 | 2.9807 | 1.3509 | 10.7266 | 34.1515 | 16725.3359 |
| 9 | 2.6162 | 1.3509 | 9.6259 | 32.6218 | 17803.0430 |

GENERAL RESULTS

VELOCITIES (FT/SEC)
RUN NUMBER 32

| POINT | V1 | V2 | W1 | W2 | U1 | U2 |
|---|---|---|---|---|---|---|
| 1 | 1077.36328 | 242.01395 | 678.67090 | 575.14404 | 418.85059 | 423.98730 |
| 2 | 1058.00562 | 232.69995 | 636.31982 | 581.46729 | 444.01099 | 449.45630 |
| 3 | 1058.29004 | 216.44083 | 602.89697 | 564.04712 | 480.27197 | 486.16211 |
| 4 | 979.92944 | 216.12202 | 497.84912 | 601.83301 | 518.38306 | 524.74048 |
| 5 | 961.74756 | 212.15552 | 448.06494 | 615.91431 | 556.12402 | 562.94434 |
| 6 | 906.65039 | 211.66402 | 376.85962 | 658.28198 | 588.31470 | 595.52979 |
| 7 | 875.18652 | 210.88635 | 321.41577 | 655.48096 | 629.01587 | 636.72998 |
| 8 | 848.35034 | 214.36365 | 282.91382 | 667.54639 | 663.42676 | 671.56299 |
| 9 | 848.87915 | 243.27753 | 256.61719 | 631.34473 | 705.97778 | 714.63574 |

TEMPERATURES (DEG R )

| POINT | PLENUM TOTAL | STATOR DISCHARGE | ROTOR DISCHARGE | ISENTROPIC FROM T1 | TOTAL DISCHARGE |
|---|---|---|---|---|---|
| 1 | 596.05835 | 499.47339 | 510.63477 | 499.51709 | 515.50854 |
| 2 | 596.39209 | 503.24683 | 509.20996 | 499.80786 | 513.71582 |
| 3 | 597.05884 | 503.86353 | 508.10937 | 498.53223 | 512.00757 |
| 4 | 597.05884 | 517.15356 | 508.19019 | 509.37891 | 512.07690 |
| 5 | 597.05884 | 520.09131 | 505.86572 | 507.71973 | 509.61108 |
| 6 | 596.72559 | 528.32422 | 504.79419 | 514.27661 | 508.52222 |
| 7 | 596.05835 | 532.32202 | 505.97852 | 512.45142 | 509.67920 |
| 8 | 596.05835 | 536.17090 | 506.65405 | 513.59888 | 510.47778 |
| 9 | 595.72485 | 535.76270 | 509.09790 | 509.25195 | 514.02271 |

FLOW ANGLES (DEGREES FROM AXIAL)

RUN NUMBER 32

| POINT | ALPHA 1 | ALPHA 2 | BETA 1 | BETA 2 | DELTA BETA |
|---|---|---|---|---|---|
| 1 | 75.96136 | -26.77655 | 67.35133 | -67.93442 | 135.28575 |
| 2 | 75.99814 | -23.06314 | 66.27835 | -68.39478 | 134.67313 |
| 3 | 76.19102 | -9.55927 | 65.23016 | -67.76537 | 132.99553 |
| 4 | 74.95389 | -10.19390 | 59.27167 | -69.30226 | 128.57393 |
| 5 | 75.04497 | -4.18564 | 56.36424 | -69.90741 | 126.27165 |
| 6 | 74.12514 | -7.72282 | 48.84682 | -71.42027 | 120.26709 |
| 7 | 73.98924 | 4.32282 | 41.32071 | -71.28787 | 112.60858 |
| 8 | 73.59174 | 10.26967 | 32.10794 | -71.58015 | 103.68810 |
| 9 | 74.17421 | 29.51349 | 25.56148 | -70.40727 | 95.96875 |

EFFICIENCIES AND LOSSES

| POINT | EFFICIENCY TOTAL STATIC | EFFICIENCY TOTAL TOTAL | ZETA ROTOR | ZETA STATOR |
|---|---|---|---|---|
| 1 | 0.73897 | 0.77189 | 0.28770 | 0.11427 |
| 2 | 0.75891 | 0.79019 | 0.25048 | 0.11783 |
| 3 | 0.77754 | 0.80508 | 0.26566 | 0.10535 |
| 4 | 0.77887 | 0.80644 | -0.04106 | 0.21401 |
| 5 | 0.79883 | 0.82607 | -0.06240 | 0.21131 |
| 6 | 0.80887 | 0.83649 | -0.35679 | 0.28544 |
| 7 | 0.79391 | 0.82079 | -0.22107 | 0.29110 |
| 8 | 0.78394 | 0.81124 | -0.23044 | 0.31767 |
| 9 | 0.75301 | 0.78720 | -0.00466 | 0.27875 |

MACH NUMBERS AND DEGREE OF REACTION

RUN NUMBER 32

| POINT | REACTION HUB | REACTION MEAN | REACTION TIP | ABSOLUTE MACH 1 | RELATIVE MACH 1 |
|---|---|---|---|---|---|
| 1 | -0.1127 | -0.0004 | 0.1398 | 0.9834 | 0.6195 |
| 2 | -0.1063 | 0.0308 | 0.1519 | 0.9621 | 0.5787 |
| 3 | -0.0775 | 0.0477 | 0.1773 | 0.9618 | 0.5479 |
| 4 | -0.0487 | 0.0683 | 0.2008 | 0.8791 | 0.4466 |
| 5 | -0.0208 | 0.1085 | 0.2258 | 0.8603 | 0.4008 |
| 6 | 0.0066 | 0.1222 | 0.2475 | 0.8047 | 0.3345 |
| 7 | 0.0344 | 0.1737 | 0.2694 | 0.7738 | 0.2842 |
| 8 | 0.0617 | 0.1960 | 0.2896 | 0.7474 | 0.2493 |
| 9 | 0.0993 | 0.2338 | 0.3164 | 0.7482 | 0.2262 |



STATOR PRESSURE RATIO AND THROAT BLOCKAGE FACTOR

| POINT | PRESSURE RATIO | BLOCKAGE FACTOR |
|---|---|---|
| 1 | 0.49304 | 0.91360 |
| 2 | 0.50562 | 0.91097 |
| 3 | 0.51117 | 0.90776 |
| 4 | 0.52033 | 0.90663 |
| 5 | 0.53545 | 0.90455 |
| 6 | 0.54228 | 0.90302 |
| 7 | 0.56424 | 0.90384 |
| 8 | 0.57263 | 0.90468 |
| 9 | 0.59092 | 0.90864 |

REPORT



TURBO PROPULSION LABORATORY USNPGS, MONTEREY, CALIF.

REDUCED PERFORMANCE DATA OF TURBINE FROM TESTS WITH TRANSONIC TURBINE TEST RIG

TURBINE TYPE CIRCULAR-ARC I STATOR I RADIAL ROTOR TIP CLEAR.= .009 IN. AXIAL CLEAR. STATOR-ROTOR= 0.250 IN.
TEST RUN NO. 32 DATE OF TEST 5/21/68 DATA REDUCTION METHOD MF

| POINT | PRESSURE RATIO | ISENTROPIC HEAD COEFF. (R=4.240 IN.) | EFFICIENCY TOT-STATIC PERCENT | REFERRED FLOW RATE LBM/SEC | REFERRED TORQUE FT-LB | REFERRED POWER HP | REFERRED SPEED RPM | DEGREE OF REACTION (HUB) | DEGREE OF REACTION (TIP) |
|---|---|---|---|---|---|---|---|---|---|
| 1 | 2.0276 | 7.4668 | 73.90 | 1.3702 | 16.219 | 32.602 | 10559 | -.1127 | .1398 |
| 2 | 2.0258 | 6.6408 | 75.89 | 1.3662 | 15.655 | 33.348 | 11190 | -.1063 | .1519 |
| 3 | 2.0305 | 5.6990 | 77.75 | 1.3614 | 14.829 | 34.147 | 12097 | -.0775 | .1773 |
| 4 | 2.0265 | 4.8795 | 77.89 | 1.3597 | 13.709 | 34.077 | 13057 | -.0487 | .2008 |
| 5 | 2.0318 | 4.2537 | 79.88 | 1.3564 | 13.118 | 34.981 | 14008 | -.0208 | .2258 |
| 6 | 2.0265 | 3.7862 | 80.89 | 1.3537 | 12.486 | 35.232 | 14823 | 0.0066 | .2475 |
| 7 | 2.0247 | 3.3047 | 79.39 | 1.3517 | 11.425 | 34.490 | 15857 | 0.0344 | .2694 |
| 8 | 2.0300 | 2.9807 | 78.39 | 1.3509 | 10.727 | 34.151 | 16725 | 0.0617 | .2896 |
| 9 | 2.0212 | 2.6162 | 75.30 | 1.3509 | 9.626 | 32.622 | 17803 | 0.0993 | .3164 |

FOR POINTS 1 TO 9 AVG. PRESSURE RATIO= 2.0272 , MAX.DEVIATION +0.226 PCT. -0.295 PCT., PAVG./PATMO= 1.1669

629

TURBINE CIRCULAR ARC I
STATOR I

RUN NUMBER 33 SPACING 0.250 TIP CLEAR. 0.009

| POINT | FLOW RATE | RPM | PRESSURE RATIO | HORSEPOWER |
|---|---|---|---|---|
| 1 | 1.5694 | 12640.0000 | 2.5358 | 56.3838 |
| 2 | 1.5723 | 13070.0000 | 2.5416 | 57.0580 |
| 3 | 1.5762 | 14000.0000 | 2.5365 | 57.8311 |
| 4 | 1.5492 | 14980.0000 | 2.5154 | 59.0277 |
| 5 | 1.5524 | 15950.0000 | 2.5311 | 60.7246 |
| 6 | 1.5426 | 17080.0000 | 2.5276 | 61.2334 |
| 7 | 1.5427 | 17920.0000 | 2.5020 | 61.0611 |
| 8 | 1.5385 | 19470.0000 | 2.5104 | 61.5244 |

DIMENSIONLESS PERFORMANCE PARAMETERS

| POINT | K ISENTROPIC | REFERRED FLOW RATE | REFERRED TORQUE | REFERRED POWER | REFERRED SPEED |
|---|---|---|---|---|---|
| 1 | 7.8914 | 1.3668 | 18.7382 | 41.3960 | 11605.2930 |
| 2 | 7.4104 | 1.3703 | 18.3335 | 41.8407 | 11988.9023 |
| 3 | 6.4308 | 1.3720 | 17.3476 | 42.4586 | 12857.3984 |
| 4 | 5.5670 | 1.3481 | 16.5525 | 43.3718 | 13764.7695 |
| 5 | 5.0629 | 1.3721 | 16.0440 | 44.2123 | 14476.2227 |
| 6 | 4.4242 | 1.3621 | 15.0679 | 44.3898 | 15475.9180 |
| 7 | 3.9898 | 1.3630 | 14.3136 | 44.1904 | 16218.3320 |
| 8 | 3.3957 | 1.3622 | 13.2917 | 44.5508 | 17607.6523 |

GENERAL RESULTS

VELOCITIES (FT/SEC)
RUN NUMBER 33

| POINT | V1 | V2 | W1 | W2 | U1 | U2 |
|---|---|---|---|---|---|---|
| 1 | 1289.63599 | 279.42017 | 840.54761 | 631.35254 | 467.69165 | 473.42725 |
| 2 | 1287.03613 | 271.74951 | 823.09814 | 620.65771 | 483.60205 | 489.53320 |
| 3 | 1230.52710 | 266.79199 | 738.53198 | 638.63477 | 518.01294 | 524.36572 |
| 4 | 1228.33325 | 252.13721 | 698.32300 | 631.50928 | 554.27393 | 561.07153 |
| 5 | 1268.18994 | 268.32153 | 703.86011 | 593.65674 | 590.16504 | 597.40259 |
| 6 | 1236.12891 | 273.90576 | 635.50928 | 604.89526 | 631.97583 | 639.72656 |
| 7 | 1236.00073 | 295.99170 | 605.22388 | 581.53101 | 663.05664 | 671.18848 |
| 8 | 1172.39966 | 300.95093 | 497.01172 | 625.65991 | 720.40820 | 729.24316 |

TEMPERATURES (DEG R )

| POINT | PLENUM TOTAL | STATOR DISCHARGE | ROTOR DISCHARGE | ISENTROPIC FROM T1 | TOTAL DISCHARGE |
|---|---|---|---|---|---|
| 1 | 615.26172 | 476.86694 | 502.93848 | 469.48779 | 509.43530 |
| 2 | 616.41113 | 478.57373 | 503.37500 | 469.94067 | 509.52002 |
| 3 | 614.93311 | 488.93408 | 500.93286 | 480.53003 | 506.85571 |
| 4 | 614.27563 | 488.72534 | 496.74976 | 470.54199 | 502.03979 |
| 5 | 629.63452 | 495.80444 | 508.41797 | 476.42822 | 514.40894 |
| 6 | 631.74341 | 504.59448 | 508.57446 | 483.62720 | 514.81738 |
| 7 | 633.20117 | 506.07861 | 509.32104 | 480.98828 | 516.61133 |
| 8 | 634.17212 | 519.79565 | 508.84302 | 488.60034 | 516.37964 |

FLOW ANGLES (DEGREES FROM AXIAL)

RUN NUMBER 33

| POINT | ALPHA 1 | ALPHA 2 | BETA 1 | BETA 2 | DELTA BETA |
|---|---|---|---|---|---|
| 1 | 76.99704 | -21.36789 | 69.80518 | -65.65991 | 135.46509 |
| 2 | 76.98311 | -15.63952 | 69.37848 | -65.06241 | 134.44089 |
| 3 | 76.02126 | -12.74319 | 66.26637 | -65.95438 | 132.22075 |
| 4 | 77.30249 | -4.14075 | 67.25517 | -66.53308 | 133.78825 |
| 5 | 77.46133 | 13.79737 | 66.97333 | -63.96379 | 130.93712 |
| 6 | 77.19234 | 19.74188 | 64.45714 | -64.77330 | 129.23044 |
| 7 | 77.63324 | 30.21010 | 64.06329 | -63.90504 | 127.96834 |
| 8 | 77.08606 | 31.74139 | 58.18478 | -65.85362 | 124.03841 |

EFFICIENCIES AND LOSSES

| POINT | EFFICIENCY TOTAL STATIC | EFFICIENCY TOTAL TOTAL | ZETA ROTOR | ZETA STATOR |
|---|---|---|---|---|
| 1 | 0.73678 | 0.76941 | 0.50211 | -0.01596 |
| 2 | 0.74121 | 0.77207 | 0.51053 | -0.01697 |
| 3 | 0.75266 | 0.78305 | 0.37546 | 0.06909 |
| 4 | 0.78863 | 0.81750 | 0.44126 | -0.01185 |
| 5 | 0.78527 | 0.81694 | 0.52172 | -0.05299 |
| 6 | 0.79523 | 0.82876 | 0.45036 | -0.00895 |
| 7 | 0.79878 | 0.83886 | 0.50170 | -0.05458 |
| 8 | 0.80323 | 0.84482 | 0.38327 | 0.00992 |

MACH NUMBERS AND DEGREE OF REACTION

RUN NUMBER 33

| POINT | REACTION HUB | REACTION MEAN | REACTION TIP | ABSOLUTE MACH 1 | RELATIVE MACH 1 |
|---|---|---|---|---|---|
| 1 | -0.0716 | 0.0516 | 0.1698 | 1.2048 | 0.7852 |
| 2 | -0.0642 | 0.0602 | 0.1780 | 1.2002 | 0.7676 |
| 3 | -0.0418 | 0.0574 | 0.2012 | 1.1353 | 0.6814 |
| 4 | -0.0301 | 0.1281 | 0.2191 | 1.1335 | 0.6444 |
| 5 | -0.0096 | 0.1338 | 0.2355 | 1.1619 | 0.6449 |
| 6 | 0.0226 | 0.1429 | 0.2630 | 1.1226 | 0.5771 |
| 7 | 0.0425 | 0.1741 | 0.2779 | 1.1208 | 0.5483 |
| 8 | 0.0843 | 0.2123 | 0.3087 | 1.0491 | 0.4447 |

STATOR PRESSURE RATIO AND THROAT BLOCKAGE FACTOR

| POINT | PRESSURE RATIO | BLOCKAGE FACTOR |
|---|---|---|
| 1 | 0.41648 | 0.91140 |
| 2 | 0.41934 | 0.91372 |
| 3 | 0.41892 | 0.91483 |
| 4 | 0.45397 | 0.89892 |
| 5 | 0.45424 | 0.91488 |
| 6 | 0.45899 | 0.90823 |
| 7 | 0.47753 | 0.90885 |
| 8 | 0.49469 | 0.90830 |

REPORT



TURBO PROPULSION LABORATORY USNPGS, MONTEREY, CALIF.

REDUCED PERFORMANCE DATA OF TURBINE FROM TESTS WITH TRANSONIC TURBINE TEST RIG

TURBINE TYPE CIRCULAR-ARC I STATOR I RADIAL ROTOR TIP CLEAR.= .009 IN. AXIAL CLEAR. STATOR-ROTOR= 0.250 IN.
TEST RUN NO. 33 DATE OF TEST 5/22/68 DATA REDUCTION METHOD ME

| POINT | PRESSURE RATIO | ISENTROPIC HEAD COEFF. (R=4.240 IN.) | EFFICIENCY TOT-STATIC PERCENT | REFERRED FLOW RATE LBM/SEC | REFERRED TORQUE FT-LB | REFERRED POWER HP | REFERRED SPEED RPM | DEGREE OF REACTION (HUB) | DEGREE OF REACTION (TIP) |
|---|---|---|---|---|---|---|---|---|---|
| 1 | 2.5358 | 7.8914 | 73.68 | 1.3668 | 18.738 | 41.396 | 11605 | -.0716 | .1698 |
| 2 | 2.5416 | 7.4104 | 74.12 | 1.3703 | 18.334 | 41.841 | 11988 | -.0642 | .1780 |
| 3 | 2.5365 | 6.4308 | 75.27 | 1.3720 | 17.348 | 42.459 | 12857 | -.0418 | .2012 |
| 4 | 2.5154 | 5.5670 | 78.86 | 1.3481 | 16.553 | 43.372 | 13764 | -.0301 | .2191 |
| 5 | 2.5311 | 5.0629 | 78.53 | 1.3721 | 16.044 | 44.212 | 14476 | -.0096 | .2355 |
| 6 | 2.5276 | 4.4242 | 79.52 | 1.3621 | 15.068 | 44.390 | 15475 | 0.0226 | .2630 |
| 7 | 2.5020 | 3.9898 | 79.88 | 1.3630 | 14.314 | 44.190 | 16218 | 0.0425 | .2779 |
| 8 | 2.5104 | 3.3957 | 80.32 | 1.3622 | 13.292 | 44.551 | 17607 | 0.0843 | .3087 |

FOR POINTS 1 TO 8 AVG. PRESSURE RATIO= 2.5250 , MAX.DEVIATION +0.656 PCT. -0.912 PCT., PAVG./PATMO= 1.2499

TURBINE CIRCULAR ARC I
STATOR I

RUN NUMBER 34 SPACING 0.250 TIP CLEAR. 0.009

| POINT | FLOW RATE | RPM | PRESSURE RATIO | HORSEPOWER |
|---|---|---|---|---|
| 1 | 1.5638 | 13080.0000 | 2.5368 | 56.9356 |
| 2 | 1.5651 | 13080.0000 | 2.5000 | 56.9356 |
| 3 | 1.5755 | 13070.0000 | 2.5170 | 56.9750 |
| 4 | 1.5815 | 13050.0000 | 2.5377 | 56.7222 |
| 5 | 1.5974 | 13060.0000 | 2.5130 | 56.1028 |

DIMENSIONLESS PERFORMANCE PARAMETERS

| POINT | K ISENTROPIC | REFERRED FLOW RATE | REFERRED TORQUE | REFERRED POWER | REFERRED SPEED |
|---|---|---|---|---|---|
| 1 | 7.4897 | 1.3727 | 18.2834 | 41.4678 | 11914.5898 |
| 2 | 7.3174 | 1.3663 | 18.2689 | 41.6311 | 11971.0352 |
| 3 | 7.3174 | 1.3669 | 18.2567 | 41.7377 | 12009.7148 |
| 4 | 7.2855 | 1.3643 | 18.2374 | 41.9466 | 12022.5742 |
| 5 | 7.1124 | 1.3667 | 17.9957 | 41.6982 | 12172.3242 |

GENERAL RESULTS

VELOCITIES (FT/SEC)
RUN NUMBER 34

| POINT | V1 | V2 | W1 | W2 | U1 | U2 |
|---|---|---|---|---|---|---|
| 1 | 1318.88477 | 267.69214 | 853.66870 | 596.26221 | 483.97217 | 489.90747 |
| 2 | 1279.49170 | 269.61963 | 814.51025 | 626.52783 | 483.97217 | 489.90747 |
| 3 | 1257.67358 | 275.64624 | 794.72070 | 641.65601 | 483.60205 | 489.53320 |
| 4 | 1210.93018 | 291.96460 | 752.07837 | 678.17187 | 482.86230 | 488.78369 |
| 5 | 1153.45264 | 304.01587 | 697.10840 | 704.95728 | 483.23193 | 489.15845 |

TEMPERATURES (DEG R )

| POINT | PLENUM TOTAL | STATOR DISCHARGE | ROTOR DISCHARGE | ISENTROPIC FROM T1 | TOTAL DISCHARGE |
|---|---|---|---|---|---|
| 1 | 625.07959 | 480.33618 | 511.87354 | 473.18994 | 517.83643 |
| 2 | 619.19824 | 482.97217 | 505.99438 | 472.22339 | 512.04346 |
| 3 | 614.27563 | 482.65601 | 501.43115 | 473.24316 | 507.75366 |
| 4 | 605.03418 | 483.01636 | 492.29102 | 475.66357 | 499.38428 |
| 5 | 597.05884 | 486.34937 | 485.91309 | 477.04297 | 493.60400 |

FLOW ANGLES (DEGREES FROM AXIAL)

RUN NUMBER 34

| POINT | ALPHA 1 | ALPHA 2 | BETA 1 | BETA 2 | DELTA BETA |
|---|---|---|---|---|---|
| 1 | 77.21069 | -9.62638 | 70.00117 | -63.72823 | 133.72940 |
| 2 | 77.24178 | -17.58957 | 69.70180 | -65.78139 | 135.48319 |
| 3 | 76.74695 | -20.86003 | 68.72781 | -66.33249 | 135.06030 |
| 4 | 75.83826 | -28.40329 | 66.80083 | -67.74727 | 134.54810 |
| 5 | 75.24397 | -33.75546 | 65.07465 | -68.98868 | 134.06332 |

EFFICIENCIES AND LOSSES

| POINT | EFFICIENCY TOTAL STATIC | EFFICIENCY TOTAL TOTAL | ZETA ROTOR | ZETA STATOR |
|---|---|---|---|---|
| 1 | 0.73465 | 0.76386 | 0.56665 | -0.04325 |
| 2 | 0.75133 | 0.78259 | 0.50833 | -0.03380 |
| 3 | 0.74804 | 0.78065 | 0.45138 | 0.01050 |
| 4 | 0.74744 | 0.78452 | 0.30288 | 0.09065 |
| 5 | 0.74858 | 0.79010 | 0.17661 | 0.14345 |

MACH NUMBERS AND DEGREE OF REACTION

RUN NUMBER 34

| POINT | REACTION HUB | REACTION MEAN | REACTION TIP | ABSOLUTE MACH 1 | RELATIVE MACH 1 |
|---|---|---|---|---|---|
| 1 | -0.0655 | 0.0496 | 0.1770 | 1.2276 | 0.7946 |
| 2 | -0.0730 | 0.0761 | 0.1765 | 1.1877 | 0.7561 |
| 3 | -0.0681 | 0.0659 | 0.1791 | 1.1678 | 0.7380 |
| 4 | -0.0595 | 0.0507 | 0.1823 | 1.1240 | 0.6981 |
| 5 | -0.0648 | 0.0648 | 0.1815 | 1.0670 | 0.6449 |

STATOR PRESSURE RATIO AND THROAT BLOCKAGE FACTOR

| POINT | PRESSURE RATIO | BLOCKAGE FACTOR |
|---|---|---|
| 1 | 0.41544 | 0.91529 |
| 2 | 0.43279 | 0.91100 |
| 3 | 0.42565 | 0.91146 |
| 4 | 0.41579 | 0.90968 |
| 5 | 0.42578 | 0.91131 |

REPORT



TURBO PROPULSION LABORATORY USNPGS, MONTEREY, CALIF.

REDUCED PERFORMANCE DATA OF TURBINE FROM TESTS WITH TRANSONIC TURBINE TEST RIG

TURBINE TYPE CIRCULAR-ARC I STATOR I RADIAL ROTOR TIP CLEAR.= .009 IN. AXIAL CLEAR. STATOR-ROTOR= 0.250 IN.
TEST RUN NO. 34 DATE OF TEST 5/23/68 DATA REDUCTION METHOD ME

| POINT | PRESSURE RATIO | ISENTROPIC HEAD COEFF. (R=4.240 IN.) | EFFICIENCY TOT-STATIC PERCENT | REFERRED FLOW RATE LBM/SEC | REFERRED TORQUE FT-LB | REFERRED POWER HP | REFERRED SPEED RPM | DEGREE OF REACTION (HUB) | DEGREE OF REACTION (TIP) |
|---|---|---|---|---|---|---|---|---|---|
| 1 | 2.5368 | 7.4897 | 73.46 | 1.3727 | 18.283 | 41.468 | 11914 | -.0655 | .1770 |
| 2 | 2.5000 | 7.3174 | 75.13 | 1.3663 | 18.269 | 41.631 | 11971 | -.0730 | .1765 |
| 3 | 2.5170 | 7.3174 | 74.80 | 1.3669 | 18.257 | 41.738 | 12009 | -.0681 | .1791 |
| 4 | 2.5377 | 7.2855 | 74.74 | 1.3643 | 18.237 | 41.947 | 12082 | -.0595 | .1823 |
| 5 | 2.5130 | 7.1124 | 74.86 | 1.3667 | 17.996 | 41.698 | 12172 | -.0648 | .1815 |

FOR POINTS 1 TO 5 AVG. PRESSURE RATIO= 2.5209 , MAX.DEVIATION +0.669 PCT. -0.830 PCT., PAVG./PATMO= 1.2525

## APPENDIX II

## EVALUATION OF THE FORCE ACTING ON THE STATOR ASSEMBLY BY THE STATOR DISCHARGE PRESSURE

The pressure at the stator discharge $P_1$ varies between the pressure $P_{h1}$ at the hub and the pressure $P_{t1}$ at the tip. This pressure is not necessarily a linear function of radius r. In the present study the pressure $P_1$ will be assumed to vary parabolically from $P_{h1}$ at $R_{h1}$ to $P_{t1}$ at $R_{t1}$ such that at the mean radius $R_{m1}$ the pressure is $(1 + \epsilon) P_{m1}$, where $P_{m1} = (P_{h1} + P_{t1})/2$. The value of the factor $\epsilon$ will be determined by comparing momentum results with those from the continuity equation.

Let

$$P_1 = P_{h1} + \frac{P_{t1}-P_{h1}}{R_{t1}-R_{h1}}(r-R_{h1}) + \Delta P = P_{h1} + \delta(r-R_{h1}) + \Delta P \quad (64)$$

where

$$\delta = \frac{P_{t1} - P_{h1}}{R_{t1} - R_{h1}} \quad (65)$$

and

$$\Delta P = A_o + A_1 r + A_2 r^2 \quad (66)$$

The constant factors $A_o$, $A_1$, and $A_2$ are obtained from the conditions $\Delta P = 0$ at $r = R_{h1}$, $\Delta P = 0$ at $r = R_{t1}$, and $\Delta P = P_{m1}$ at $r = R_{m1} = (R_{t1} + R_{h1})/2$. Thus

$$0 = A_o + A_1 R_{h1} + A_2 R_{h1}^2$$

$$0 = A_o + A_1 R_{t1} + A_2 R_{t1}^2$$

$$\epsilon P_{m1} = A_o + A_1 R_{m1} + A_2 R_{m1}^2$$

The above simultaneous equations are solved by Cramer's Rule, with

$$C = \begin{vmatrix} 1 & R_{h1} & R_{h1}^2 \\ 1 & R_{t1} & R_{t1}^2 \\ 1 & R_{m1} & R_{m1}^2 \end{vmatrix} = (R_{t1} - R_{h1})[R_{m1}^2 - R_{m1}(R_{t1} + R_{h1}) + R_{h1}R_{t1}]$$

with $R_{m1} = (R_{h1} + R_{t1})/2$

$$C = (R_{t1} - R_{h1})[\tfrac{1}{4}(R_{h1} + R_{t1})^2 - \tfrac{1}{2}(R_{h1} + R_{t1})^2 + R_{h1}R_{t1}]$$

$$C = -\tfrac{1}{4}(R_{t1} - R_{h1})^3 \qquad (67)$$

Thus

$$A_o = 1/C \begin{vmatrix} 0 & R_{h1} & R_{h1}^2 \\ 0 & R_{t1} & R_{t1}^2 \\ \epsilon P_{m1} & R_{m1} & R_{m1}^2 \end{vmatrix} = \frac{\epsilon P_{m1}\left[R_{t1}^2 R_{h1} - R_{h1}^2 R_{t1}\right]}{C}$$

with Eq. (67)

$$A_o = -4\epsilon P_{m1} \frac{R_h R_{t1}}{(R_{t1} - R_{h1})^2} \qquad (68)$$

with Eq. (67), in like manner

$$A_1 = \frac{4\epsilon P_{m1}(R_{t1} + R_{h1})}{(R_{t1} - R_{h1})^2} \qquad (69)$$

$$A_2 = - \frac{4 \epsilon P_{m1}}{(R_{t1} - R_{h1})^2} \tag{70}$$

Substituting Eqs. (68), (69), and (70) into Eq. (66)

$$\Delta P = \frac{4 \epsilon P_{m1}}{(R_{t1} - R_{h1})^2} [- R_{h1} R_{t1} + (R_{t1} - R_{h1})\, r - r^2] \tag{71}$$

The force on the stator assembly due to the stator discharge pressure is

$$F_{sD} = 2\pi \int_{R_{h1}}^{R_{t1}} P_1 r \, dr \tag{72}$$

with Eqs. (64) and (71)

$$F_{sD} = 2\pi \int_{R_{h1}}^{R_{t1}} [(P_{h1} - \delta R_{h1}) r + \delta r^2 + \Delta P r] \, dr$$

$$= \pi (P_{h1} - \delta R_{h1})(R_{t1}^2 - R_{h1}^2) + \frac{2\pi}{3} \delta [R_{t1}^3 - R_{h1}^3] + 2\pi \int_{R_{h1}}^{R_{t1}} \Delta P \, r \, dr$$

with Eq. (65)

$$F_{sD} = \pi (P_{h1} - R_{h1} \frac{P_{t1} - P_{h1}}{R_{t1} - R_{h1}})(R_{t1}^2 - R_{h1}^2) + \frac{2\pi}{3} \frac{P_{t1} - P_{h1}}{R_{t1} - R_{h1}} (R_{t1}^3 - R_{h1}^3)$$

$$+ \frac{2\pi 4 \epsilon P_{m1}}{(R_{t1} - R_{h1})^2} \left[ - R_{h1} R_{t1} \frac{(R_{t1}^2 - R_{h1}^2)}{2} + (R_{h1} + R_{t1}) \frac{(R_{t1}^3 + R_{h1}^3)}{3} - \frac{R_{t1}^4 - R_{h1}^4}{4} \right]$$

Simplifying

$$F_{sD} = \frac{\pi}{3}P_{h1}[R_{t1}^2 + R_{h1}R_{t1} - 2R_{h1}^2] + \frac{\pi}{3}P_{t1}[2R_{t1}^2 - R_{h1}R_{t1} - R_{h1}^2]$$

$$+ 2/3\,\pi \frac{\epsilon P_{m1}}{(R_{t1} - R_{h1})^2}[(R_{t1}^2 - R_{h1}^2)(R_{t1} - R_{h1})^2]$$

With $P_{m1} = (P_{h1} + P_{t1})/2$, the final expression for the force $F_{sD}$ acting on the stator assembly by the pressure at the stator exit is

$$F_{sD} = 2\pi \int_{R_{h1}}^{R_{t1}} P_1 r\,dr = \frac{\pi}{3}P_{h1}[(1+\epsilon)R_{t1}^2 + R_{h1}R_{t1} - (2+\epsilon)R_{h1}^2] \tag{73}$$

$$+ \frac{\pi}{3}P_{t1}[(2+\epsilon)R_{t1}^2 - R_{h1}R_{t1} - (1+\epsilon)R_{h1}^2]$$

INITIAL DISTRIBUTION LIST

| | | Copies |
|---|---|---|
| 1. | Defense Documentation Center<br>Cameron Station<br>Alexandria, Virginia 22314 | 20 |
| 2. | Library<br>Naval Postgraduate School<br>Monterey, California 93940 | 2 |
| 3. | Commander, Naval Air Systems Command<br>Navy Department<br>Washington, D.C. 20360 | 1 |
| 4. | Commandant of the Marine Corps (Code A03C)<br>Headquarters, U.S. Marine Corps<br>Washington, D.C. 20380 | 1 |
| 5. | Commander, Naval Ship Systems Command<br>Navy Department<br>Washington, D.C. 20360 | 1 |
| 6. | Professor M. H. Vavra<br>Department of Aeronautics<br>Naval Postgraduate School<br>Monterey, California 93940 | 3 |
| 7. | Chairman, Department of Aeronautics<br>Naval Postgraduate School<br>Monterey, California 93940 | 1 |
| 8. | Professor A. E. Fuhs<br>Department of Aeronautics<br>Naval Postgraduate School<br>Monterey, California 93940 | 1 |
| 9. | Professor R. D. Zucker<br>Department of Aeronautics<br>Naval Postgraduate School<br>Monterey, California 93940 | 1 |
| 10. | Dr. E. S. Lamar (Code 03C)<br>Chief Scientist, Research and Technology<br>Naval Air Systems Command<br>Navy Department<br>Washington, D.C. 20390 | 1 |
| 11. | Commander<br>Naval Ordnance Systems Command<br>Navy Department<br>Washington, D.C. 20390 | 1 |

| | | |
|---|---|---|
| 12. | Dr. O. H. Johnson<br>Naval Air Systems Command (Code 330 B)<br>Navy Department<br>Washington, D.C. 20360 | 1 |
| 13. | Head, Department of Engineering<br>Naval Academy<br>Annapolis, Maryland 21402 | 1 |
| 14. | Superintendent<br>Naval Academy<br>Annapolis, Maryland 21402 | 1 |
| 15. | Mr. I. Silver, Code 330<br>Propulsion Administrator<br>Research and Technology<br>Naval Air Systems Command<br>Navy Department<br>Washington, D.C. 20390 | 1 |
| 16. | Office of Naval Research<br>Air Programs Office<br>Navy Department<br>Washington, D.C. 20360 | 1 |
| 17. | Capt. A. Bodnaruk, USN<br>Naval Ship Systems Command (Code 6140)<br>Navy Department<br>Washington, D. C. 20360 | 1 |
| 18. | Office of Naval Research (Power Branch)<br>Attn: Mr. J. K. Patton, Jr.<br>Navy Department<br>Washington, D. C. 20360 | 1 |
| 19. | Dr. F. I. Tanczos<br>Technical Director, Research and Technology<br>Naval Air Systems Command<br>Navy Department<br>Washington, D. C. 20390 | 1 |
| 20. | Captain Martin J. Lenzini<br>100 Lakewood Place<br>Highland Park, Illinois 60035 | 2 |

## DOCUMENT CONTROL DATA - R & D

*Security classification of title, body of abstract and indexing annotation must be entered when the overall report is classified)*

1 ORIGINATING ACTIVITY (Corporate author)
Naval Postgraduate School
Monterey, California 93940

2a. REPORT SECURITY CLASSIFICATION
UNCLASSIFIED

2b. GROUP

3 REPORT TITLE
CALIBRATION OF TURBINE TEST RIG WITH IMPULSE TURBINE AT HIGH PRESSURE RATIOS

4 DESCRIPTIVE NOTES (Type of report and inclusive dates)
Thesis

5 AUTHOR(S) (First name, middle initial, last name)
Martin J. Lenzini, Captain, U. S. Marine Corps

6. REPORT DATE
June 1968

7a. TOTAL NO. OF PAGES
144

7b. NO. OF REFS
9

8a. CONTRACT OR GRANT NO.

b. PROJECT NO.

c.

d. Unlimited dist

9a. ORIGINATOR'S REPORT NUMBER(S)

9b. OTHER REPORT NO(S) (Any other numbers that may be assigned this report)

10. DISTRIBUTION STATEMENT
This document is subject to special export controls and each transmittal to foreign governments or foreign nationals may be made only with prior approval of Naval Postgraduate School.

11. SUPPLEMENTARY NOTES

12. SPONSORING MILITARY ACTIVITY
Naval Postgraduate School
Monterey, California 93940

13 ABSTRACT

The Transonic Turbine Test Rig of the Turbo-Propulsion Laboratory, Department of Aeronautics, of the Naval Postgraduate School was designed to investigate the performance of turbines with transonic or supersonic rotor inlet velocities. The test rig has provisions for testing single stage axial turbines at high pressure ratios and at variable axial and radial clearances. The present study describes the calibration of the turbine test rig with an impulse turbine at high pressure ratios. The turbine stage consists of a double circular-arc rotor with sharp leading edges and a stator with converging nozzle type blading. The results of the flow rate calibration and labyrinth seal leakage tests are described. The instrumentation necessary to separate rotor and stator losses is also discussed.

| 14 KEY WORDS | LINK A | | LINK B | | LINK C | |
|---|---|---|---|---|---|---|
| | ROLE | WT | ROLE | WT | ROLE | WT |
| Impulse Turbine | | | | | | |
| Transonic Turbine | | | | | | |
| Transonic Turbine Test Rig | | | | | | |



thesL527
Calibration of turbine test rig with imp
3 2768 002 12055 2
DUDLEY KNOX LIBRARY C.1